

**SOIL LOSS ESTIMATION AND SPATIAL MAPPING USING RUSLE
AND GIS- A CASE STUDY IN KURUMANPUZHA SUB WATERSHED OF
CHALIYAR RIVER BASIN**

By

AISHWARYA M S

(2019-18-002)



Department of Irrigation and Drainage Engineering

Kelappaji College of Agricultural Engineering and Technology

Tavanur-679 573, Malappuram

2022

**SOIL LOSS ESTIMATION AND SPATIAL MAPPING USING
RUSLE AND GIS- A CASE STUDY IN KURUMANPUZHA SUB
WATERSHED OF CHALIYAR RIVER BASIN**

By

AISHWARYA M S

(2019-18-002)

Thesis

Submitted in partial fulfillment of the

Requirement for the award of degree of

Master of Technology

In

Agricultural Engineering

(Soil and Water Conservation Engineering)

Faculty of Agricultural Engineering and Technology

Kerala Agricultural University



Department of Irrigation and Drainage Engineering

Kelappaji College of Agricultural Engineering and Technology

Tavanur-679 573, Malappuram.

2022

DECLARATION

I hereby declare that this thesis entitled “Soil Loss Estimation And Spatial Mapping using RUSLE and GIS- A case study in Kurumanpuzha Sub Watershed of Chaliyar river basin” is a bonafide record of research work done by me during the course of research and the thesis has not previously formed the basis for the award to me for any degree, diploma, associateship, fellowship or other similar title of any other university or society.

Place: Tavanur

Date : 24-05-2022

Aishwarya M.S
Aishwarya M S

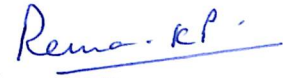
(2019-18-002)

CERTIFICATE

Certified that this thesis entitled “Soil loss estimation and spatial mapping using RUSLE and GIS-A case study in Kurumanpuzha sub watershed of Chaliyar river basin” is a bonafide record of research work done independently by Ms. Aishwarya M S (2019-18-002), under my guidance and supervision and that it has not previously formed the basis for the award of any degree, diploma, fellowship or associateship to her.

Place: Tavanur

Date: 24-5-22



Dr. Rema K P

Professor

Department of Irrigation and


Drainage Engineering

KCAET, Tavanur

Malappuram, Kerala

CERTIFICATE

We, the undersigned, members of the Advisory Committee of **Ms. Aishwarya M S**, a candidate for the degree of Master of Technology in Agricultural Engineering majoring SOIL AND WATER Engineering agree that the thesis entitled **“Soil loss estimation and spatial mapping using RUSLE and GIS - A case study in Kurumanpuzha sub watershed of Chaliyar river basin”** may be submitted by **Ms. Aishwarya M S**, in partial fulfillment of the requirement for the degree.



Dr. Rema K. P.

(Chairman, Advisory Committee)

Professor & head,
Dept of IDE,
KCAET, Tavanur.



Dr. Sathian K.K.

(Member, Advisory Committee)

Dean of faculty (Agrl.Engg),
Dept of SWCE,
KCAET, Tavanur.



Dr. Divya Vijayan

(Member, Advisory Committee)

Assistant Professor,
Dept of Remote Sensing & GIS,
College of Forestry,
Vellanikkara, Trissur

Dr. Sasikala

(Member, Advisory Committee)

Professor (Retd.)
Department of IDE,
KCAET, Tavanur.

ACKNOWLEDGEMENT

ACKNOWLEDGEMENT

First of all, I am thankful to **God Almighty** for his invisible helping hand in this covid pandemic situation that guided me through the right way to pursue my journey to the completion of this project.

At the very outset I express my sincere regards, my heartfelt gratitude to my guide **Dr. Rema K. P.** Professor, Department of Irrigation and Drainage Engineering, KCAET, Tavanur, for her constant guidance, support, valuable suggestions, warm encouragement, insightful decision provided for my entire work. Her timely interventions, knowledge, confidence and blessings were the main source and cause for the timely and successful completion of this project.

I am also indebted to **Dr. Sathian K. K.**, Dean (Agri.Engg), Kelappaji College of Agricultural Engineering and Technology, Tavanur, for all the support offered during the course of my research work and for providing me with the necessary permissions to carry out my research work with ease and correction of the thesis.

I avail this opportunity to express my sincere thanks to my advisory committee members **Dr. Divya Vijayan V**, Assistant Professor & PI, STCR, Dept. of Soil Science & Agri. Chemistry, College of Horticulture, Vellanikkara, **Dr. Sasikala**, Professor, Dept. of IDE KCAET, Tavanur for their valuable suggestions, encouragement and remarks throughout this study.

I am extremely thankful to **Dr. Anu Varughese**, Assistant Professor, Department of Irrigation and Drainage Engineering KCAET, Tavanur who has shown interest to clarify the doubts in ArcGIS and given timely helps to move forward during my research work very confidently. I greatly appreciate and thank for her most sincere and lovable approach towards me.

With immense pleasure, I express my heartfelt thanks to my batchmates **Er. N.Subhasree, Er. Adarsh, Er. Alankar, Er.Chithra ,Er.Hari Sankar** and **Er. Rathinavel** for the great support and encouragement provided throughout my study. I whole heartedly thank my respected seniors **Er. Chethan, Er. Chandrashekhar, Er. Adwaith, Er. Kalyan, Er. Amith Er.Mahesh baabu, Er. Venkata Reddy, Er. Kari Venkat Sai** and **Er. Srinivas** for their timely support and help during my research. I am also thankful to my best friend **Devika** for her love and support during M.Tech journey.

I engrave my deep sense of gratitude to **Jayanth Kanavi G.B, Anand Subramanyan, Er.Premakumar, Adarsh K and Shaheemath Suhara K K** for their valuable suggestion and support throughout the project work.

I have no words to express my gratitude and love to my dearest parents **M N Shylashekhar , Pramodini , Savitha Rani** and **Shree Harsha**, sister **Chandana** and to my beloved extended family **Chithrashekharaiyah , Premakumari** and **Prashanth Aradhya** who constantly supported me throughout this venture. I can't count the immense blessings, encouragement, sacrifices, prayers and love they have showered on me which were the major source of power for me to complete this venture.

Once again, I am expressing my heartfelt thanks to each and everyone those who helped me in one way or the other in carrying out this endeavor.

Tavanur

Aishwarya M S

Date

DEDICTAION

This thesis is dedicated to my father

CONTENTS

Chapter No.	Title	Page No.
	LIST OF TABLES	i
	LIST OF FIGURES	ii
	LIST OF PLATES	iv
	SYMBOLS AND ABBREVIATIONS	vii
I	INTRODUCTION	1 - 6
II	REVIEW OF LITERATURE	7 - 40
III	MATERIALS AND METHODS	41-74
IV	RESULTS AND DISCUSSION	75-112
V	SUMMARY AND CONCLUSION	113-117
	REFERENCES	118 -136
	APPENDICES	137 – 139
	ABSTRACT	140-142

LIST OF TABLES

Table No.	Title	Page No.
2.1	Variation of K factor proposed by Stone and Hilborn with respect to textural class and organic matter content.	26
2.2	P factor values (Wischmeier and Smith, 1978)	31
3.1	Indication of form factor value	51
3.2	Indication of drainage density values	52
3.3	Indication of stream frequency value	53
3.4	Indication of drainage texture values	55
3.5	Indication of length of overland flow	56
3.6	Indication of Ruggedness number	58
3.7	Indication of HI Values	60
3.8	Annual rainfall (mm) of Nilambur rain gauge station	63
3.9	P factor variation with land use and land slope %	72
4.1	Slope classes identified in the watershed	79
4.2	Area under different Land use/Land cover	82
4.3	Stream order and its mean stream length of Kurumanpuzha sub watershed	86
4.4	Stream length ratio of Kurumanpuzha sub watershed	86

4.5	Bifurcation ratio of Kurumanpuzha sub watershed	90
4.6	Linear aspects of Kurumanpuzha sub watershed	91
4.7	Areal aspects of Kurumanpuzha sub watershed	93
4.8	Relief aspects of Kurumanpuzha Sub Watershed	94
4.9	Rainfall erosivity factor R ($\text{MJ mm ha}^{-1} \text{ h}^{-1} \text{ y}^{-1}$)	96
4.10	K factor values for the Kurumanpuzha sub watershed	99
4.11	Variation of range of C factor with respect to the land use	105
4.12	Soil erosion risk classification and area coverage	108
4.13	Average annual soil loss (A) in different land uses	110
4.14	Average annual soil loss (A) corresponds to different slope lands	110

LIST OF FIGURES

Figure No.	Title	Page No.
3.1	Location map of Kurumanpuzha sub watershed	42
3.2	Annual rain fall(mm) from 2000-2020	63
3.3	Soil map of Chaliyar river basin	66
3.4	Flowchart for the estimation of the LS factor	69
3.5	ArcGIS interface for raster calculator	70
3.6	Image analysis tool with Landsat 8 image clipped for the study area	71
3.7	Methodology flow chart adopted for RUSLE model	73
4.1	DEM map of the watershed	75
4.2	Flow Direction map of the Watershed	76
4.3	Flow accumulation map of Kurumanpuzha sub watershed	78
4.4	Slope map of the watershed	79
4.5	Aspect map of Kurumanpuzha sub watershed	80
4.6	Land use/Land cover map of the watershed	82
4.7	Drainage network map of the watershed	85
4.8	Regression plot of logarithm of stream number v/s stream order	87

4.9	Regression plot of logarithm of total stream length and stream order	88
4.10	Hypsometric curve of Kurumanpuzha sub watershed	95
4.11	Average annual rainfall erosivity factor (R) graph for (2000-2020) Years	97
4.12	Soil map of Kurumanpuzha sub watershed	100
4.13	Spatial distribution of soil erodibility factor(K factor)	101
4.14	Spatial distribution of topographic (LS factor)	102
4.15	NDVI map of Kurumanpuzha sub watershed	103
4.16	Spatial distribution of C factor of Kurumanpuzha sub watershed	104
4.17	Spatial variation of C factor with respect to Land use	105
4.18	Spatial distribution of P factor for the watershed	106
4.19	Soil loss map of Kurumanpuzha sub watershed	107
4.20	Spatial distribution of soil erosion in Kurumanpuzha sub watershed	108
4.21	Soil conservation measures suggested for the study area	112

LIST OF PLATES

Plate No.	Title	Page No.
1	Canolly plot (outlet of Kurumanpuzha sub watershed)	76
2	Higher elevated part in Kurumanpuzha sub watershed	83
3	Field photographs of different land uses of the study area	84
4	3 rd order stream of Kurumanpuzha sub watershed	85
5	4 th order stream of Kurumanpuzha sub watershed	89

SYMBOLS AND ABBREVIATIONS

%	:	Percentage
<	:	Less than
>	:	Greater than
Σ	:	Sum
\leq	:	Less than or equal to
\geq	:	Greater than or equal to
$^{\circ}$:	Degree
'	:	Minute
"	:	Second
&	:	And
$^{\circ}\text{C}$:	Degree Celsius
cm	:	centimeter
CSWCRTI	:	Central Soil & Water Conservation Research & Training Institute
DEM	:	Digital Elevation Model
E	:	East
ESRI	:	Environmental System Research Institute
e.g.	:	Example
et al.,	:	and others
etc	:	etcetera
Fig.	:	Figure
GIS	:	Geographical Information System
GPS	:	Global Positioning System
h	:	Hour
ha	:	hectare
I30	:	30 minute intensity
IMD	:	Indian Meteorological Department

IRS	:	Indian Remote-Sensing Satellite
ISRO	:	Indian Space Research Organization
J	:	Joule
km	:	Kilometer
km ⁻¹	:	per kilometre
km ²	:	square kilometer
km ⁻²	:	per square kilomere
km h ⁻¹	:	Kilometer per hour
LISS	:	Linear Imaging And Self Scanning
LULC	:	Landuse Land Cover
m	:	meter
MFI	:	Modified Fournier Index
MJ	:	Mega Joule
mm	:	millimeter
Mg	:	Mega gram
m-tonnes	:	Million tonnes
MUSLE	:	Modified Universal Soil Loss Equation
N	:	North
NBSSLUP	:	National Bureau of Soil Survey and Land Use Planning
NDVI	:	Normalized Difference Vegetation Index
NIR	:	Near infrared
R ²	:	Coefficient of Determination
RUSLE	:	Revised Universal Soil Loss Equation
s	:	Second
S	:	South
SRTM	:	Shuttle Radar Topography Mission
USDA	:	United States Department of Agriculture
USGS	:	United States Geological Survey
USLE	:	Universal Soil Loss Equation
UTM	:	Universal Transverse Mercator Co-ordinate System
vfS	:	Very fine sand

W	:	West
WEPP	:	Water Erosion Prediction Project
WGS	:	World Geodetic System
WOI	:	Weighted Index Overlay
yr	:	year

INTRODUCTION

CHAPTER -I

INRODUCTION

Natural resources have played a dynamic role in balancing the ecosystem. Ever since the rise of modern human civilization and expansion of human activities to wider domains and spaces such as urbanization, industrialization, intensified agricultural practices and much more in different countries, serious environmental problems have originated. The portion of the biosphere, the two main components, i.e., the “soil” and “water”, are much prone to serious environmental threats.

“Soil”, the earth’s subtle skin that anchors all life on earth, is a dynamic complex of minerals and organic matter supporting plant growth. The combined influence of climate, topography, and living organisms overtime on the parent material paves the way to soil formation. In simple terms, soil can be defined as a non-renewable dynamic natural resource consisting of organic and inorganic material, which provides structural support for the life to grow.

Natural and human activities upon the soil over the years have resulted in erosion of the upper layer of soil from the earth's surface, though the soil being the important component of the biosphere, supporting all life forms directly or indirectly, is facing a serious threat of erosion globally since the last century. In primitive teams, “Soil erosion” can be defined as the detachment and movement of topsoil (Jackson *et al.*, 1986) and to be specific, Soil erosion is a process that involves detachment, transportation, and accumulation of fertile surface soil (Jain *et al.*, 2001). Soil erosion is one such geological process that occurs naturally over a period, causing no serious problem, but when human activities and interference assist such natural processes, the rate is accelerated. Such accelerated soil erosion is an alarming situation, resulting in the removal of nutritive layers of soil and further resulting in loss of life.

The soil erosion process is grouped into three steps: detachment: losing of soil particles, transportation: moving of soil particles, deposition, and placement of soil particles. Soil erosion and sedimentation of eroded materials at locations away from the point of detachment involve the economic loss to individuals and society as a whole due

to loss of productive topsoil and applied nutrients on croplands, damage to crops and crop yield, and pollution of water bodies (Flanagan *et al.*, 2013).

Water and wind are the major agents that contribute to the degradation of soils. Out of 329 M ha, 144 M ha is affected by wind and water erosion and is primarily confined to the States of Rajasthan, Gujarat and Haryana. The severity of wind erosion is reciprocally associated with the rainfall amount. Lesser the rainfall more would be the wind erosion (Guerra *et al.*, 2020). The soil particles from sloping and bare lands were washed due to runoff. The wind blows loosed soil particles and detaches them from flat and unprotected lands. Productivity is directly affected by soil erosion, and it depends on parameters such as soil profile and horizonation, terrain, soil management, and climate characteristics (Balasubramanian , 2017).

In case of water erosion, the impact of raindrops and run-off water moving over the soil surface are responsible for soil particles detachment. The high striking velocities (up to 9 ms^{-1}) and many drops produce strong hydro-dynamic force, which detaches a large amount of soil particles. The variation in rainfall, run-off, soil characteristics, topography, and cover conditions contribute to soil erosion by water. Generally, water erosion can be grouped into four categories, (1) Splash erosion: splattering and loosening of small soil particles caused by raindrops affecting a wet soil surface, (2) Sheet erosion: it is more-or-less uniform removal of soil from the surface by flow of water across the soil surface, (3) Rill erosion involves the concentration of flowing water into small channels less than 0.3m and (4) gully erosion occurs when concentrated runoff cuts deep channels into the soil. Apart from water and wind, which are equally as well as unequally subsidised to the rate of soil erosion in the specified regions such as characteristics of soil, temperature, landscape, organic matter in the soil, topographic characteristics, watershed characteristics, and crop pattern.

Out of 329 M ha 174 M ha (53%), India is estimated to be affected by various land degradation problems. Average annual soil erosion in India is $16.35 \text{ t ha}^{-1} \text{ yr}^{-1}$ *i.e.*, 5334 MT of soil is being removed annually due to various reasons. About 29% is lost permanently to the seas, 10% is deposited in the reservoirs and the remaining 61% is dislocated from one place to another, causing land degradation problems. The storage

capacity of major reservoirs is depleting 1-2% every year due to high siltation rates (Naidu *et al.*, 2021).

Several erosion models have been developed to understand and predict stream erosion and upland soil, as well as the transportation and deposition of sediments. Soil erosion models are useful to estimate soil loss and runoff rates from agricultural land, plan land use tactics, provide relative soil loss indices, and guide government policy and strategy on soil and water conservation (Igwe *et al.*, 2017). Earlier models of estimation and prediction, such as surveys, multi-slot devices and Coshocton wheel sampler methods were difficult and time-consuming and needed a wide number of data collection. Therefore, Soil loss estimation models were improved over the years by adding new variables and factors.

Modelling provides a consistent and quantitative methodology to estimate soil erosion and sediment yield under a wide range of conditions and is desired to guide the broad control of soil erosion. Models differ in complexity and input requirements; therefore, the application of these models relies on the soil type and climate of the given area. Information about current erosion, its trends and scenario analysis can be provided by effective modelling. (Ganasri and Ramesh, 2016).

With advancements in technology and a wide range of input availability, modern soil loss estimation models have come into the limelight. These models are interdisciplinary and reflect numerous scientific approaches to better understand soil erosion phenomena with variable temporal and spatial scales, methodologies, and research goals.

Soil erosion models are classified into three types, Empirical or Statistical, Conceptual; and Physical based models. Those be subject to the physical processes simulated by the model, the model algorithms relating to these processes and the data dependence of the model (Merrit *et al.*, 2003).

The development of the Universal Soil Loss Equation (USLE) was one of the major innovations in soil and water conservation during the past century, an empirical model used around the world to estimate soil erosion by raindrop impact and surface runoff

(Wischmeier and Smith 1978). Its revised version, named RUSLE; the Modified Universal Soil Loss Equation (MUSLE); Water Erosion Prediction Project (WEPP); and the European Soil Erosion Model (EUROSEM), have been used for soil erosion estimation by academicians and decision-makers.

Model accuracy differed in determining soil erosion areas according to the model's parameters (Sadeghi *et al.*, 2014). The RUSLE model is considered one of the widely accepted empirical models to predict soil erosion lost by water. However, the RUSLE model is based on the energy erosion of rainfall, susceptibility of soils to erosion, topography, vegetation, and maintenance (Abdo and Salloum 2017). The RUSLE is a computerized version of the USLE. It incorporates improvements in many factor estimates, including a new procedure to calculate cover factor, new algorithms to reflect rill to inter-rill erosion in slope length and steepness factors. Further-enhanced Windows version of the software, known as RUSLE2, was released in the year 2003 for estimating erosion rates, sediment delivery and guiding conservation planning.

Modelling soil loss is a complex process due to the spatial variation of controlling factors and the huge data involved (Bhattarai and Dutta 2007). Still, the possibility of this process is achievable with the well-established use of geospatial technologies like GIS and RS, spatial interpolation techniques, and the use of a wide range of environmental data. The Geographic Information System (GIS) has emerged as a powerful decision-making tool allowing to handle spatial information and interaction with erosion models (Renschler and Harbor, 2002). The computerized system can execute predefined tasks such as capturing, storing, integrating, analysing, and visualization of data linked to coordinates or locations (ESRI, 2005). Soil erosion models are vital to designing and implementing soil management and conservation strategies (Panagos *et al.*, 2015b). As a result, estimating the rate of soil loss and categorising its spatial intensities will enable soil conservation and management procedures (Zhang *et al.*, 2009; Yang *et al.*, 2012).

Numerous methods can be taken to conserve this vital resource. Because the causes of soil erosion differ from one area to the next, different measures must be implemented to combat the problem in each area. Some of the important methods consist

of contour bunding, contour tillage, and construction of check dams, terrace farming, checking the extension of gullies, stripcropping and shelter belts, afforestation, ban on shifting cultivation, controlled grazing, mixed cropping, mixed farming, rotation of crops and mulching.

The Kerala state of India has a unique land form between the Arabian Sea in the west and the western ghats in the east, with over 90% of the geographical area either in the midland or high land category. The average annual rainfall of Kerala is about 3000mm. With such unique geological characteristics having high lands and high rainfall, this state is much more prone to natural hazards such as landslide, flooding, tsunami, etc. Such natural hazards are directly or indirectly contributing factors to soil erosion and vice-versa.

The devastating floods of 2018 and its continued repeated spells in 2019 August have caused a serious threats by washing off the fertile top soils. A study on the 2018 Kerala floods on soil erosion has found that the soil erosion rates increased rapidly by 80% due to the 2018 floods. This high increase in soil erosion is not sustainable, given that shorter rainfall events in future can easily erode more soil and trigger landslides in the coming days. Chaliyar river basin in Malappuram district has experienced several landslide events during 2018 & 2019. Quantifying the rate of soil loss on a sub-watershed scale is important for the effective and sustainable management of watersheds. Therefore, the present study in the Kurumanpuzha sub-watershed of the Chaliyar river basin located in the Malappuram district envisages the estimation of soil loss with the existing land use and management practices in a sub-watershed scale and to identify erosion-prone areas, for implementation of best soil conservation and management practices leading to better policy decisions.

In the present case, the Revised Universal Soil Loss Equation (RUSLE) model is integrated within the Geographic Information System (GIS) to estimate the Soil loss from the Kurumanpuzha sub-watershed of the Chaliyar river basin.

The specific objectives are:

1. To collect the hydro morphological parameters influencing erosion in the watershed.

2. To estimate potential average annual soil loss from the watershed using RUSLE.
3. To map the spatial distribution of soil erosion hazards using GIS.
4. To suggest suitable soil conservation and management protocol for the watershed.

REVIEW OF LITERATURE

CHAPTER – II

REVIEW OF LITERATURE

Soil erosion is a serious environmental threat, estimation of erosion in a specified area is important to predict present/future soil losses and suggest conservation measures to control soil erosion. Though there are different methods and models to predict and evaluate soil erosion, the present study of soil loss in the Kurumanpuzha Sub-Watershed of the Chaliyar river basin is estimated by the Revised Universal Soil Loss Equation (RUSLE) model integrated within the Geographic Information System (GIS) to identify erosion-prone areas. This chapter reviews the earlier research done on the hydro morphological parameters, potential average annual soil loss computations and suggestions for suitable soil conservation and management protocols for the watersheds. Further mentioned topics are reviewed in this chapter, *i.e.*, soil erosion process factors affecting soil erosion, soil erosion estimation models, Revised Universal Soil Loss Equation (RUSLE), and presents an overview of the Geographic Information System (GIS) in which the Revised Universal Soil Loss Equation (RUSLE) model will be implemented for soil erosion modelling.

2.1 HYDRO GEOMORPHOLOGICAL CHARACTERISTICS OF WATERSHEDS

Sreedevi *et al.* (2009) studied morphometric analysis of a watershed in south India using SRTM Data and GIS. The drainage morphometry and its impact on the Wailapalli watershed's hydrology in South India have been investigated. They used SRTM data to create a DEM, aspect grid, slope maps, and GIS to evaluate morphometric parameters' linear, areal, and relief aspects. According to the results, the drainage basins were in the early stages of the fluvial geomorphic cycle. Lower-order streams dominate the basin. Rainfall impacts the development of stream segments in the basin area. The directing impact of thrusting and faulting is largely responsible for the basin's elongated shape. The subsurface Lithology of the basin has a significant impact on fluvial erosional processes. The relief ratio suggests that these watersheds have a high discharge capability but a low groundwater potential. These studies are extremely beneficial for watershed management and rainwater harvesting.

Muluneh and Mamo (2014) conducted a study on morphometric analysis of the Didessa river catchment in the Blue Nile basin, Western Ethiopia. The objective of this study was to see how morphometric parameters affected the basin's hydrology and morphology. The basin's Linear, areal, and relief aspects were estimated based on the software analysis results. The results showed that geospatial approaches and DEM data effectively extract stream networks, describe watershed morphology and compute basin morphometry indices. The results of this study gave suitable information for watershed planning and management.

Chandrashekhar *et al.* (2015) studied GIS-based morphometric analysis of two reservoir catchments of Arkavati river, Ramanagaram district, Karnataka. The Manchanabele reservoir catchment and the Nellegudde reservoir catchment of the Arkavati river system were subjected to a detailed morphometric investigation using ArcGIS. This study used high-resolution satellite data and GIS to better know the status of land forms and their processes, soil erosion, drainage management, and ground water potential conditions to plan and manage reservoir catchments more efficiently.

Son (2017) conducted a study on assessing morphometric characteristics of Chakrar watershed in Madhya Pradesh, India using geospatial techniques to delineate and calculate the morphometric characteristics. This analysis was carried out to provide a measurable assessment of the watershed and plan and manage water resources. Linear, Areal, and Relief are the three major features described in the study. According to research, the watershed has a well-developed basin network and a mature geomorphic stage. The Dd number denotes terrain with a moderate slope, sparse to dense vegetation, a higher infiltration rate, moderate surface runoff, and less dissection. The watershed and its sub-watersheds have an extended shape, making them less prone to flooding, erosion, and sediment movement. As a result, morphometric parameters provide useful information on the watershed's topography characteristics and hydrological behaviour. The combination of morphometric analysis with watershed assessments would be useful in preparing a drainage basin management plan.

Kabite and Gessesse (2018) conducted a study on hydro-geomorphological characterization of the Dhidhessa river basin, Ethiopia. For this study, the study's SRTM

DEM, geology, and hydrological maps were employed in an ArcGIS10.3 environment. According to the study, total stream length and stream order of the basin were high, while stream length ratio, bifurcation ratio and hydrologic storage coefficients were low. Likewise, the watershed was large, and stream frequency was coarse with an elongated basin shape. Drainage density was medium, and infiltration number was low, the overland flow was long and constant channel maintenance was high throughout the Dhidhessa river catchment.

2.2 FACTORS INFLUENCING SOIL EROSION

The term erosion is of Latin origin, derived from the verb *erodere*, which means "to eat away" (*rodere*, "to go away," "to excavate"). The term erosion was first used in geology to describe the formation of hollows by water and the wearing of solid material by river water (Zorn and Komac, 2011).

Soil erosion is a dynamic process that involves the detachment, transportation, and accumulation of productive surface soil across the earth's surface. Soil erosion is a global environmental issue that affects the productivity of all-natural ecosystems and agriculture, endangering the lives of most smallholder farmers (Gessesse *et al.*, 2015).

The erosion factors are the natural and anthropogenic conditions that have the greatest impact on the erosion process's rise, development, and results. (Dvorak and Novak, 1994). The most important erosion factors are the climatic, hydrological, topographic, soil, geological, and vegetation conditions, as well as the human society's economic, technical, and socioeconomic conditions. The section that follows summarises the effects of various factors on soil erosion.

Climatic Factors

Precipitation, temperature, and wind speed are the primary climatic factors influencing an area's erosion processes.

Precipitation

Soil erosion considerably depends on storm characteristics, mainly upon the

intensity of rainfall, rain droplet size, duration of rainfall and volume of rainfall in a particular area over some time.

Rainfall intensity is a critical factor in storm characteristics. The close relationship between water erosion and rainfall intensity is due to the following factors: (1) higher rainfall intensity results in higher rates of infiltration and excess runoff and a much greater transport of suspended sediment load. (Roose, 1986) and (2) In high-intensity storms, the impact of raindrops on the soil surface causes increased soil particle detachment. (Van Dijk *et al.*, 2002).

Parsons and Stone (2006) analysed the effect of storm patterns on runoff and erosion from three different soils with the same total rainfall kinetic energy in five different storm patterns on three soil types. They concluded that no steady difference in runoff was noticed across the three soil types, but significant differences in eroded sediment were observed. In particular, the constant-intensity storm caused 75% less erosion than the average value for the variable-intensity storms. The kinetic energy governs soil sealing and particle detachment. However, regardless of storm pattern effects, the effect of storms with the same average intensity on surface soil is different.

Mohamadi and Kavian (2015) studied the effects of rainfall patterns on runoff and soil erosion in field plots and showed that two forms of function could categorize the relationship between soil loss and rainfall intensities: (1) in low rainfall intensities, a linear function is fitted to soil loss-rainfall intensity, and (2) in high rainfall intensities nonlinear functions are fitted to soil loss-rainfall intensity. Further, ANOVA revealed no consistent differences in runoff coefficient across all storm patterns, but there were significant differences in the total runoff, soil loss, and sediment concentration. Storms with increasing rainfall intensity, in particular, resulted in a greater runoff, soil loss, and sediment concentration.

Atmospheric temperature

One of the important factors influencing soil properties is atmospheric temperature, which controls soil surface temperature. The temperature of the soil is determined by heat flux in the soil and heat interactions between the soil and the

atmosphere. (Elias *et al.*, 2004). It is also defined as a function of the soil's internal energy. Temperature affects the top organic layer of soil; a constant difference in water temperature and solar radiation results in soil thawing, which causes serious erosion.

Al-Ali *et al.* (2016) studied the effect of fine-grained soil temperature on soil erodability. The test was conducted by holding all other parameters which influence fine-grained soil erodability as constant except the temperature. Soil temperature was successfully brought to and maintained at temperatures above room temperature, while varying soil temperature with a custom heating system. Comparing test results from room temperature and heated samples revealed a direct relationship. Soil samples tested at temperatures higher than room temperature exhibited more erosion than soil samples tested at room temperature.

Wind

The wind is another climatic factor that affects soil erosion. Wind also produces its effects on raindrops. Raindrops do not fall vertically due to wind speed and wind direction and usually hit in an inclined position over the surface of the soil, which in turn affects soil loss by water (Pedersen and Hasholt, 1995; Sharon and Arazi, 1997). Schmidt *et al.* (2017) studied wind effects on soil erosion by water and suggests that wind impact alters the spatial distribution of soil loss and deposition and changes the overall magnitude of soil loss within the catchment. The wind is a severe ecological and environmental problem worldwide, especially in arid and semiarid regions resulting in soil erosion (Borrelli *et al.*, 2016). It may even adversely affect sustainable ecological functions and social and economic development globally (UNCCD, 2017)

Topography

Topography is a factor that directly relates to and reflects soil loss spontaneously. Topographical factors such as slope shape, steepness, and length are of concern. The major topographical factor influencing soil erosion is the land slope. The slope has a complex geometrical shape in nature, having different characteristics, *viz.*, slope shape, slope length, slope steepness (depth).

Sabzevari and Talebi (2019) studied the effect of hill slope topography on soil erosion and sediment yield using the USLE model on nine different complex hill slopes having different plans (parallel, convergent and divergent) and different curvatures (concave, convex and straight). According to the results, the mean erosion of convex hill slopes was 1.43 times that of concave and 1.19 times that of straight slopes. The effect of curvature shape on erosion was much greater than the effect of plan shape. Convex divergent slopes experienced the most erosion, while divergent concave slopes experienced the least.

Sun *et al.* (2014) studied the effects of land use and topography on soil erosion and concluded that with the increase of slope gradient, soil erosion significantly amplified under the same land-use type. Though, significant differences in soil erosion responding to slope gradients differed from land uses. Inland uses with less vegetation cover, the effectiveness of slope gradients was increased. Further, the research reported that hilly terrain with steep slopes leads to serious erosion, which results in the formation of rills and gullies. Further steepness of the slope exerts high impacts on the soil erosion compared to other slope features.

Vegetation

In general terms, vegetation refers to the ground cover provided by plants, the importance of plant cover in controlling soil erosion by water is significant. Plant cover protects the soil against erosion by reducing water runoff and by increasing water infiltration into the soil matrix. Vegetation influences erosion primarily by intercepting rainfall and protecting the soil surface from the impact of raindrops and obstructing runoff velocity. Additionally, vegetation influences water and sediment fluxes by expanding soil-aggregate stability and cohesion and improving water infiltration. (Wainwright *et al.*, 2002).

Zheng Fen-Li (2006) conducted a study on vegetation changes on soil erosion on the Loess Plateau in Ziwuling secondary forest region, China. The study revealed that after the primary loss of vegetation, secondary vegetation was restored over the Loess Plateau in Ziwuling, which resulted in low soil erosion. Further, the impacts of rainfall

and slope gradient on soil erosion were small. Gully erosion was ceased, and sediment deposition occurred in gully channels, and the vegetation effect on soil erosion was predominant. Thereby, the effect of soil erosion was minimal after the secondary restoration of vegetation. Later the destruction, secondary forests of field plots (human activities) resulted in a great soil erosion increase and The findings revealed that accelerated erosion caused by vegetation destruction was a major contributor to soil degradation and eco-environmental deterioration in deforested areas.

Duran *et al.* (2007) studied soil-erosion and runoff prevention by plant covers and reported that the effects of vegetation on soil could be divided into two major related categories: bio-protection and bio-construction.

Zuazo and Pleguezuelo (2009) reported that the plant cover changes have a greater impact on runoff and erosion than canopy cover changes alone and a reduction in plant cover can intensify erosion processes that diminish soil quality.

A study assessing the effects of land use and topography on soil erosion on the Loess Plateau in China by Sun *et al.* (2014) concluded that Soil erosion was controlled by forest, shrub, and dense grassland cover, whereas cropping on slopes caused the most serious soil erosion. Over the decade, reductions in the rate of change of soil loss by erosion were greater in areas having lower vegetation cover, such as woodland and grassland with moderate and sparse density.

Soil erodibility

Soil is the unconsolidated mineral or organic material on the instantaneous surface of the earth. The soil properties greatly dominate soil erosion. Soils with faster infiltration rates, higher levels of organic matter and improved soil structure are more resistant to erosion.

The susceptibility of soil to erosion is determined by inherent soil properties such as texture, structure, soil organic matter content, clay minerals, exchangeable cations and water retention and transmission properties. Climatic proximity includes rain drop size distribution and intensity, rainfall amount and frequency, run-off volume and rate,

and wind velocity. (Kathiravelu *et al.*, 1993)

The study conducted by Romkens *et al.* (2002) on soil erosion under different rainfall intensities, surface roughness and soil water regimes ascertains that a sequence of rainstorms of decreasing intensity on an initially air-dry smooth surface caused more soil loss than a sequence of similar storms of increasing intensity. The surface roughness sediment concentration relationship was not monotonic. Further, initially smooth and uniform surfaces may yield less soil loss than initially rough surfaces; inter rill runoff occurs as spatially varying flow in which flow patterns determine the locations of rills.

Soil erodability is an estimation of the ability of soils to resist erosion based on the physical features of each soil. Texture, organic matter, and permeability are the principal characteristics affecting erodability. Intense tillage and cropping pattern reduces soil organic matter, which in turn contributes to an increase in soil erodability. Sand, sandy loam and loam-textured soils tend to be less erodible than silt, very fine sand and certain clay-textured soils. (Balasubramanian, 2017)

Vannoppen *et al.* (2017) conducted a study on whether plant root and soil characteristics affect the erosion with a prime objective to assess the erosion-reducing potential of both fibrous and tap roots in sandy soils. Plant roots were very effective at reducing concentrated flow erosion rates in sandy soils compared to root-free bare soils. Furthermore, the findings confirmed that fibrous roots outperformed thick tap roots. Furthermore, the results indicated that the effectiveness of plant roots in controlling concentrated flow erosion rates depended on apparent soil cohesion, with fine root systems being most effective in non-cohesive soils and tap root systems being most effective in cohesive soils.

Tillage practice

Tillage is defined as the mechanical management of the soil for crop production, which significantly impacts soil characteristics such as soil temperature, infiltration, and evapotranspiration processes. One of the purposes of tillage practice is to decrease the bulk density of the soil to ensure regular air and water movement through the soil profile (Lampurlanes and Martinez 2003). These activities can degrade soil and adversely

affect soil quality. Tillage has a negative impact by allowing material redistribution and disconnecting the most critical flowpaths. Tillage (particularly the ploughing direction in relation to the slope), crop selection, planting direction or orientation, and the amount, distribution, and intensity of rainfall or irrigation all impact water-induced soil erosion.

Basic *et al.* (2004) conducted a study on tillage and crop management effects on soil erosion in central Croatia over a plot of land using five different crops for five years and concluded that with no-tillage, soil erosion from the maize and soybean crops was reduced by 40 and 65% compared to ploughing up and down a slope. Even when the planting direction was still up and down the slope and ploughing and planting perpendicular to the predominant slope were effective soil conservation practices.

Mhazo *et al.* (2016) conducted a study of tillage impact on soil erosion by water reports with the main objective of study based on 282 runoff plots comparing NT (No-Tillage) and CT (conventional tillage) worldwide. This was done to quantify the benefits of applying NT on soil losses, runoff, and sediment concentration and to identify soil and environmental factors that could influence NT performance variability. Results from the study demonstrated that NT caused lower soil erosion relative to CT, and in overland flow, no differences were found, and it is supposed that NT adoption in temperate climatic zones is likely to yield a significant decline in soil loss compared to tropical regions.

2.3 Estimation of soil loss

This Section deals with estimating soil loss by different conventional methods and using soil loss estimation models.

Reconnaissance method

Reconnaissance methods estimate the amount of erosion in a given situation/plot of land. That approximation may be needed to examine the level of erosion, or it could be followed by more precise studies if required.

The main advantage of reconnaissance methods is that they are inexpensive and simple to implement, and many measurements can be taken. The results can be reliable

and representative. Other advantages include that reconnaissance methods can usually be operated by semi-skilled personnel and may require little maintenance.

This widely-used method involves driving a pin into the soil so that the top of the pin gives a datum from which changes in the soil surface level can be measured by which the extent of soil erosion is measured.

In another example of the pin, method, pins were installed at 1.5 m intervals on six selected profile lines in western Colorado as part of a long-term hydrology study in a 5 ha basin. All runoff and sediment from the basin are captured in a reservoir at the basin outlet, allowing estimates of loss from the pins to be compared to sediment measurements from reservoir surveys. A heavy storm with an assessed return period of 25 years occurred shortly after the pins were installed and the first reservoir survey, allowing an assessment of the storm's isolated effect. The average soil loss calculated from the pin results was 2.7 mm, compared to the estimated sediment held in the reservoir, corresponding to a depth loss of 2.3 mm. (Haveren *et al.*, 1987).

Runoff plots

Runoff plots are structures used to measure the overland flow and soil loss under controlled conditions. They are constructed directly in the field. For erosion/soil loss studies, these are cropped with the crops considered for the study. The soil type and slope of the plot can be changed as per requirement. The devices such as H-flumes, water level recorders and sediment samplers are a few important instruments required for a runoff plot systems.

For estimating the soil loss from the runoff plot, it is very important to collect the water sample from the collecting tank accurately, the water sample volume is taken out, and soil particles are filtered and oven-dried. Later dried soil mass is measured, and now the determined soil mass of a given volume of runoff is converted into kg/unit area.

Multi slot divisor and Coshocton wheel

When the situations come to meet a large volume of soil loss and runoff, installing a large plot is necessary. In some situations, a series of connected plots can

be implemented. Coarser particles are permitted to settle in the first tank. The outflow from the tank is directed to the multi-slot divisors containing numerous slots, out of which one slot is active at a time which permits passing known quantity of water to the lower tank. The sediment samples are collected, dried and weighed to predict the soil loss. Multi-slot divisors and storage tanks were set up to estimate the sediment deposition from small plots in New South Wales, Australia. The designed system has superior storage capacity. The sludge tank and storage tank capacity were 0.3 cm and 10 cm separately. The permissible flow rate was $0.009\text{m}^3 \text{ s}^{-1}$ (Moore and Wilson 1992). Due to the restricted capacity of such samplers, multi-slot divisors are limited to small watersheds.

The Coshocton wheel sampler is used to evaluate soil loss directly from the field. The known quantity of discharge from the measuring flume drops over a water wheel, taking a slight inclination from vertical. At each wheel rotation, the slot splits across the jet from the flume and reflects a small fraction of the flow (Moore and Wilson 1992). Karthick *et al.* 2017 installed a multi-slot divisor in the cotton field of Perumbalur district, Tamil Nadu, for the daily evaluation of soil erosion rate. Soil erosion under cotton crops grown on runoff plots was $10.86 \text{ t ha}^{-1} \text{ yr}^{-1}$.

2.3.1 SOIL LOSS ESTIMATION MODEL

Modelling is useful in estimating soil loss because it improves our understanding of the environment and estimates likely outcomes. Soil erosion models are useful for estimating soil loss and runoff rates from agricultural land, planning land-use strategies, calculating relative soil loss indices, and guiding government policy and strategy on soil and water conservation. Effective modelling can provide data on current erosion, trends, and scenario analysis. (Ganasri and Ramesh, 2016)

Igwe *et al.* (2017) reported that Soil erosion models are classified into threetypes based on the physical processes simulated by the model, the model algorithms used to describe these processes, and the model's data dependence: empirical or statistical models, conceptual models, and physics-based models.

Universal Soil Loss Equation (USLE)

The Universal Soil Loss Equation is an empirical model developed by Wischmeier and Smith (1978), which is widely used worldwide to assess and predict soil erosion due to water runoff. Originally, USLE was designed to estimate soil erosion in croplands or gently sloping topography. (Ganasri and Ramesh, 2016).

The model quantifies soil erosion as the product of factors representing rainfall and runoff erosivity (R), soil erodibility (K), slope length (L), slope steepness (S), cover and management practices (C), and supporting conservation practices (P)

The equation is:

$$A = R K L S C P$$

...(2.1)

Where erosion A is the estimated soil loss per unit area ($t\ ha^{-1}\ yr^{-1}$)

R = Rainfall-runoff erosivity factor ($MJ\ mm\ ha^{-1}\ h^{-1}\ yr^{-1}$)

K = Soil erodibility factor ($t\ h\ ha\ MJ^{-1}\ ha^{-1}\ mm^{-1}$)

L = Slope length factor (dimensionless)

S = Slope steepness factor (dimensionless)

C = Cover management factor (dimensionless)

P = Supporting practices factor (Wischmeier and Smith, 1978)

Though this method is widely used, it has few drawbacks as USLE is a totally empirical relationship for computing soil loss. Theoretically, it does not contain the actual soil erosion process. It does not compute gully erosion, does not compute sediment deposition and can only predict average annual soilloss.

Modified Universal Soil Loss Equation (MUSLE)

Williams and Berndt (1977) exposed that the estimate of stream sediment yield for individual storms could be simplified by using the USLE with its rainfall factor (R) replaced by a runoff factor and developed a modified model by analysing 778 storm-runoff events collected from 18 small watersheds, with areas varying from 15 to 1500 ha, slopes from 0.9 to 5.9% and slope lengths of 78.64 to 173.74 m

The MUSLE is given as follows (eq 2.2) :

$$S = 11.8(Q_{qp})^{0.56} K L S C P \quad \dots (2.2)$$

Where S is sediment yield in tonnes or tonne/ha, Q is a volume of runoff in m³, qp is the peak flow rate in m³ s⁻¹ and K, L, S, C, and P are, respectively, the soil erodibility (Mg MJ⁻¹ mm⁻¹), slope length (dimensionless), slope steepness, crop management and conservation practice factors similar to the USLE model. The dimensions are not similar on both sides of the equation since the model has been empirically and logically developed.

Arekhi *et al.* (2012) used the MUSLE model to estimate storm wise sediment yield in the Kengir watershed of Iyvan City, Ilam province, Iran. The runoff factor of MUSLE was calculated using the measured values of runoff and the peak rate of runoff at the drainage outlet. Sediment yield at the basin outlet was simulated for six storm events spread over the year 2000 and validated with the measured values. Results revealed a high coefficient of determination Value (0.99), showing that the MUSLE model sediment yield predictions are satisfactory for practical purposes.

MUSLE is a modification of the USLE. MUSLE is similar to USLE except for the energy component. The source of erosive energy for USLE is purely rainfall. MUSLE simulates erosion and sediment yield using storm-based runoff volumes and runoff peak flows (Alewell *et al.*, 2019).

RUSLE

The RUSLE soil erosion model calculates annual soil loss value and estimates soil erosion intensity in a catchment. The RUSLE model is built on the USLE erosion model structure, which was established by Wischmeier & Smith (1978). The first USLE, released in 1965, was widely used in the United States and a few other countries. Following that, its application revealed severe flaws in the conditions for which it was appropriate and the outcomes obtained. McCool and Renard (1990) proposed RUSLE that maintained the USLE's essential framework. RUSLE is especially useful for predicting soil erosion in agricultural, pasture, and forest sectors watersheds. Five

parameters are used in the RUSLE model to estimate soil loss. They are rainfall erosivity (R), soil erodability (K), slope length and steepness factor (LS), cover management factor (C) and conservation practice factor (P). Referring to RUSLE model, the relationship is expressed as:

$$A = R * K * LS * C * P \quad \dots(2.3)$$

LU *et al.* (2004) conducted research work to evaluate soil erosion risk in Brazilian Amazonia based on a combination of RUSLE, remote sensing, and GIS and found that it was an effective way to map the spatial distribution of soil erosion risks in a large area.

RUSLE PARAMETERS

RUSLE model works based on certain specific factors, such as Rainfall erosivity factor (R), Soil erodibility factor (K), Slope length and steepness factor (LS), Crop management factor (C) and conservation practice factor (P), which are either derived from RS data or through conventional data collection systems. The following section deals with specific parameters influencing the calculation of erosivity using the RUSLE model.

Rainfall erosivity factor (R)

The rainfall erosivity factor specifies the erosive force of a specific rainfall. It is an important parameter influencing soil erosion. Further, due to the lack of long rainfall intensity data, an empirical equation is needed to calculate R- factor.

Pluviograph data for at least 20 years are required to compute original rainfall erosivity for a given study area in (R)USLE (Renard *et al.*, 1996), but such data are not available for many places in the world. To overcome such difficulties, simplified approaches investigate correlations between rainfall erosivity and readily available rainfall parameters.

Wischmeier and Smith developed an empirical formula for calculating erosivity (R). Calculation of the R factor is a complex process and involves collecting 10,000

plot years of data. Wischmeier and Smith determined that the energy available to move sediment during a rainstorm is the product of the total amount of kinetic energy (E) contained within a storm and the intensity (I) of the storm.

The rainfall erosivity factor (R) is the average annual sum of individual storm erosion index values, EI_{30} , where E is the total storm Kinetic energy per unit area, and I_{30} is the maximum 30-minute rainfall intensity. To compute storm EI_{30} , continuous rainfall intensity data of 20 years of rainfall is recommended by Wischmeier and Smith (1978). This factor considers the characteristics of rainfall, such as the duration, intensity and amount of rainfall (Eq.2.4).

$$R = \sum (EI_{30}) \quad \dots(2.4)$$

After determining the E and I_{30} values for each storm throughout the record, they are multiplied by each other and then summed on per year basis. The average of these annual sums over the period shall be the R-factor

$$R = \frac{1}{n} \sum_{i=1}^n \left[\sum_{k=1}^m (E)(I_{30})^k \right] j \quad \dots(2.5)$$

Where k is the number of the individual storm up to m , the total number of storms in a year, j is the number of the years up to n , the total number of years over which data was collected, and E is the kinetic energy.

Another approach developed by Arnoldus (1980) is to take both annual precipitation and monthly rainfall amount into an account, and a new Index called Fournier Index was introduced for calculating the erosivity factor. The modified Fournier index (MFI) developed by Arnoldus (1980) for Morocco is the annual sum of the square of the monthly maximum amount of rainfall divided by annual precipitation.

$$MFI = \sum_{i=1}^{12} \left[\frac{P_i}{P} \right] \quad \dots (2.6)$$

Where P is annual precipitation (mm), and P_i is the monthly rainfall amount ($i = 1, \dots, 12$) from January to December.

Further, the Erosivity Factor R can be calculated as $R = mF + n$ (where m and n vary according to regions) (Ferro *et al.*, 1991). Correlation analysis can be used as an indirect measure to predict rainfall erosivity in areas where pluviograph data are not directly recorded (Morgan, 2009)

Eltaif *et al.* (2010) correlated the erosivity factor R values in both the USLE and RUSLE with annual rainfall amount or modified Fournier index (F_{mod}). Pluviometric data recorded at 18 weather stations covering North Jordan were taken to predict R values, according to the Eltaif *et al.* (2010)

$$R = 23.61 \times e^{(0.0048p)} \quad \dots (2.7)$$

Where p is the mean annual precipitation in mm and e is the Kinetic energy in $\text{MJ ha}^{-1} \text{mm}^{-1}$.

$$e = 0.119 + 0.0873 \log_{10} i$$

A power relationship was also found between R and F_{mod}

$$R = 14.616 \times e^{0.0734 F_{mod}}$$

Farhan *et al.* (2015) studied the Spatial assessment of soil erosion risk using RUSLE and GIS techniques in the Wadi Kerak drainage basin in southern Jordan. Rainfall data of 40 years average for five weather stations distributed over or close to the watershed were used to calculate R values based on the equation elaborated by Eltaif *et al.*, (2010).

Rahaman *et al.* (2015) calculated annual average soil loss by RUSLE modelling in the Kallar watershed, Tamil Nadu. The watershed has an area of about 1281.2 km^2 . Thirty years of monthly rainfall data (1980 to 2010) were collected from the Indian meteorological department for the estimation of the R factor. The rainfall erosivity value was obtained using the formula modified by Arnoldus (1980), as shown in Eq. (2.8)

$$R = \sum_{i=1}^{12} 17.35 \times \left(1.5 \frac{(P_i)^2}{P} \right) - 0.08188 \quad \dots(2.8)$$

Where R is the rainfall erosivity factor is expressed in the unit MJ mm ha⁻¹h⁻¹ y¹, annual rainfall, P, and monthly rainfall, P_i is in mm. The annual average erosivity value for the particular watershed was found in 251.5 to 798.5MJ mm ha⁻¹ h⁻¹ y⁻¹.

Libin *et al.* (2019) conducted a study on soil erosion in the Chittar Sub watershed of the Vamanapuram river basin, Kerala, based on RULSE methodology. Since E and I₃₀ data for the study area here not available, the R factor was calculated using the modified Fournier index developed by Arnolodus (1977). According to Arnolodus the F index is a good approximation of R. (F) is defined as in equation 2.9:

$$F = \sum_{i=1}^{12} \left[\frac{(P_i)^2}{P} \right] \quad \dots(2.9)$$

P_i is monthly rainfall (in mm) and P is the annual rainfall (in mm).

Kebede *et al.* (2021) conducted a study on a watershed level in the upper beles, Ethiopia, approached the study using the readily available regression equation to estimate R-factor from annual rainfall total P in mm

$$R = -8.12 + (0.562 \times P) \quad \text{Hurni (1985)} \quad \dots(2.10)$$

Furthermore, to reduce rainfall distribution variation and achieve a representative estimate of R-factor in the drainage basin, this study derived the mean R-factor map using mean annual rainfall derived from monthly rainfall data from different stations from 1992 to 2016.

Olorunfemi *et al.* (2020) conducted a GIS-based assessment of the potential soil erosion and flood hazard zones in Ekiti State, South western Nigeria, using RULSE and Hand models. In this study, the calculation of the R-factor was by way of the Rosee (1976) equation. R factor represents the effect of energy and intensity of rainfall. The product of event rainfall kinetic energy in MJ ha⁻¹ and the maximum rainfall intensity in 30 min in mm per hour for a long-term annual average (Wischmeier and Smith, 1978; Renard and Freimund, 1994), data were not available for the study area, hence

approached R by quantifying monthly rainfall data of 37 years (1981–2017) using an equation developed by Roose (1986).

$$R = 0.5 \times P \quad \dots (2.11)$$

R is the rainfall erosivity ($\text{MJ mm ha}^{-1} \text{h}^{-1} \text{yr}^{-1}$) and P represents the mean annual rainfall (mm).

Soil erodibility factor (K)

The soil erodibility factor “K” measures the intrinsic susceptibility of a given soil to erosion. The RUSLE calculates the K factor based on soil properties related to soil erodibility. K is a quantitative value determined experimentally by taking five soil parameters: texture, structure, organic matter content, and permeability. (Wischmeier *et al.*, 1971).

A relationship connecting soil texture, soil structure, percentage of organic matter content in soil and permeability was developed by (Wischmeier *et al.*, 1971) as follows:

$$K = [2.1 \times 10^{-4} (12 - M) [(Si + vfS)(100 - C)]^{1.14} + 3.25(A - 2) + 2.5(P - 3)] / 759 \quad \dots (2.12)$$

Where,

M = percentage of organic matter content in the soil.

Si = percentage composition of silt.

vfS = percentage composition of very fine sand.

C = percentage composition of clay.

A = Value corresponding to structural classes

P = Value corresponding to permeability classes

Specifically, soil erodibility is a function of particle size distribution, organic matter content, structure and permeability (Renard *et al.*, 1996). Prasannakumar *et al.* (2011) conducted a study of the Siruvani river watershed in Attapady valley, Kerala, for soil loss estimation by RUSLE equation and estimated K factor of Soils in the watershed by classifying the soil into 11 textural types and the corresponding K values

were identified from the table proposed by Stone and Hilborn (2000). The Soil erodibility factor is calculated using the soil type data. Collecting soil data and assigning K factor values from the field is costly and time-consuming. Hence the soil maps published by the National Bureau of Soil Survey and Land Use Planning (NBSS & LUP), Govt. of India, are used to calculate the K factor (Biswas,2012).

Kebede *et al.* (2021) modelled soil erosion using RUSLE and GIS in Ethiopia's upper beles. The lack of data on soil properties is a serious obstacle to soil erosion modelling. Due to the lack of soil properties in Ethiopia's condition, the K value was determined by soil colour type, which was suggested by Hurni (1985)

Table 2.1 Variation of K factor proposed concerning textural class and organic matter content.

Textural class	Organic Matter Content		
	Average	Less Than 2%	More Than 2%
Clay	0.22	0.24	0.21
Clay loam	0.30	0.33	0.28
Coarse sandy loam	0.07	-	0.07
Fine sand	0.08	0.09	0.06
Fine sandy loam	0.18	0.22	0.17
Heavy clay	0.17	0.19	0.15
Loam	0.30	0.34	0.26
Loamy fine sand	0.11	0.15	0.09
Loamy sand	0.04	0.05	0.04
Loamy very fine sand	0.39	0.44	0.25
Sand	0.02	0.03	0.01
Sandy clay loam	0.20	-	0.20
Sandy loam	0.13	0.14	0.12
Silt loam	0.38	0.41	0.37
Silty clay	0.26	0.27	0.26
Silty clay loam	0.32	0.35	0.30
Very fine sand	0.43	0.46	0.37
Very fine sandy loam	0.35	0.41	0.33

Topographical factor (LS)

LS-factor describes the effects of slope length and slope steepness on soil erosion. The topographic factor (LS) comprises two sub-factors: a slope gradient factor (S) and a slope-length factor (L).

As the slope length (L) increases, the total soil erosion loss per unit area increases due to the progressive accumulation of runoff in the downslope. As the slope steepness increases, soil erosion increases as the velocity and erosivity of runoff increases. The effect of slope steepness on soil erosion loss is greater than the effect of slope length. LS factor in RULSE is such that the ratio of soil loss experienced under the given length of slope and steepness to that of slope length of 72.6 feet and steepness of 9% (Wischmeier and Smith, 1978). The equation to calculate the topographical factor by connecting slope length and the land slope is as follows:

$$LS = L^{0.5} / 100 (0.76 + 0.53S + 0.076S^2) \quad \dots (2.13)$$

Where L = slope length in ft and S = land slope in %

They further derived and proposed equation to calculate slope steepness as follows:

$$S = (65.41 \times \sin^2\theta) + (4.56 \times \sin\theta) + 0.065 \dots (2.16) \quad \dots (2.14)$$

Where θ represents slope angle in degrees.

The following equation adopted from Mitasova *et al.* (1996) was used to calculate the LS factor:

$$LS(r) = (m+1) \times [A(r)/a_0]^m \times [\sin b(r)/b_0]^n \quad \dots (2.15)$$

Where, A(r) upslope contributing area per unit contour width, b(r) slope; m = 0.6; n = 1.3 are parameters, $a_0 = 72.6$ ft is the slope length, $b_0 = 0.09 = 9\% = 5.16^\circ$ is the slope of the standard USLE plot.

Farhan *et al.* (2013) estimated the LS factor of the Wadi Kerak catchment to the southeast of the Dead Sea, east of the Lisan Peninsula. The Digital Elevation Model

(DEM) was drawn with a 20 m contour interval from 1:50,000 topographic sheets. Mitasova equation was employed to derive the LS factor.

Terranova *et al.* (2009) studied soil erosion risk scenarios in the Mediterranean environment in Calabria. The LS factor was determined based on the Mitasova equation.

Prasanakumar *et al.* (2011) derived a combined LS factor for the watershed through ArcInfo ArcGIS spatial analyst extension. Using ArcGIS spatial analyst plus and arc hydro extension, the flow accumulation and slope steepness were calculated from the DEM. The below equation was applied to a DEM of cell size, 20 m².

$$LS = (\text{flow accumulation} \times \text{cell size} / 22.13)^{0.4} \times (\sin \text{slope} / 0.0896)^{1.3} \dots (2.16)$$

(Moore and Burch, 1986)

Where flow accumulation denotes the collected upslope contributing area for a given cell, LS = combined slope length and slope steepness factor, cell size = size of the grid cell (for this study, 20 m) and sin slope = slope degree value in sin.

A Study conducted at Karst Basin of Southwest China by Hao *et al.* (2017) for soil loss estimation has determined the LS-factor from the DEM data through ArcGIS spatial analysis tool. The L-factor was generated by the formulation proposed by Wischmeier and Smith.

$$L = \frac{\lambda}{22.13} \dots (2.17)$$

Where λ is the slope length (m); $\lambda = Fa \times \text{Cell size}$

Where Fa is flow accumulation representing the accumulative upslope area that drains into a given cell, Cell size is the grid size of DEM is an exponent dependent on the value of the slope angle: 0.5 for slope $\geq 2.86^\circ$, 0.4 for slopes of $1.72-2.85^\circ$, 0.3 for slopes of $0.57-1.72^\circ$, and 0.2 for slopes $< 0.57^\circ$; Further, the S-factor was evaluated by two approaches based on slope angle. On slope angle $< 10^\circ$, the approach of McCool *et al.* (1989) was used. On slope angle $> 10^\circ$, the approach of Liu *et al.* (1994) was used.

The constituent was calculated in different scenarios:

$$S=10.8 \times \sin\theta + 0.03, \theta < 5^\circ \quad S=16.8 \times \sin\theta - 0.50, 5^\circ \leq \theta < 10^\circ$$

$$S=21.91 \times \sin\theta - 0.96, \theta \geq 10^\circ; \text{ Where } \theta \text{ is the angle of slope in degrees.}$$

Cover management factor (C)

The C-factor value is defined as soil loss from cropped land to the corresponding loss from clean-tilled, continuous fallow land (Wischmeier and Smith 1978). The cover management factor quantifies the impact of plants, crop sequence, and other cover surfaces on soil loss.

Like the other RUSLE factors, the C value is a ratio comparing the existing surface conditions at a site to the unit's standard conditions. RUSLE uses a sub factor method to compute soil loss ratios (SLR), SLR are the ratios of soil loss at any given time in the cover management sequence to soil loss from the standard condition, and sub factors used to compute a soil loss ratio value are prior land use, canopy cover, surface cover, surface roughness, and soil moisture. There are two C factor options in RUSLE, a time-invariant option and a time-variant option (Toy *et al.*, 1999).

The outdated method for spatial estimation of the C factor is assigning values to land cover classes using classified remotely sensed images of study areas. Different researchers have developed many methods to estimate C using normalized difference vegetation index (NDVI) for soil loss assessment with USLE/RUSLE.

Markose and Jayappa (2016) studied soil loss estimation in the Kali River basin, Karnataka. C value was determined using Normalized Differential Vegetation Index (NDVI) values for soil loss assessment with RUSLE. The NDVI, one of the vegetation indices, measures the amount of green vegetation. The spectral reflectance difference between Near Infrared (NIR) and red is used to calculate NDVI.

The formula can be expressed as follows:

$$NDVI = \frac{(NIR-RED)}{(NIR+RED)} \quad \dots (2.18)$$

Prasannakumar *et al.* (2011) and Markose *et al.* (2016), in their respective case studies, have approached C factor estimation by the normalized difference vegetation index (NDVI), an indicator of the vegetation vigour and health, by application of the following equation to generate the C factor value image for the study area respectively.

$$C = \exp\left[-\alpha \frac{NDVI}{\beta-NDVI}\right] \quad \dots(2.19)$$

Where α and β are dimensionless parameters that determine the shape of the curve relating to NDVI and the C factor.

Practice factor (P)

It is also known as the support practice factor. P factor is obtained by finding the ratio of soil loss under given conservation practices to that from up and down the slope. The number of conservation practices are implemented depending on the slope of the field. Contour cropping, terracing, bunding, mulching, and strip cropping are some commonly used conservation practices in agricultural lands. The value of P factor varies from 0 to 1 (Wischmeier and Smith, 1978) as given in Table 2.1 and varies according to the land slope. The lands with no conservation practices convey higher P values as one (Shiono *et al.*, 2002).

Singh (1994) suggested P factor for different percentage ranges of land slopes as 0.6, 0.5, 0.5, 0.6, 0.7, 0.8 and 0.9 respectively for the slopes 1-3, 3-6, 6-9, 9-13, 13-17, 17-21 and 21-25. Biswas (2012) implemented this method in the Upper Kangsabati catchment. To ignore this factor in soil erosion estimation, Kouli *et al.* (2009) assigned the P factor as one throughout the watershed. Sahu *et al.*, (2017) allocated 0.28 and 1 for paddy fields and fields other than paddy, respectively.

Table 2.2 P factor values for different land slope % (Wischmeier and Smith,1978)

Land use	Land slope %	P factor
Agriculture	0-5	0.10
	5-10	0.12
	10-20	0.14
	20-30	0.19
	30-50	0.25
	50-100	0.33
	>100	0.35
Other land uses		1

Alexakis *et al.* (2013) prepared a land-use map of Yialias river at Potamia catchment area in the broader region of Nicosia – Cyprus from the two GeoEye-1 satellite images to formulate a P factor map. The value of 1 was given for the areas with no support practices. On the other hand, the terrace areas measured to be less prone to erosion were given a value of 0.55.

2.4 RUSLE MODEL STUDIES IN GIS ENVIRONMENT

Shiono *et al.* (2002) used the RUSLE model paired with GIS to estimate soil erosion and geographical distribution under present farming conditions in a pilot research area of around 3,009 ha in Japan, which included 11544 crop fields. The average soil erosion rate was projected to be $10.5 \text{ t ha}^{-1} \text{ yr}^{-1}$ over the period 1994- 1999. The USLE's K-factor was calculated based on a sedimentation assessment carried out in a small catchment area. The LS factor was calculated using field data, and a DEM created with ERDAS. According to the study, the soil erosion rate calculated with RUSLE and GIS proved extremely valuable for soil conservation planning.

Srinivas *et al.* (2002) used the Revised Universal Soil Loss Equation in a GIS context to perform a soil erosion research in Nagpur district, Maharashtra, with the goal of prioritising the study region for soil conservation and delineating eligible conservation units. Separately, an isoerodent map, a topographic factor map, and a land

cover-land use map were created, and nine conservation units were defined using a multi-criteria over landing method.

Pandey *et al.* (2007) used USLE to identify important erosion-prone locations in the Karson watershed in Hazaribagh, Jharkhand state, covering an area of 27.93 km² by utilising geographic information systems software, image processing software (ERDAS IMAGINE 8.4) provided spatial input data to the erosion model, while the USLE was used to predict the spatial distribution of the sediment yield on-grid basis. The study region was divided into 200×200 grid cells, and the average yearly rainfall was calculated for each cell of the watershed to identify the critical erosion-prone areas for prioritization. The model and data gathered from the stream gauging station placed at the watershed's exit were used to predict sediment yields, and the results were compared. Finally, the RUSLE model was proven to be accurate. Karso's yearly average soil erosion of 3.66 t ha⁻¹ of the watershed was estimated. In this study, efforts were made to use remote sensing data to generate land use/land cover data, which are required to generate USLE factors. Thus, remote sensing and geographic information systems (GIS) can play an important role in generating parameters from remote areas of watersheds/river basins for sediment yield modelling and watershed management.

Zhou *et al.* (2008) conducted a study in the Upper Min river (UMR) watershed, Sichuan, China, to determine the impact of plant cover on soil erosion. The RUSLE technique was used on a pixel-by-pixel basis to assess the soil erosion rate. A multivariate geostatistic co-kriging model was used to create a raster map of the R factor. By combining Landsat ETM+ scenes and field data with appropriate settings, vegetation cover was calculated using the k-NN algorithm. The root mean square errors and significance of biases at the pixel were used to select the best parameters. A regression programme was used to estimate the accuracy of vegetation cover using Landsat ETM+ bands, field data, and the Normalized Difference Vegetation Index (NDVI).

Sharma (2010) identified a probable soil erosion risk region in the Maithon reservoir basin from 1988 to 2004. Using terrain and vegetation indices, the study region was divided into four soil erosion potential classes using three terrain indices: Topographic Wetness Index (TWI), Stream Power Index (SPI), and vegetation indices

like the Normalized Difference Vegetation Index (NDVI). Finally, the RUSLE model validated the resulting erosion potential map, which demonstrated good agreement with the results. The results revealed a significant change in the watershed's erosion potential and a progressive transition from lower to greater erosion potential classes.

Vemu and Pinnamaneni (2011) conducted a study on estimating spatial patterns of soil erosion using remote sensing and GIS for the Indravati catchment. R, K, LS, C, and P, all thematic layers were prepared, analysed, and eventually, generated a 200m x 200m pixel erosion risk map inside the GIS environment to determine the spatial distribution of soil loss. The yearly average soil erosion rate was calculated using 20 year-average rainfall data. The annual soil loss ($t\ ha^{-1}\ y^{-1}$) was computed using the yearly R factor and assumed that the remaining variables were constant. All 424 sub-watersheds in the Indravathi basin were prioritised according to the intensity of soil loss for soil conservation purposes. 18 t/ha/y was the predicted average erosion, and sediment yield near the catchment outlet was 22.3 MTyr⁻¹. The predicted values were tested with the observed data.

Prasannakumar *et al.* (2012) assessed the soil erosion risk inside a small hilly sub-watershed in the Pamba river basin by the RUSLE model. The used climatic and terrain factors in the soil loss estimation equation were calculated from rainfall data obtained from Indian Meteorological Department (IMD), soil texture map of soil survey organization, Kerala, satellite image and Survey of India (SOI) toposheets. In the area, vegetation parameters were calculated from IRS-P6 LISS-III digital data with a resolution of 23.5 m for the year 2008. Rainfall erosivity factors were calculated by using Wischmeier and Smith (1978) and modified by Arnoldus (1980). The average soil erosion rate for the study area ranges from 0 to 17.73 t h⁻¹ y⁻¹. The expected average annual soil erosion of the Pamba sub-watershed was assembled into distinct classes, and the spatial distribution of each class was obtained. From the spatial patterns, it was seen that the severe and high level of soil erosion risk zones are disseminated in the grassland, deciduous forest areas, and degraded plantation, and they need immediate attention to conservation.

Abdel Rahman *et al.* (2016) used GIS and remote sensing techniques to evaluate

the soil fertility condition in physically degraded land in the Chamarajanagar district of Karnataka, India. He used satellite data to conduct a qualitative assessment of soil eroded areas and discovered that the data allowed for better-eroded area definition. Soil erosion was observed in the tone of none, modest to very severe, using the visual interpretation of IRS data and the field survey method, but it was moderate to high by the RUSLE approach. He also discovered that compaction affects the soil's water penetration capability, promoting erosion. Soil loss increases as the slope increases up to a certain point. According to this study, the majority of the watershed falls under the moderate erosion class.

Ganasri and Ramesh (2016) evaluated soil erosion by the RUSLE model by RS and GIS in the Nethravathi river basin. The assessed rainfall erosivity, soil erodibility, and topographic and crop management factors range from 2948.16 to 4711.4 MJ mm⁻¹ ha⁻¹ hr⁻¹ y⁻¹, 0.10 to 0.44 t ha⁻¹.MJ⁻¹.mm⁻¹, 0 to 92,774 and 0 to 0.63 respectively. The study concluded that the empirical soil erosion models are comparatively simple and easy to interpret physically, require minimal resources and can be driven out with readily available inputs. They found that the annual average soil loss obtained using the RUSLE model is about 473,339 t yr⁻¹ in the Nethravathi Basin. By considering the impact of the increase in an agricultural area on soil erosion, they decided that as increased agricultural area increases erosion risk due to the agricultural practices. By implementing Weighted Index Overlay (WIO) method, they categorised the area into different zones based on the probability of soil erosion which finally helped to suggest proper protection measures.

Hao *et al.* (2017) used remote sensing and GIS to simulate the soil erosion rate in a Karst catchment using the empirical and current RUSLE model. Each RUSLE factor was estimated in the context of GIS. The potential soil erosion map was created to identify regions experiencing severe soil erosion. The erosion rate was categorised into six categories: 1) minimal, 2) low, 3) medium, 4) high, 5) very high, and 6) extremely high.. The erosion rate was estimated to be 30.24 Mg ha⁻¹ yr⁻¹ from the 1980s through the 2000s, which was in line with the results produced through in-situ measurements from 1980 to 2009.

Ostovari *et al.* (2017) predicted the soil erosion in Dembecha Watershed, Northwestern Ethiopia. The study was made to investigate the effect of the K factor on soil erosion. ArcGIS was used to run the model. The K factor was derived in two ways. One was by using an erosion plot and the other by adopting the USLE method. The results indicated that the average measured K factor was two times lower than the expected K by USLE K-factor. The annual average of soil erosion obtained by the RUSLE model was $5.70 \text{ t h}^{-1} \text{ yr}^{-1}$ and equivalent to measured soil loss, but it was two times higher than the measured K values. The spatial distribution of soil erosion in most areas came under a very low category (73.6%). Furthermore, this study proves that the RUSLE model, integrated with GIS and RS, is useful for determining soil erosion loss and identifying high-risk areas.

Singh and Panda (2017) conducted a study on Grid-cell-based soil erosion potential for identifying critical erosion-prone areas using RUSLE, GIS and remote sensing: A case study in the Kapgari watershed, India. The R factor was calculated using the study area's annual rainfall data. The K value was calculated using soil survey data, and the LS factor was estimated using the DEM of the study area. The C and P factors were calculated using the land use map. After generating all parameters, the soil erosion was estimated using the USLE model and a spatial information analysis approach. The average annual soil loss in the study area was discovered to be $8 \text{ t ha}^{-1} \text{ yr}^{-1}$, with only 4% of the total area subject to extreme erosion risk. This study also demonstrates that the USLE soil erosion model combined with GIS is an efficient tool for handling large data needed for soil loss studies in the catchment area.

Thomas *et al.* (2017b) projected soil erosion rate on Pambar river basin area extend of 289 km^2 by integrating the RUSLE and TLSD function with GIS software. The RUSLE R factor was obtained from the Fournier index allowing the monthly rainfall data gathered from the meteorological stations of the river basin. K factor was estimated from the field sample by the Wischmeier and Smith (1978) formula. DEM for the study area was built from the topographic map obtained from the SOI. For the computation of P, the LULC map was prepared from the LISS III image with ground truth verification. The projected mean gross and net erosion rate was $11.7 \text{ t ha}^{-1} \text{ yr}^{-1}$.

Zare *et al.* (2017) projected the effects of land-use changes on soil erosion in the Kasilian drainage basin of Iran for the year 2030, and they considered the patterns in the years 1981 to 2011. The RUSLE model, along with GIS, was adopted to predict soil erosion. The land use map was obtained from the satellite imageries through maximum probability classification and regulated by running the Markov chain model by IDRISI Kilimanjaro software. There was a 45% increase in the obtained result of mean erosion potential from the estimated erosion $104.52 \text{ t ha}^{-1} \text{ yr}^{-1}$ by 2030. Moreover, the results showed the land-use change in the forest areas. They found that the main key factor for the change of erosion was converting forest to urban and settlement areas.

Kayet *et al.* (2018) estimated the soil erosion rate for Kiruburu and Meghahatuburu mining areas, Jharkhand, using the RUSLE model. The GIS environment and remote sensing data were used to run the model for the study. To generate the LULC map and LS factor, Landsat image of the year 2015 and CARTOSAT DEM of the year, 2014 were used. Rainfall data were obtained from the IMD. Using field images and DGPS survey data, verification was done. The C factor classification was done by a support vector machine algorithm. Karl Pearson coefficient of correlation was used to predict the correlation of soil erosion with the slope and altitude, which was seen to be 0.998 in both cases. $40 \text{ t ha}^{-1} \text{ yr}^{-1}$ area was the estimated soil erosion.

Teng *et al.* (2018) calculated and obtained soil loss rate in the Tibetan Plateau using by RUSLE and CMIP models. By integration of RUSLE with ArcGIS, soil erosion for the years 2002 to 2016 was estimated. R factor was obtained from TRMM data and the daily rainfall data from the rain gauge stations. To combine these two rainfall data collocated co krigging option was used. The epic model was adopted to calculate the K factor, which mainly considers soil organic carbon content and texture of the soil. The prediction of soil erosion in 2050 was made using multi linear regression model and CMIP model. The estimated rate of erosion was 2.76 t ha^{-1} .

Thomas *et al.* (2018) estimated soil erosion rate in Pambar River Basin northern part of Idukki district Kerala, using the RUSLE model and transport limited sediment delivery function. The transport limited accumulation function accumulates the

sediment flux subject to the rule that the sediment outflow from any cell is the minimum of the sediment in flow into the cell plus the soil erosion in the cell. This study calculated the TLSD function using the Terrain Analysis using Digital Elevation Models (TauDEM) toolbox in ArcGIS. The R factor was calculated using the modified Fournier Index (F). A continuous raster surface of the K factor was generated by spatial interpolation in ArcGIS. The LS factor was calculated in ArcGIS using the ArcHydro tool. NDVI value was calculated from the LISS III images, and a C factor map was obtained for the watershed. The value one was given as the P-value for forest and open scrub. Mean gross soil loss was $14.36 \text{ t ha}^{-1} \text{ yr}^{-1}$ in the study location, of which 25% was obtained as the net soil erosion rate. The erosion was reclassified into six classes based on the net erosion values, which ranged from slight to very severe. The LS and C factors compared to other parameters.

Zerihun *et al.* (2018) have done a soil erosion assessment in the Dembecha district, Ethiopia, by integrating the RUSLE model with the GIS environment. Rainfall data were obtained from the eight rain gauge stations situated in the study area, and the interpolation technique was used throughout the watershed in ArcGIS. The different types of soils have different k values, such as 0.25 for Alisols, 0.15 for vertisols and 0.3 for fluvisols. The DEM having a resolution of 30m was used for LS factor calculation. Erosion severity classes were prepared based on the quantitative assessment of soil erosion. The mean annual rate of soil erosion obtained was $49 \text{ t ha}^{-1} \text{ yr}^{-1}$. The double mass curve verified the model's reliability plotted using rainfall data.

Barman *et al.* (2020) studied the soil erosion assessment using the RUSLE model and geo-spatial technology for the upper Tuirial river basin, Mizoram. Because of its delicate geomorphic-pedological properties, shifting agriculture is prone to significant soil loss and land degradation. The Study's goal was to find annual soil erosion in the upper Tuirial river basin by RUSLE, which took into account various factors those were rainfall erosivity factor (R), soil erodibility factor (K), slope length (L), slope steepness factor (S), crop management factor (C), and practice management factor (P), for the preparation of crop management factor map, Sentinel 2A multispectral satellite data of 10 m spatial resolution was used and thus land use and land cover map of the study area was prepared. Their findings showed that the river basin has an average

annual soil loss of 115.4 Mg ha⁻¹ yr⁻¹ and an annual sediment loss of 6.161 million Mg yr⁻¹. Approximately one-fourth (24.78%) of the overall basin might be classified as a very high to very severe soil erosion-prone area needing rapid conservation measures. Besides, the erosional activities were perceived as directly proportional to the slope values in the basin.

2.5 PLANNING OF CONSERVATION MEASURES

Sadgir *et al.* (2006) conducted a study on sustainable watershed development by refilled continuous contour trenching technology. They found that a continuous contour trench helped to boost water levels in surrounding areas/dug wells and tube wells, resulting in increased agricultural productivity due to a shift in cropping pattern from food grains to cash crops. This would help soil stabilisation by preventing soil erosion and increasing grass coverage. Trenching with a consistent contour was better for tree development than any other method. Refilled continuous contour trenching (RCCT) technology provided a cost-effective and efficient solution for long-term watershed development.

Amdihun *et al.* (2014) conducted a study on suitability and scenario modelling to support soil and water conservation interventions in Ethiopia's Blue Nile basin. They concluded that soil loss in the Blue Nile basin could be decreased by up to 600 million tonnes in 5-10 years by properly adopting soil and water conservation strategies. According to net soil loss reduction calculations, conservation measures executed successfully in only four administrative zones (out of 17) may potentially cut up to 60% of overall soil loss in the drainage basin.

Krios and Schulte (2014) studied GIS-based multi-criteria evaluation to identify potential sites for soil and water conservation techniques in the Ronquillo watershed, northern Peru. The different thematic layers of drainage lines, stream orders, soil characteristics, slope, and LULC were integrated into the GIS for finding suitable areas for different soil and water conservation interventions, and the set of criteria was used in three steps. The slope of the topographical area and the vertical and horizontal intervals required between structures were utilised as preliminary criteria to determine the specific locations and number of structures. Due to the limited availability of runoff

potential in semi-arid rain-fed regions, these locations were further optimised based on the runoff available after storage by existing structures. After current storage, an average year's runoff volume from the entire watershed is expected to be 8,70,000 m³. Twenty-five rockfill dams, 74 agricultural ponds, and five check dams were deemed suitable. The suitability of the selected sites with the collected ground truth was tested using Google Earth.

Pandey *et al.* (2016) conducted a study on RS and GIS to identify of suitable sites for soil and water conservation structures. They provided a conceptual framework for developing a site suitability map for soil and water conservation by combining thematic maps such as drainage, land use, and soil texture. Using remote sensing data in conjunction with auxiliary data and sufficient ground truth information, it was possible to identify and delineate numerous geomorphologic features that serve as direct or indirect indicators for selecting a suitable structure. The recommended soil conservation strategies are converting wasteland to cropland and installing check dams across 2nd and 3rd order streams. Percolation tanks are suggested for increasing the irrigated area and groundwater recharge in the study area. In particular, RS and GIS tools provide a suitable platform for convergent analysis and decision-making on large-scale multidisciplinary data in the watershed development plan.

Patode *et al.* (2017) carried out a study on the planning of conservation measures for watershed management and development by adopting geospatial technology for Patur Watershed in Akola, Maharashtra District. They prepared thematic maps from various data sets like IRS- LISS-III multispectral images, SRTM data with 30 m resolution and Survey of India toposheet. Concerning RS and GIS data compared to ground truth, various conservation measures/structures such as recharge wells, farm ponds, CNB, gully plug, CCT, and other soil and water conservation structures have been suggested for groundwater recharge development, environmental management and by considering the slope of the watershed. Different in-situ soil and water conservation measures should be adopted along with the construction of temporary, semi-permanent and permanent structures on the drainage lines for harvesting the runoff from rainwater.

Krishna *et al.* (2018) carried out study on planning of soil and water conservation

measures in a micro-watershed at College of Agricultural Engineering (CAE) Campus Madakasira. For spatial data analysis, QGIS software was used. Google earth map was used for the delineation of watershed. The area slope was measured using Abneys level and the land use was mapped using GPS. In order to provide drainage line treatments, a longitudinal and cross-section of streams were created using a dumpy level and staff. Surfer software was used to create the contour map. In the QGIS environment, maps of land use, slope, and proposed engineering structures were generated.

MATERIALS AND METHODS

CHAPTER - III

MATERIALS AND METHODS

This chapter explains the details of the study area, methods used in studying different aspects of the watershed, soil erosion models and procedures adopted for the study. Different factors necessary for the estimation of soil erosion were identified and detailed. Revised Universal Soil Loss Equation (RUSLE) was selected for the study, and the use of this model in assessing soil erosion was evaluated. Satellite imageries were used as the basic data to define the effect of vegetation on spatial variation of soil erosion in the sub-watershed.

3.1 DESCRIPTION OF THE STUDY AREA

Kurumanpuzha sub-watershed of the Chaliyar river basin was selected for the study. Kurumanpuzha is a tributary of Kerala's Chaliyar river. This river originates in the forests that border the districts of Malappuram and Kozhikode in Nilambur taluk. It connects with the Chaliyar near Vadapuram, just before Kuthirappuzha meets the Chaliyar. The total length of the Kurumanpuzha river is 19.084 km. The sub-watershed is located at almost the central portion of the Chaliyar river basin. The total catchment area of the watershed is 2911 sq km, out of which the Kurumanpuzha sub watershed occupies 3.55% of the area with an aerial extent of 103.6 km².

3.1.1 Location

The selected watershed is located in between the latitude-longitude range of 11⁰17'30" North, 76⁰7'0" East and 11⁰23'0" North, 76⁰12'30" East. Fig.3.1 shows the location map of the watershed. The maximum elevation of the sub-watershed is 2226 m. The topography of the Chaliyar river basin comprises 3 natural divisions; lowland, midland and highland. The low land stretches along the sea coast, the midland in the centre and the highland region towards the east and northeastern parts, rich with evergreen forests, ravines, hills and dales, rivers and brooks. The Kurumanpuzha watershed has undulating topography starting from the hilltops covered with thick forests and gradually slopes down to the valleys and the small hills, before finally

ending on the sandy flat of luxuriant coconut groves and palm-fringed coasts in the west.

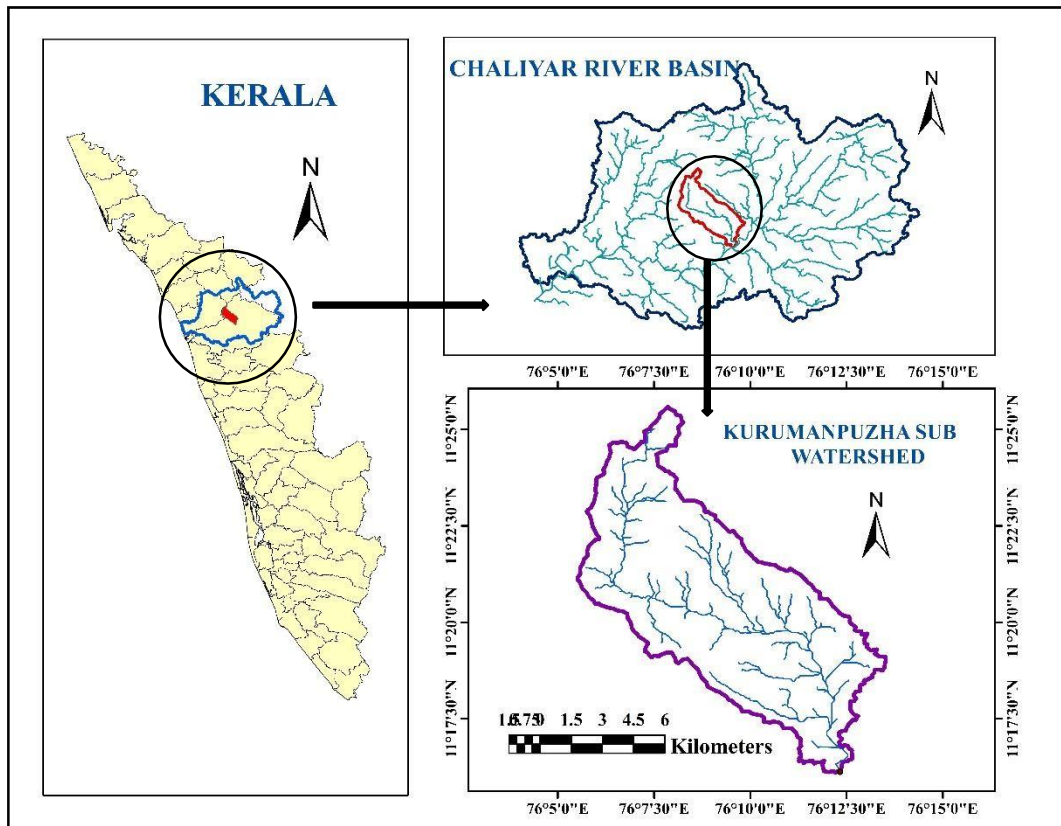


Fig. 3.1. Location map of Kurumanpuzha sub watershed

3.1.2 Climate

The sub-basin falls under a humid tropical climatic areas. The rainfall distribution in the catchment varies seasonally with hot summers and heavy monsoon rainfall. On average, the basin receives 2419 mm of rain per year. In Kerala, the main rainy seasons are the southwest (June-September) and northeast (October-November) monsoons. Major thunderstorm activity characterizes the pre-monsoon months (March-May), while minimal cloudiness and rainfall characterize the winter months (December-February) (Ananthakrishnan *et al.*, 1979). The southwest monsoon (June-September) accounts for the majority of the average annual rainfall (> 300 cm), while the northeast monsoon (October- January) accounts for approximately 50-60 cm. The

mean annual temperature of the watershed is 27.8°C.

3.1.3 Soil

The soils of this watershed are very deep, moderately well-drained, moderately fine-textured, pale brown to dark yellowish-brown medium acidic soils. These soils are located on very gently sloping to moderately sloping natural levees along the river course with slope gradients ranging from 1 to 3 %. These soils are formed as a result of the deposition of alluvial materials by the rivers. Laterite can be found in abundance in the midlands. It is economically exploited for construction purposes, and hundreds of quarries cutting laterite stone known as Vettukallu are in operation, employing thousands. Granite building stone is another important mineral in terms of economic importance.

3.1.4 Cultivation

Crops cultivated in the study area are diverse due to variations in climate, rainfall, slope, terrain, and soil type. Crop selection is based on physiological characteristics and efficient use of the particular location by farmers. Mainly the watershed consists of agricultural plantation crops like Coconut, Rubber, Arecanut, Cashew and Pepper. Major field crops like paddy and horticultural crops like Banana are also cultivated.

3.2 SOFTWARE AND TOOLS USED

The software and tools that were used in the study are listed below. The research was done on a GIS platform.

3.2.1 ArcGIS 10.2

Environmental System Research Institute developed ArcGIS, a proprietary Geographic Information System (GIS) software. The investigation was conducted using ArcGIS 10.2. This version was launched in the year 2013. Because GIS software can manage geographical data (including both spatial and attribute data), it is more popular than other information systems. It is possible and simple to perform geographical and

temporal data analysis in a GIS system. ArcHydro, spatial analyzer, and hydrological tools were employed in addition to the built-in GIS capabilities. The hydrology tool was used to define the boundaries of the specific area.

3.2.2 ERDAS IMAGINE

ERDAS imagine is an easy to use, raster-based software designed specifically to extract information from images. It is the most powerful package for derived information, supporting multiple workflows, including Data conversion, colour balancing, mosaicking and compression, land-cover mapping, terrain categorization, etc. A geographic imagine toolset extends the capabilities of IMAGINE essentials by adding more precise mapping, with sensor model support and geospatial data processing functions. In this study the ERDAS imagine software was mainly used to prepare the land use map.

3.3 COLLECTION OF REMOTE SENSING DATA

RS is the pre-processing of data obtained by getting details about object areas on an earth line that is positioned at a distance without actually coming into touch with the object. Today, we define satellite remote sensing as the use of satellite-borne sensors to observe, measure, and record the electromagnetic radiation reflected or transmitted by the earth and its condition for the purpose of data analysis and extraction.

For the study area, satellite images, digital elevation models, soil data (including structural and textural features), and rainfall data (daily and monthly rainfall amounts) were gathered. The essential data sources used in this investigation are listed below.

3.3.1 USGS Earth Explorer

The Earth Explorer is used to download satellite images to develop the study area's land use land cover (LULC) map. Imageries from many satellites such as ISRO Resourcesat, Landsat, Sentinel, RADAR, and others are available through USGS Earth Explorer. It is a user interface system that allows users to search for online data using interactive and query features. The system allows users to specify search criteria such as the location's coordinates, a predefined area, a shapefile, and the needed data range.

It also can change the cloud in addition to these criteria.

3.3.2 Bhuvan

The Bhuvan, an Indian Geo-platform developed by ISRO, was used to download CartoSat-DEM satellite imageries with a resolution of 30 metres. The downloaded image was used to delineate the watershed boundary. To fix the entire research region, two tiles of imageries were necessary. Images with the least amount of cloud cover were chosen. In ArcGIS, the downloaded images were pan-sharpened.

3.4 WATERSHED DELINEATION

3.4.1 Fill DEM

To avoid the discontinuous flow problem when water is trapped in a cell surrounded by cells of a higher rise, the elevation values were first revised by filling the sinks in grids. This was accomplished in ArcGIS by using the Fill tool in the Hydrology section of the Spatial Analyst tool function. The presence of sinks may lead to an incorrect flow direction raster. The elevation ranges of the watershed were identified after the DEM was filled. Flow direction and accumulation must be processed when this method is finished.

3.4.2 Flow direction

The flow direction map was created using the filled DEM. For the most part, the Flow direction tool takes a terrain surface and recognises each cell's down-slope direction. The water flow direction on the surface from one cell to one of the eight nearby cells is shown in this network. This was accomplished using the Flow direction tool in the hydrology portion of the spatial analyst tool function in ARCGIS.

3.4.3 Flow accumulation

A cell number represents the direction of the water. Cells with an unclear flow direction will simply receive flow and not contribute to any downstream flow. The Flow accumulation tool determines how much surface flow accumulates in each cell. Stream or river channels are commonly found in cells with high accumulation values.

It also recognises local topographic highs, or areas of zero flow accumulation, such as mountain peaks and ridge lines, using the flow accumulation tool in the hydrology section of the spatial analyst tool function in ArcGIS.

3.5.5 Delineation of watershed

The watershed boundary was digitally demarcated using the ArcGIS Hydrology tool. In the ArcGIS window, the DEM of the study region (resolution 30 m) was loaded. Expanding the spatial analyst tool in the main window yielded the hydrology tool. The hydrology tool created the fill sink raster, flow direction raster, flow accumulation raster, and watershed raster was all created throughout the delineation process. To create the fill sink raster, the DEM of the study region was used as the input raster, which will help prevent the defects of the chosen DEM. The fill sink raster was chosen to create the flow direction raster, which shows the flow direction. A flow direction raster was used to construct a flow accumulation raster. Finally, the flow accumulation raster was used to create a watershed raster. The created watershed raster was converted to a polygon using a conversion tool. The polygon feature matching the research location was taken from the acquired polygon features, clipped out, and stored as a shapefile for further activities.

3.4.4 Aspect

Aspect refers to the slope orientation in relation to the north. This is used to indicate the direction of the streamflow. In creating an output slope raster, the aspect indicates the downslope direction from one cell to neighbouring cells. The aspect values of the output raster will be measured in the compass direction. In other words, from N-NE-E-SE-S-SW-W-NW to N-NE-E-SE-S-SW-W-NW (0-360 degrees in a clockwise direction). Arrows will indicate the aspect on the slope. The aspect map was created in ArcGIS from the slope map created from the DEM.

3.5.5 Slope map

The slope is an important parameter in determining the catchment's morphometric characteristics. This represents the topographical structures with a

degree of inclination about a horizontal plane surface. We can also get the slope grid by using the Arc toolbar. To create a slope grid using Arc Toolbox, select Terrain pre-3D analyst tool-raster surface - Slope. Confirm that the input is dem_clip, and the output will be a slope grid with the default name (Slope). The number of classes and percentage of a class interval of slope can be changed in properties (use properties->symbology).

3.5.6 Preparation of land use the land cover map

The 2020 satellite image for the Kurumanpuzha watershed was obtained from Landsat 8 data sets. Landsat data sets can be found from the United States Geological Survey (USGS) Earth Explorer online portal. The Landsat 8 OLI data set consists of nine spectral bands with a spatial resolution of 30 metres. These data sets were used in the creation of the LULC map. The data that was downloaded was in the Geo tiff file format. Each image band displays intensity values for a single wavelength. Images with cloud cover and unwanted shade significantly reduce classification accuracy. As a result, high-quality, cloud-free scenes were used in this study. March is the best month for single image estimation (Alexandridis *et al.*, 2015). The unsupervised classification was done based on the image processing in ERDAS IMAGINE 2015 software. Image pre-processing includes image rectification, layer stacking, image enhancement, and extraction before classification. The number of unsupervised classes was set to 150. The classes are automatically clustered by the unsupervised classification. Aerial imageries, google imageries, and ground truth data were also utilized to confirm the areas while preparing the training sites needed to prepare the land use map, as shown in Fig.4.6.

3.5 HYDRO GEOMORPHOLOGICAL PARAMETERS OF THE WATERSHED

A systematic description of watersheds' geometry and stream channel system is known as hydro geomorphologic characterisation. The following elements of measurements are required for the watershed's geometry and stream channel network: (1) linear aspect, (2) areal aspect and (3) relief aspect of the channel and contributing ground slants. The first two types of estimation were planimetric (that is, properties were treated as though they were projected onto a horizontal datum plane), whereas the third kind examined the vertical inequalities of drainage basin morphologies. Horton's (1945) technique for scientific ordering of channels reflected the quantitative analysis

of channel systems.

Strahler (1952) proposed a modification to Horton's ordering system because of its simplicity and greater flexibility from subjective decisions. The following geomorphological parameters of a watershed's stream network are necessary to analyse the watershed's hydrologic behaviour so that resource planning and management can be done sequentially after prioritisation.

3.5.1 Linear aspects of the drainage network

The linear aspects *viz.*, stream number (N_u), stream order (U), average basin width (B), basin length (L), mean stream length (L_m), stream length (L_u), bifurcation ratio (R) and stream length ratios (R_L) were determined and their detailed procedure is explained in the following subheadings.

3.5.1.1 Stream order

It remains the classification system of stream/river rank in the watershed. Stream order provides a type of stream classification; for example, the smallest stream in the watershed has the lowest order. The largest stream, on the other hand, gets the highest order. The lowest order streams are tributaries or rivulets, while the highest order stream is the stream reaching the watershed outlet.

3.5.1.2 Stream number

According to the law of stream number, the number of stream segments of each order forms an inverse geometric sequence with the order number. expressed as Eq.3.1 as

$$N_u = R_b^{k-u} \quad \dots(3.1)$$

Where,

N_u =number of stream segments of order 'u'. The no streams of any order is fewer than for the next lower order, but more in numbers than the next higher order

R_b =Bifurcation ratio

3.5.1.3 Stream length

The length of a stream in a watershed indicates the characteristics of the drainage system and its contributing area. The stream length was determined by using the flow length tool in ArcGIS using the drainage map of the study area. The obtained channel length represents the true length, which is a little less due to projection on the horizontal plane.

3.5.1.4 Mean stream length

It demonstrates drainage network components and contributing surfaces (Strahler 1964). It was estimated by dividing the total length of order 'u' stream segments by the number of stream segments in the order.

3.5.1.5 Stream length ratio

It is the ratio of the total stream length of one stream segment to the next lower order of stream segment. An increasing trend in the stream length ratio from lower to higher-order indicates that they have reached their mature geomorphic stage. As a result, there is no classification for stream length ratio.

3.5.1.6 Bifurcation ratio (R_b)

It is the ratio of a specific number of stream segments to the number of streams in the next higher order. The R_b is a dimensionless property. R_b values are divided into two categories: low and high. Horton's law of stream numbers states that the number of streams of each successive order N in an order watershed forms an inverse geometric sequence with stream order I , which may be written as Eq. 3.2;

$$N_i = R_b^{k-I} \quad \dots(3.2)$$

Where R_b is the bifurcation ratio, which is given as

$$R_b = \frac{N_{i-1}}{N_i} \quad \dots(3.3)$$

Where,

N_{i-1} = Number of (i-1) order streams

N_i = Number of 'i' order streams

After putting it into a linear form by taking the logarithm of both sides, the value of R_b for the drainage area was calculated using the least-squares approach in the regression analysis of equation 3.2. Because of random variations in watershed shape, the bifurcation proportion won't be the same from one region to the next, but it will likely remain stable across the arrangement. In areas of steeply plunging rock strata where narrow valleys are constrained between edges, abnormally high bifurcation proportions may be usual. The bifurcation ratio was determined for the Kurumanpuzha watershed.

3.5.2 Areal aspects of the drainage network

3.5.2.1 Drainage area (A)

The drainage area is the watershed area that contributes runoff to a single, highest-order stream segment that leads to an outlet. ArcGIS 10.2 was used to measure the drainage area and perimeter along the drainage area for the watershed.

3.5.2.2 Form factor (R_f)

Horton (1932) used the phrase "form factor" to characterize the basin shape, which is defined as the ratio of basin area to basin length squared, expressed as Eq.3.4:

$$R_f = \frac{A}{L_b^2} \quad \dots(3.4)$$

Where,

R_f = Form factor, dimensionless

A = Area of the watershed, km²

L = Length of basin, km

A watershed with a greater form factor is more regular and has larger pinnacle streams for shorter-term storms, whereas a stretched watershed with a lower form factor has lower peak streams for longer-term storms. For around watershed, the form factor would almost certainly be less than 0.785.

Table 3.1 Indication of form factor value

Formfactor	Shape	Nature of Flow
0	Highly elongated	low peak for longerduration
0-0.06	Slightly elongated	peak flow for a longerduration
0.6-0.8	Perfectly circular	Moderate to high peak flow for a short duration
0.8-1.0	Circular	High peak flow for a short duration

3.5.2.3 Drainage Density(D_d)

The drainage density (D_d) reflects how close the channels are spaced (Horton, 1932). The seepage thickness is influenced by several factors, including the atmosphere, geography, invasion limit, flora and terrain of the watershed. The lower the drainage density, the more noticeable is the infiltration. Infiltration is lower, and surface overflow is higher in areas with higher drainage density. Low drainage density arises from ranges of relatively safe or permeable subsoil material, limited vegetation, and mountains. The proportion of the aggregate length of stream channels of all orders to the drainage area of the watershed is expressed as drainage density (Eq.3.5):

$$D_d = \frac{\sum_{i=1}^w \sum_{j=1}^{N_i} L_{ij}}{A} \quad \dots(3.5)$$

Where,

D_d = Drainage density, km km⁻²

L_{ij} = Total length of all order streams, km

A = Total area of the Drainage basin, km²

Table 3.2 Indication of drainage density values

Drainage density	Explanation
<1	Less
1-2	Moderate
2-3	High
3-4	Very high

3.5.2.4 Stream Frequency (F)

Stream frequency (F) is the number of streams per unit area *i.e.*, the total number of the streams of all orders to the watershed area(Eq.3.6). Lower the permeability of the land, higher the runoff, and vice versa

$$F = \frac{\sum_{i=1}^k N_u}{A_k} \quad \dots(3.6)$$

Where,

F = Stream frequency, km⁻¹

A_k = Basin area , km²

$\sum_{i=1}^k N_u$ = Total number of all order stream segments

Table 3.3 Indication of stream frequency value

Stream frequency	Number of streams km⁻²
Low	0-5
Moderate	5-10
Moderately high	10-15
High	15-20
Very high	20-25

3.5.2.5. Circulatory Ratio (R_c)

Miller (1953) coined the term "circulatory ratio" to describe the basic shape. The circularity ratio (R_c) is the ratio of the watershed's area to the area of a circle with the same perimeter as the watershed's perimeter. It denotes the dissecting stage in the research area. Its low, medium, and high values correspond to the watershed's young, mature, and old phases. The circulatory ratio approaches unity as the basin form approaches circular. The R_c is calculated using the watershed size and the perimeter p . It is written as follows (Eq.3.7):

$$R_c = \frac{4\Pi A}{P^2} \quad \dots(3.7)$$

Where,

R_c = Circularity ratio

P = Perimeter of watershed, km

A = Area of the watershed, km²

The R_c has no dimensions. R_c value varies between 0.6 and 0.7, according to Miller. For I and II order basins in homogeneous shales and dolomites. R_c value remains constant, indicating that tiny drainage basins with homogenous geologic materials have a tendency to maintain geometrical similarity.

3.5.2.6 Elongation Ratio

The proportion between the measurement of a circle of watershed range and the basin length is known as the elongation ratio (R_e) (Schumn, 1954). It generally ranges from 0.6 to 1.0 under various climatic and geologic conditions, and it approaches one as the basin's state approaches a circle. The average value is about 1 for low-relief locations and between 0.6 and 0.9 for areas with high slope and ground slope. A smaller form figure indicates more elongation of the drainage.

For prolonged storms, along watershed with a low form factor will complement the stream's peak. In terms of watershed area and length, the elongation ratio is calculated as equation 3.8 :

$$R_e = 1.128 \frac{A^{0.5}}{L} \quad \dots (3.8)$$

Where,

R_e = Elongation ratio , A = Basin area, km^2 , L = Basin length, km

3.5.2.7 Compactness Coefficient

The ratio between the perimeter of the watershed and the perimeter of the circle of the watershed area is known as the compactness coefficient (C_c). In terms of watershed perimeter P and area A , it is calculated as equation 3.9:

$$C_c = 0.28 \frac{P}{A^{0.5}} \quad \dots (3.9)$$

Where,

C_c = Compactness coefficient

P_b = Perimeter of the basin, km

A =Area of the drainage basin, km²

3.5.2.8 Drainage Texture (D_t)

It is a crucial measure that indicates the drainage line's relative spacing, which is greater in impermeable areas than in permeable areas. The texture ratio (R_t) is calculated by dividing the total number of stream segments of all orders (N) by the perimeter (p) of the watershed. Horton identified the land's infiltration capacity as the single most important factor influencing drainage texture. The formula for the calculation of texture ratio is given in equation 3.10

$$D_t = \frac{N_u}{P} \quad \dots(3.10)$$

Where,

D_t = Texture ratio, P =Basin perimeter, km

N_u =Number of u order streams

Table 3.4 Indication of drainage texture values

Drainage texture	Significant
<2	Very coarse
2-4	Coarse
4-6	Moderate
6-8	Fine
>8	Very fine

3.5.2.9 Length of overland flow (L_g)

Horton defined the mean length of overland flow as the distance between a location on the watershed divide and a point on the adjacent stream channel, projected to the level plane. He discovered that the length of an overland stream is one of the most important independent parameters determining the hydrologic and physiographic development of drainage basins. During the development of the drainage system, the mean length of overland flow is adapted to a size that is roughly comparable to half the reciprocal of the drainage density and is proportional to the size of the drainage basin. The faster the surface runoff from the streams, the shorter the length of overland flow. The formula for calculating the length of overland flow is given in equation 3.11:

$$L_g = \frac{1}{2D_d} \quad \dots(3.11)$$

Where,

L_g = Length of overland flow, km

D_d = Drainage density, km km⁻²

Table 3.5 Indication of the length of overland flow

Length of overland Flow	Significant
<0.4	More stream erosion
0.4-0.7	! Moderate stream erosion
>0.7	More sheet erosion

3.5.3 Relief aspects of drainage network

Maximum watershed relief (H), relative relief (R_R), ruggedness number (Rn), relief ratio (Rr), and time of concentration (T_c) were calculated, and the methodology is presented in the following subheadings below

3.5.3.1 Maximum watershed relief (*H*)

The variation in elevation between the basin outlet (discharge point) and the highest elevated point on the basin perimeter is the maximum watershed relief (*H*). The DEM was used to calculate the maximum watershed relief for the present research. It is given in meters.

3.5.3.2 Relative relief (*R_R*)

Relative relief is the ratio of maximum watershed relief to perimeter length. Relative relief measures the overall steepness of the basin from peak to outlet. It is calculated using the following expression (Eq.3.12):

$$R_R = 100 \frac{H}{L_p} \quad \dots(3.12)$$

Where,

R_R = Relative relief, % , H = Watershed relief, m

L_p = Length of the perimeter, m

3.5.3.3 Relief ratio (*R_r*)

The relief ratio is the maximum watershed relief divided by the maximum watershed length. The relief ratio increases the overall sharpness of the drainage basin and serves as an indicator of the intensity of the process operating as the watershed shape. It is calculated using the following equation

$$R_r = \frac{H}{L_b} \quad \dots(3.13)$$

Where,

R_r = Relief ratio

H = Maximum watershed relief, m , L_b = Maximum watershed length, km.

3.5.3.4 Ruggedness number (R_n)

Ruggedness number is defined as the product of maximum watershed relief and drainage density. A high ruggedness number occurs when there is a high relief region with a high stream density. It provides a sense of the overall roughness of a watershed. The formula for calculating the ruggedness number is given in the following equation

$$R_n = \frac{H D_d}{1000} \quad \dots (3.14)$$

Where,

R_n = Ruggedness number

H = Maximum watershed relief, m

D_d = Drainage density, km km⁻²

Table 3.6 Indication of Ruggedness number

Ruggedness Number	Prone to soil erosion
<0.18	Less
0.18-0.36	Moderately low
0.36-0.54	Moderate
0.54-0.79	Moderately high
>0.79	High

3.5.3.5 Time of concentration (T_c)

The time it takes for runoff water to travel from the watershed's most remote point to its outlet. It can be calculated using the formula below.

$$T_c = 0.0195L^{0.77}S^{-0.385} \quad \dots(3.1)$$

T_c = Time of concentration, min

S = Slope of catchment

L = Length of the watershed from remote point to an outlet, m. 3.5.4. Plotting of Hypsometric Curve (HC) and estimation of hypsometric integral

The hypsometric curve is drawn by plotting the relative area along the ordinate and relative relief beside abscissa. Which develops a relationship between the horizontal cross-sectional area of the watershed and its elevation in a dimensionless form. The relative area is calculated by dividing the area above a specific contour by the total area of the watershed encompassing the outlet.

The hypsometric integral (HI) was estimated for the watershed and calculated using the elevation relief ratio method proposed by (Pike *et al.*, 1971). The relationship is expressed below

$$E \approx HI_{si} = \frac{Elev_{mean} - Elev_{min}}{Elev_{max} - Elev_{min}} \quad \dots(3.16)$$

Where,

E is the elevation relief ratio equivalent to the hypsometric integral HI_{si} , $Elev_{(mean)}$ is the weighted mean elevation that is obtained with respect to the area of the watershed and elevation-area product valued from the identifiable contours of the delineated watershed.

$Elev_{min}$ = Minimum elevation within the watershed

$Elev_{max}$ = Maximum elevation within the watershed

Based on hypsometric integral (HI) values, the threshold limits suggested by Miller (1953), as mentioned below, were applied to decide the watershed stage.

Table 3.7 Indication of HI Values

Stage	HI value
Youthful	≥ 0.60
Equilibrium	0.35-0.60
Mature(old)	≤ 0.35

The advanced knowledge of the watershed geomorphology is important in flood control measures and engineering projects because these characteristics of river basins influence the runoff process and the occurrence of floods in these areas. Geomorphological parameters can be broadly classified into those that describe linear aspects of the watershed, areal aspects of the watershed, and relief aspects of the watershed. These aspects of the watershed were evaluated in this study to assess the nature of runoff and peak flow from the watershed and to study the susceptibility of the watershed to erosion. The findings were useful in determining the role of geomorphology in watershed runoff response and soil erosion.

3.6 ESTIMATION OF POTENTIAL SOIL EROSION

The region's climatic conditions, the proportion of estimated sand, silt, and clay particles in a specific soil, organic matter content, water permeability of the soil, slope length and slope of the field, are all factors that influence a field's vulnerability to soil erosion.

The key climatic elements are the energy related to falling raindrops, the quantity and severity of rainstorms, and the extra influence of wind on raindrop energy.

Unprotected soils can be particularly damaged by such storms, which are often accompanied by high-velocity winds. Surface, structural, and profile features are all factors that influence water erosion.

Soil erosion scientific expressions are used in PC models to refer to the linkages between various variables and procedures occurring on the landscape. Geology, meteorological elements, soil qualities, land use and land cover highlights are mostly included in these components. Most erosion models rely on USLE on the watershed in planes and channel components. The USLE is the most extensively used and acknowledged empirical soil erosion model. It was created for sheet and rill erosion based on a large test data collection from farming plots.

The USLE and its modifications are limited in their ability to estimate gross erosion and cannot process deposits along slopes, depressions, and valleys or in channels. Also, because erosion might occur merely along a streamline without the impact of the water stream itself, the USLE's coordination with the complex terrain is limited.

3.7 RUSLE

The Revised Universal Soil Loss Equation is used in most soil erosion model studies. McCool and Rendard (1990) proposed a RUSLE (Revised Universal Soil Loss Equation) that maintained the USLE's essential framework. RUSLE is especially useful for predicting soil erosion in agricultural, pasture, and forest sectors watersheds. Compared to USLE, the RUSLE is a software version of a considerably upgraded USLE.

In the present study, RUSLE model was used to calculate the soil loss in the study area. Further, the RUSLE model can calculate the yearly soil loss value and soil erosion intensity in a watershed. The spatial average soil loss of area is calculated using the following equation

$$A=R*K*LS*C*P \quad \dots(3.17)$$

Where,

A is the Computed spatial average soil loss per unit area ($t\ ha^{-1}\ yr^{-1}$)

R is the Rainfall erosivity factor ($MJ\ mm\ ha^{-1}\ h^{-1}\ yr^{-1}$),

K is the Soil erodibility factor ($ton\ h\ ha\ MJ^{-1}\ ha^{-1}\ mm^{-1}$)

LS is the Slope length, and steepness factor (dimensionless),

C is the Cover management factor (dimensionless)

P is the Conservation practice factor (dimensionless)

3.8 PREPARATION OF MAP LAYERS FOR RUSLE MODEL

3.8.1 Creation of R factor layer

The erosive power of particular rainfall or the energy of rainfall as the driving force behind soil erosion is rainfall erosivity. The RUSLE model's rainfall erosivity parameter was calculated by multiplying total storm energy by 30-minute rainfall intensity ($R = EI_{30}$) and was considered the appropriate method. Meanwhile, the study area lacks recording type rain gauge stations, and hence intensity data could not be drawn. So, monthly rainfall data for three stations, Karipur, Manjeri, and Nilambur, were collected from IMD, Pune, for the year 2000 to 2020. Further, the study area was influenced by only one rain gauge station at Nilambur, which is located near the outlet. This station data were used for further calculations (Table 3.8, Fig 3.2).

Table 3.8 Annual rainfall (mm) of Nilambur rain gauge station

Year	Annual rainfall (mm)	Year	Annual rainfall (mm)
2000	2606.1	2011	2160.5
2001	2169.9	2012	1432
2002	1707.7	2013	3093
2003	1927.5	2014	3156
2004	2297	2015	2306.4
2005	2900.6	2016	1409.6
2006	4389	2017	2280.6
2007	3838.5	2018	4413
2008	2145.3	2019	3267.8
2009	2385.8	2020	2081.6
2010	2178.9		

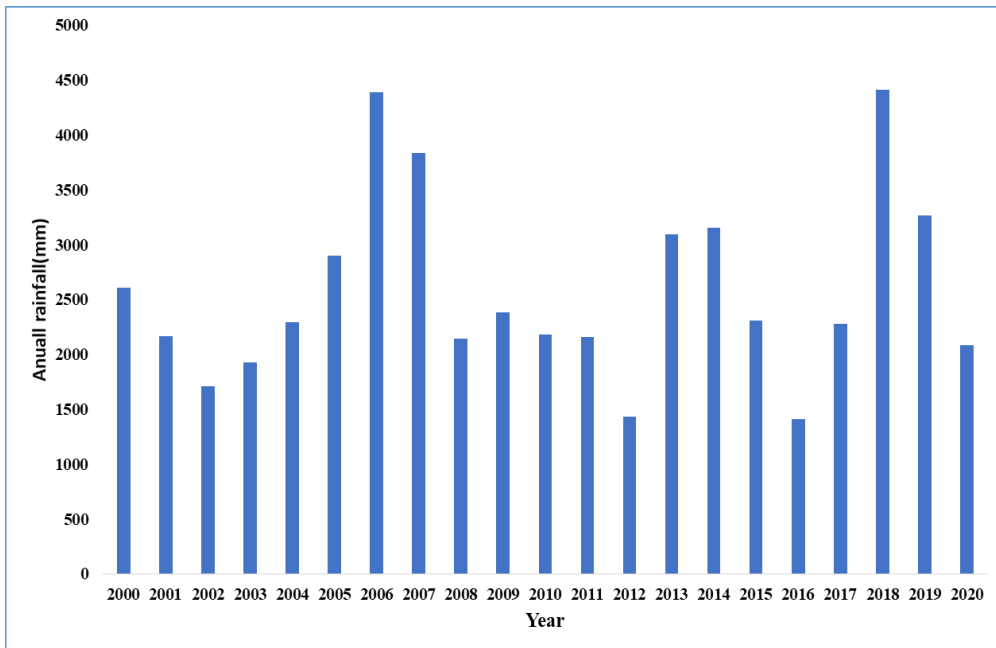


Fig. 3.2 Annual rainfall (mm) from 2000-2020

In the absence of hourly rainfall data, Fournier highlighted a directory in 1977 to characterise rain-fall aggressivity of the soil, which is known as FI.

$$\text{Fournier Index} = \frac{P_m^2}{P} \quad \dots(3.18)$$

where P_m denotes the maximum monthly rainfall depth (mm). Since Fournier's index does not consider the monthly rainfall distribution throughout the year, it does not always increase as the number of erosive rainfalls increases. To overcome this particular disadvantage, Arnoldus proposed the following modified Fournier index.

$$\text{Modified Fourier Index} = \sum_{i=1}^{12} \left(\frac{P_i^2}{P} \right) \quad \dots(3.19)$$

Where P_i is the rainfall depth in month i (mm) and P (mm) is the annual rainfall in a given location. Arnoldus demonstrated that MFI provides a good approximation of the R factor in regions where no high temporal resolution pluviographic statistics are available. The following relationship, recognised by Wischmeier and Smith (1978) and adapted by Arnoldus (1980), was used in the current study to calculate the R-factor.

$$R = \sum_{i=1}^{12} 1.735 \times 10^{(1.5 \log_{10} \frac{P_i^2}{P} - 0.08188)} \quad \dots(3.20)$$

Where R is the rain-fall erosivity factor ($\text{MJ mm ha}^{-1} \text{ h}^{-1} \text{ y}^{-1}$), P_i is rainfall depth in the month i (mm), and P (mm) is yearly precipitation in a given location.

3.8.2 Preparation of K factor layer

The erodibility factor, often known as the K factor, refers to the soil's susceptibility to eroding. The erodibility of the soil is influenced by elements such as soil structure, particle size distribution, organic matter content, permeability, and so on. The Department of Soil Survey and Soil Conservation, Kerala, provided the soil

association map of the Chaliyar river basin. The Chaliyar river basin soil map was geo referenced, and the study area map was clipped from the Chaliyar basin soil map and used to prepare the K factor layer. The original soil association map was provided with the description of each soil as a soft copy.

The description includes the following information: soil name, colour, depth of various horizons, taxonomic classes, drainage and permeability, vegetation details, land capability and land irritability class, soil fertility status, particle size distribution with percentage values for gravel, very coarse sand, coarse sand, fine sand, medium-coarse sand, very fine sand, silt, and clay.

The K factor was calculated for each series using the equation developed by Wischmeier and Smith, 1965; Renard *et al.* 1997 (Eq.3.21)

$$K = 1.2917\{(2.1 \times 10^{-4} M^{1.14} (12-a) + 3.25(b-2) + 2.5(c-3)\}/100\dots(3.21)$$

‘a’ represents the per cent of organic matter content in the soil, ‘b’ indicates value matching to structural classes, and ‘c’ indicates value relating to permeability class. In the equation $M = (\text{per cent of silt} + \text{per cent of very fine sand}) \times (100 - \text{per cent of clay})$.

The b value varies according to the following:

- 1 -indicates a very fine granular structure,
- 2 -indicates a fine granular structure,
- 3 -indicates a medium or coarse granular structure, and
- 4 -indicates a blocky, platy, or huge structure.

The following is a list of c value variations:

- 1 -indicates a fast permeability rate
- 2 -indicates a moderate to fast permeability rate
- 3 -indicates a moderate permeability rate
- 4 -indicates a slow to moderate permeability rate

- 5 -indicates a slow permeability rate
- 6 -indicates a very slow permeability rate

The series with the highest K factor was chosen from each soil association group. A nomograph for the USLE K factor was used to check the accuracy of the estimated K factor (Wischmeier and Smith,1978). Figure 3.3 shows the soil map of the Chaliyar basin that was utilized for the analysis and digitalization.

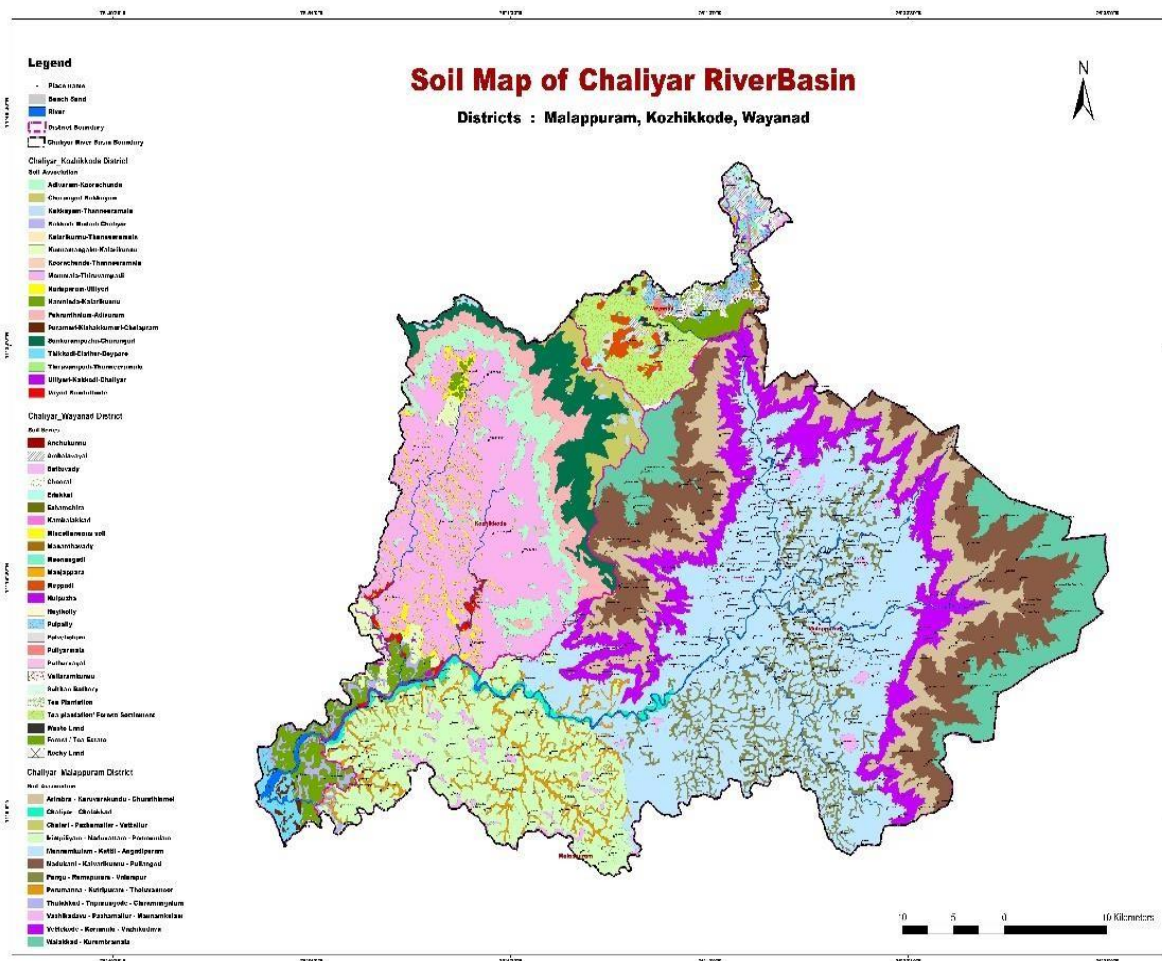


Fig. 3.3 Soil map of Chaliyar river basin

First, the map was scanned and georeferenced in the ArcGIS environment. The soil map for the study area was clipped out of the georeferenced soil map of the Chaliyar river basin using the 'Boundary' and digitized in ArcGIS using the editor tool. The

WGS_1984_UTM_43 N coordinate system was used to project.

The digitised map. In the attribute table, the K value for each series was added.

Finally, a K factor map was created for the area of study.

3.8.3 Creation of LS factor layer

The topographic characteristics, i.e., slope length (L) and slope steepness [S (gradient)], influence the total erosion in a watershed. CartoSat DEM imagery with 30m resolution was used to compute LS factor using the spatial analyst and hydrology toolkits in ArcGIS software, following the method described by Moore Burch (1986) and Mitasova *et al.* 1996. The precision of the factor depends on the resolution of the DEM.

$$LS = (\text{Flowaccumulation} * \text{Gridsize} / 22.13)^{0.5} (\sin[\text{Slope}] * 0.01745 / 0.0896)^{1.3} \dots (3.22)$$

Where, flow accumulation denotes the accumulated upslope contributing area for a given cell,

LS = combined slope length and slope steepness factor, Grid size = size of grid cell (for this study 30 m), and sin slope = slope degree value in sin.

The LS factor was calculated using the ArcHydro tool in ArcGIS using equation.3.22. The L and S factor maps were prepared separately and then combined to generate the final topographic factor map. The following procedural steps were followed to calculate slope length.

- The selected CartoSat DEM was uploaded in the ArcGIS window and converted to the projected coordinate system (WGS_1984_UTM_43_N) by the raster projection tool. The projected DEM was clipped to the study boundary and named 'Project_DEM'.
- The 'project_DEM' was loaded into the Arc window using the 'data management and terrain preprocessing' function in the Arc Hydro tool's terrain preprocessing. DEM modification was carried out by selecting fill sinks to ensure that water flowed continuously. "fill" was the term given to the filled hydro DEM.

- By selecting the flow direction option under terrain preprocessing, the 'fill' was utilised to generate a flow direction map, and the resulting map was designated 'flow direction.'
- A flow accumulation map called 'flowacc' was created from the flow direction map. The flow accumulation map is the input layer for the slope length map generation.

The slope steepness factor was calculated using the slope parameter in the spatial analyst tool. The input was 'Project DEM,' The map was created in both degrees and percentages by selecting options under the output measurement icon. Finally, the raster calculator function of map algebra was chosen under the spatial analyst tool, which uses equation (3.22) as an input function to determine the LS factor. The methods used to create the LS factor map are given in the flowchart (Fig.3.4). 'LS factor' was the name given to the prepared map. Figure 3.5 shows the raster calculator's user interface.

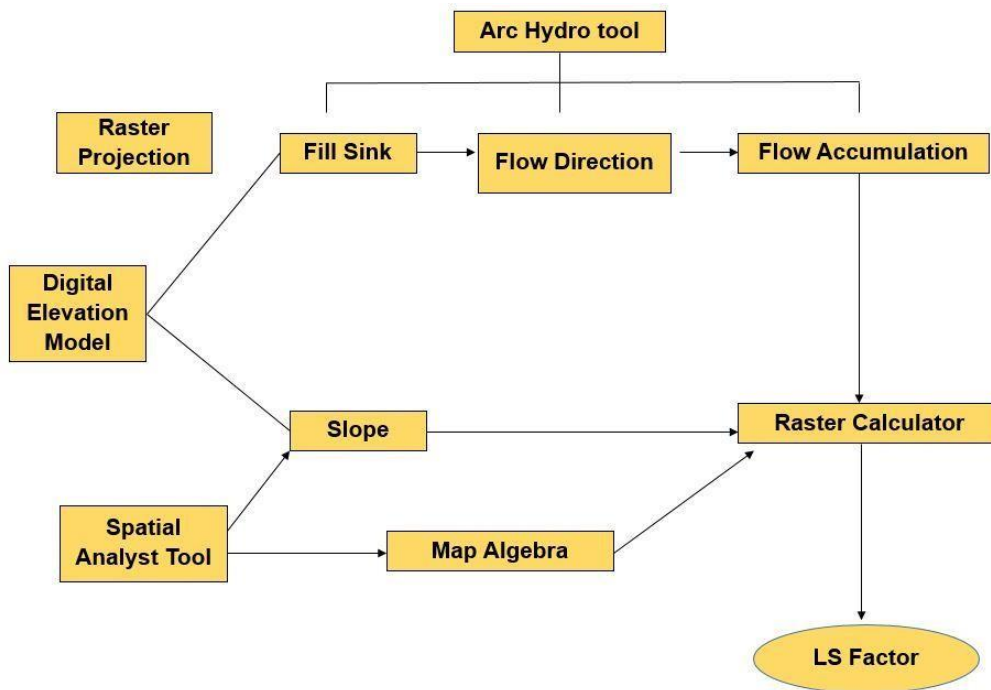


Fig.3.4 Flowchart for the estimation of the LS factor

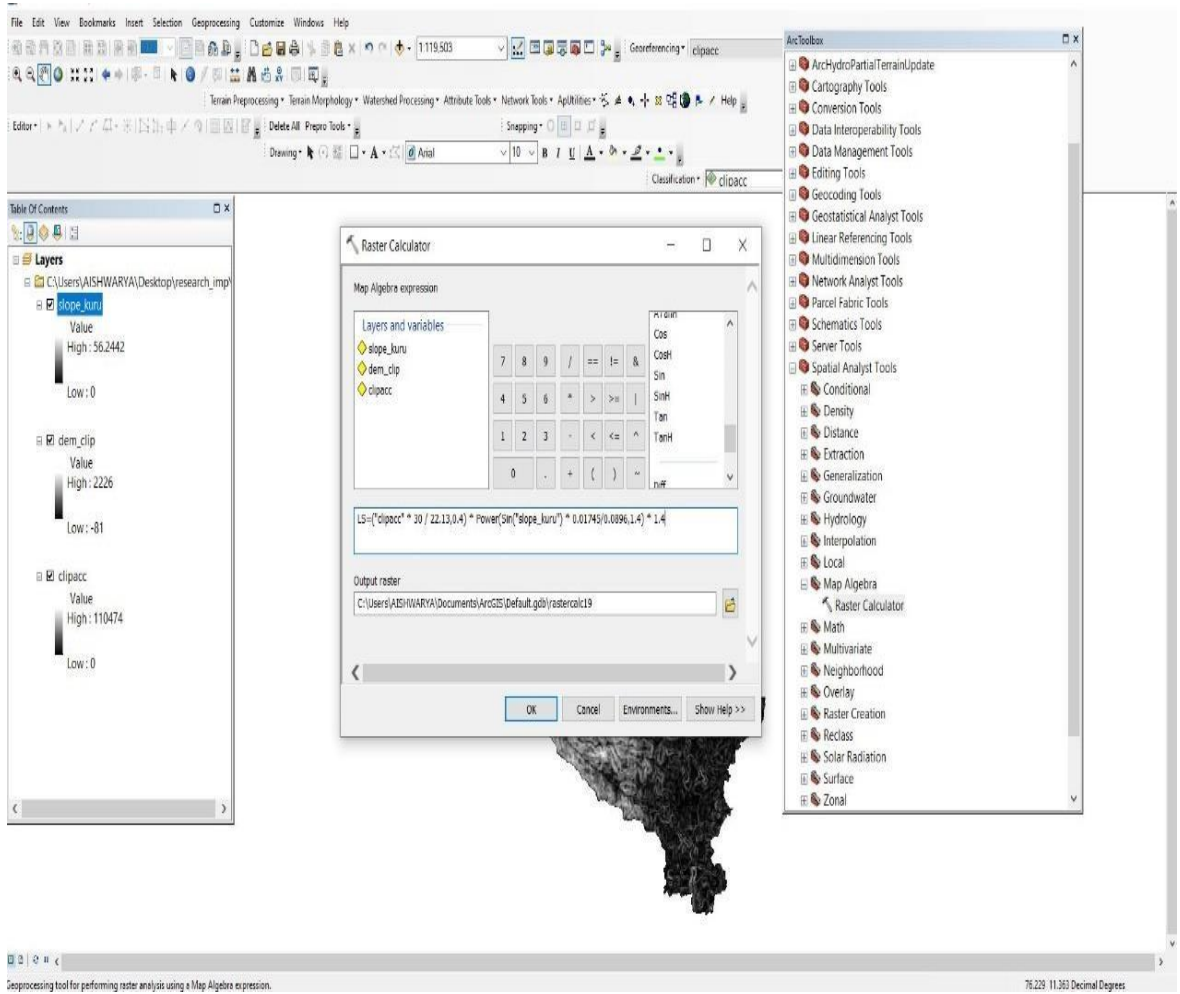


Fig. 3.5 ArcGIS interface for raster calculator

3.8.4 Creation of C factor layer

The cover management factor, often known as the C factor, is one of the most significant RUSLE parameters because effective control of the C factor can prevent soil erosion. The C factor is greatly influenced by the type of plant, its growth stage, and canopy cover. As a result, deriving the C factor from the relevant vegetation-related parameter should be highly accurate.

The most suitable and widely accepted approach for calculating the C factor from remote sensing data such as satellite images is NDVI (Kouli *et al.*, 2008). The red and near-infrared band reflectance values are needed for the calculation, and the relationship is given as follows (Eq.3.23)

$$NDVI = \frac{NIR - RED}{NIR + RED} \quad \dots(3.23)$$

The Landsat 8 satellite image of March 2020 downloaded from USGS Earth Explorer was taken for the NDVI calculation. NDVI map was obtained using ArcGIS by using the image analysis option (Fig.3.6). Out of seven bands in the satellite image, band 4 indicates red, and band 5 shows NIR.

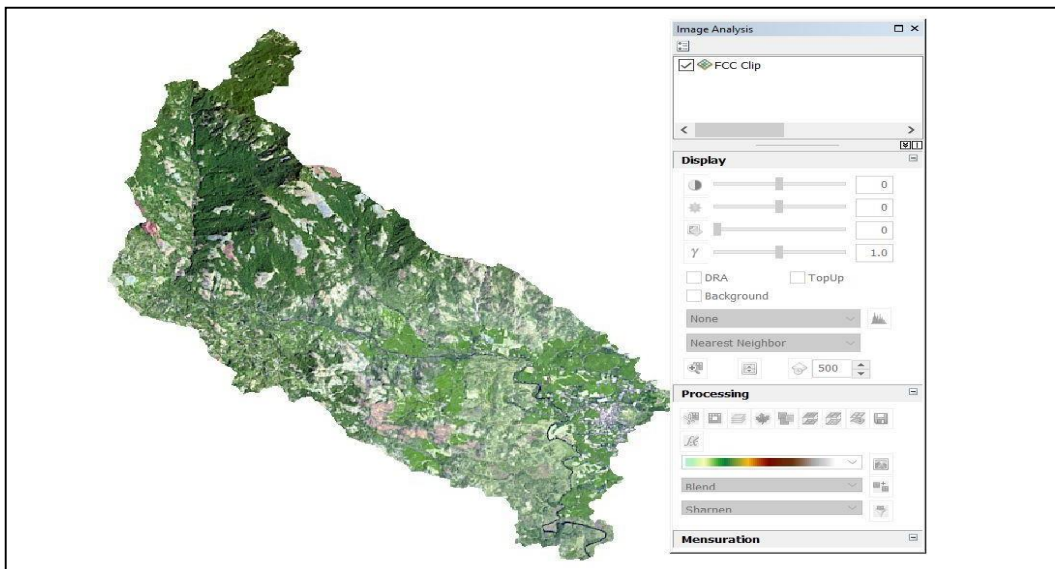


Fig.3.6 Image analysis tool with Landsat 8 image clipped for the study area

The C factor map was created by obtaining an NDVI map using the equation 3.24

$$C = EXP\left(\frac{-2NDVI}{1-NDVI}\right) \dots(3.24)$$

The calculation was done in ArcGIS 10.2 using a raster calculator. The prepared map was named as C Factor map.

3.8.5 Creation of P factor layer

The support practice factor (P-factor) is the soil erosion ratio with a specific support practice to the corresponding soil loss with up and downslope tillage. The P factor indicates the effect of various conservation and support practices being taken up in the study area for soil erosion. The various conservation measures help to decrease soil erosion by reducing the amount and rate of runoff water by influencing drainage patterns, runoff velocity, runoff concentration, and hydraulic pressures applied to the soil by runoff. Usually, conservation practices in the field is performed based on the slope and land use. In the present study, the P factor values given by Wischmeir and Smith(1978) on the basis of land use and field slope in percentage were used. The LULC map is required to use this method.

Table 3.9 P factor variation with land use and land slope %

LAND USE	LAND SLOPE,%	P FACTOR
Agriculture	0-5	0.10
	5-10	0.12
	10-20	0.14
	20-30	0.19
	30-50	0.25
	50-100	0.33
	>100	0.35
Other land uses		1.00

3.9 ESTIMATION OF AVERAGE ANNUAL SOIL EROSION USINGRUSLE

The final soil erosion map for the subwatershed was obtained by applying the RUSLE model, multiplying all the raster layers such as R factor value, K_factor, LS_factor, C_factor and P_factor using a raster calculator by maintaining a cell size of 30m for each layer. After integrating all the layers in ArcGIS,environment final erosion map was obtained. The WGS_1984_UTM_43N coordinate system and transverse Mercator projection were used to create all of the map layers. The prepared soil erosion map was analysed for further calculation. The flow chart of the methodologies adopted in the RUSLE model is shown in Fig 3.7

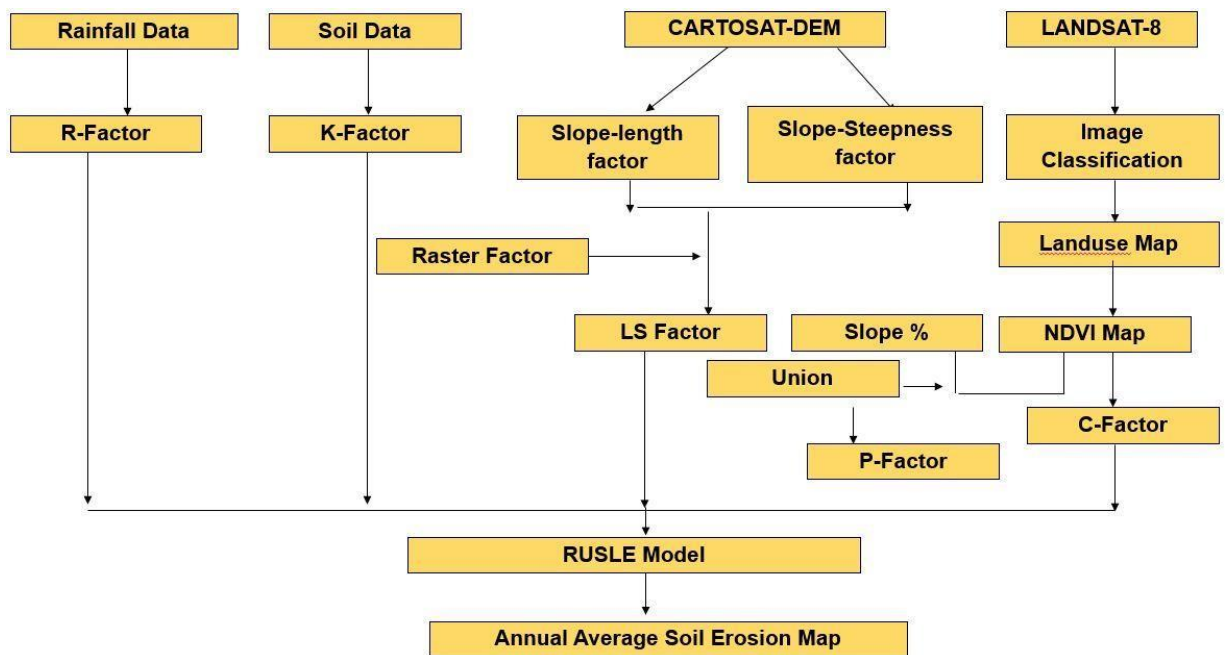


Fig.3.7 Methodology flow chart adopted for RUSLE model

3.10. Soil conservation and management protocol for the watershed

The suitability of a given type of conservation measure for an area is determined by topography, rainfall amount, intensity, distribution, soil type and depth, water holding capacity, location of the impervious soil layer, current agricultural practices, and, more often than not economics. When the steepness of the slope is less than 2%, any kind of structural measure becomes redundant, and simple agronomic practices can be sufficient. For slopes ranging from 2 to 10%, narrow or broad-based terraces can impact soil and water conservation.

In this study, in order to suggest suitable conservation practices for the watershed, the erosion risk of different land uses, and different slope classes were identified. For this, analysis was done in ArcGIS, and the generated soil loss map of the study area was spatially joined with the slope and land use maps using ArcGIS spatial join tool. The average soil loss from different land uses and slope classes were calculated. Based on the slope classes and their erosion risk, conservation measures were suggested for the study area following the guidelines published in the technical bulletin on soil erosion in Kerala by the National Bureau of Soil Survey and Land Use Planning (NBSSLUP) and Central Soil and Water Conservation Research and Training Institute (CSWCRTI) in 2014.

RESULTS AND DISCUSSION

CHAPTER- IV

RESULTS AND DISCUSSION

This chapter reveals the results of the investigation of geomorphologic aspects such as areal, linear and relief aspects of the Kurumanpuzha sub-watershed of Chaliyar river basin, Kerala, and the results of estimation gross soil erosion in the watershed. Various maps for RUSLE analysis using remote sensing and GIS are also presented.

4.1 DELINEATION OF THE WATERSHED

4.1.1 Digital Elevation Model (DEM)

The Kurumanpuzha sub-watershed of the Chaliyar river basin was delineated using the Spatial Analyst Tool in ArcGIS. The sequential procedures were DEM > Fill > Flow Direction > Flow Accumulation > Boundary delineation with the location of outlet. The outlet point of the watershed is located at Conolly plot near Nilambur, and it is where the Kurumanpuzha joins the Chaliyar river(Plate .1).

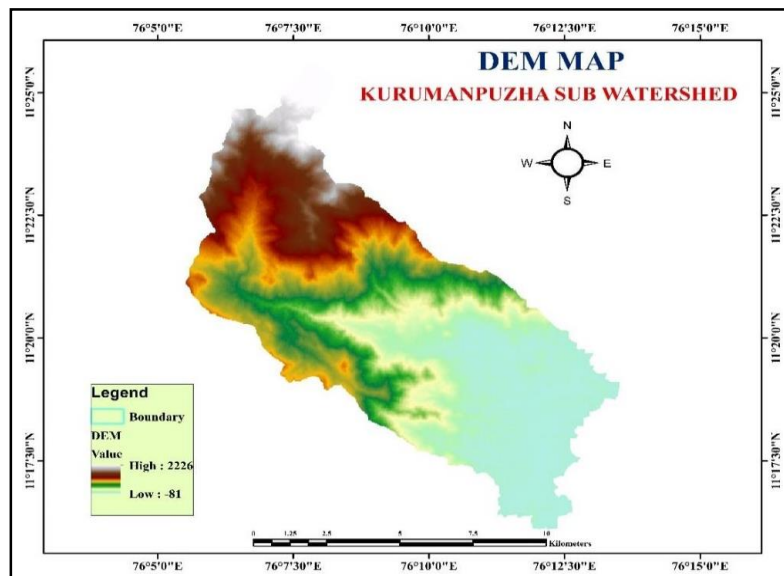


Fig 4.1 DEM map of the watershed

The area of watershed was found to be 10,359.05 ha. The obtained basin length, width, and perimeter are 19.19, 9.2, and 60.63 km, respectively.



Plate 1: Canolly plot (outlet of Kurumanpuzha sub watershed)

4.1.2. Flow Direction

The Flow Direction map was obtained by using the DEM file and Spatial Analyst Tool in the Hydrology section of ArcGIS software, as shown in Fig4.2. The blue portion of the map represents the higher flow direction values, while the brown portion of the map represents the lower flow direction values. The higher values of the flow direction were found in the western and southern parts of the watershed so that the flow is directed towards the outlet of the watershed.

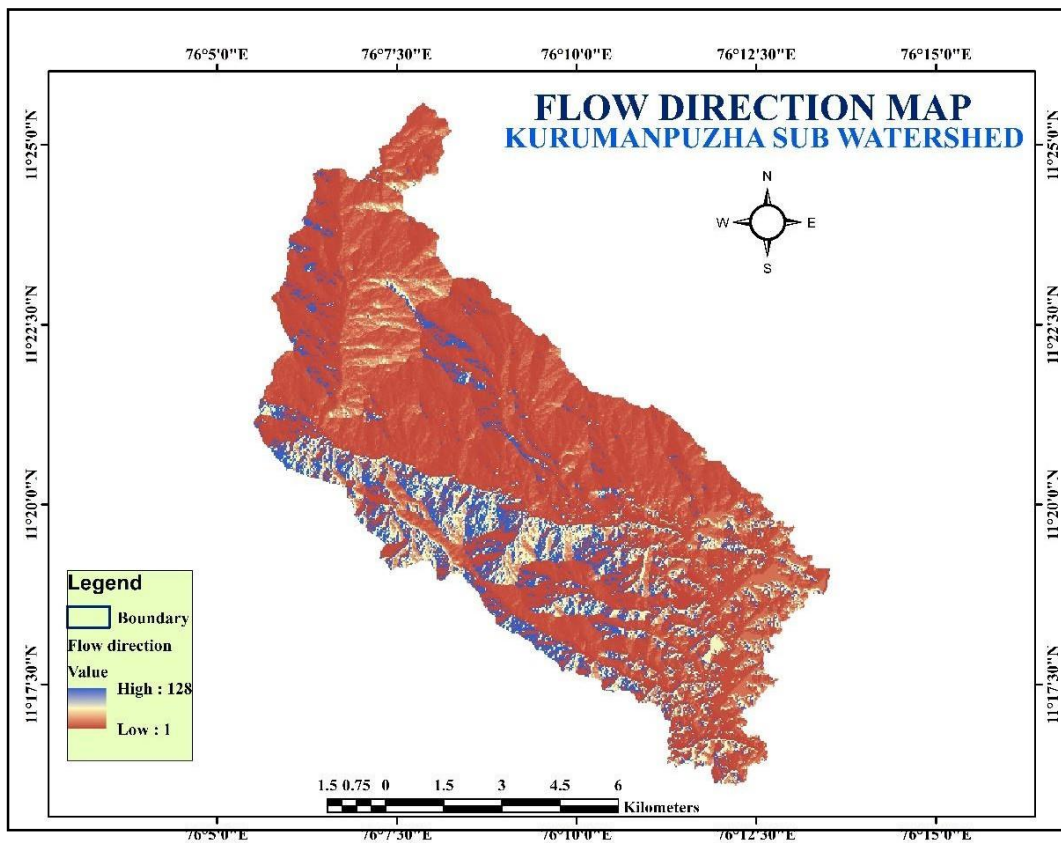


Fig.4.2 Flow Direction map of the Watershed

4.1.3 Flow accumulation

Flow accumulation map is generated from the “Flow direction” using the Spatial Analyst Tool. The result of the flow accumulation raster was in the range of 0 to 110474. The black portion represents the lesser flow accumulation values while the white portion represents the higher flow accumulation values, as shown in fig4.3. The major

flow accumulation is directed towards the southern sides of the watershed with lesser accumulation in the northern direction, and finally, the flow connects to the outlet. The watershed outlet is directed to the chaliyar river, located at the south end of the watershed.

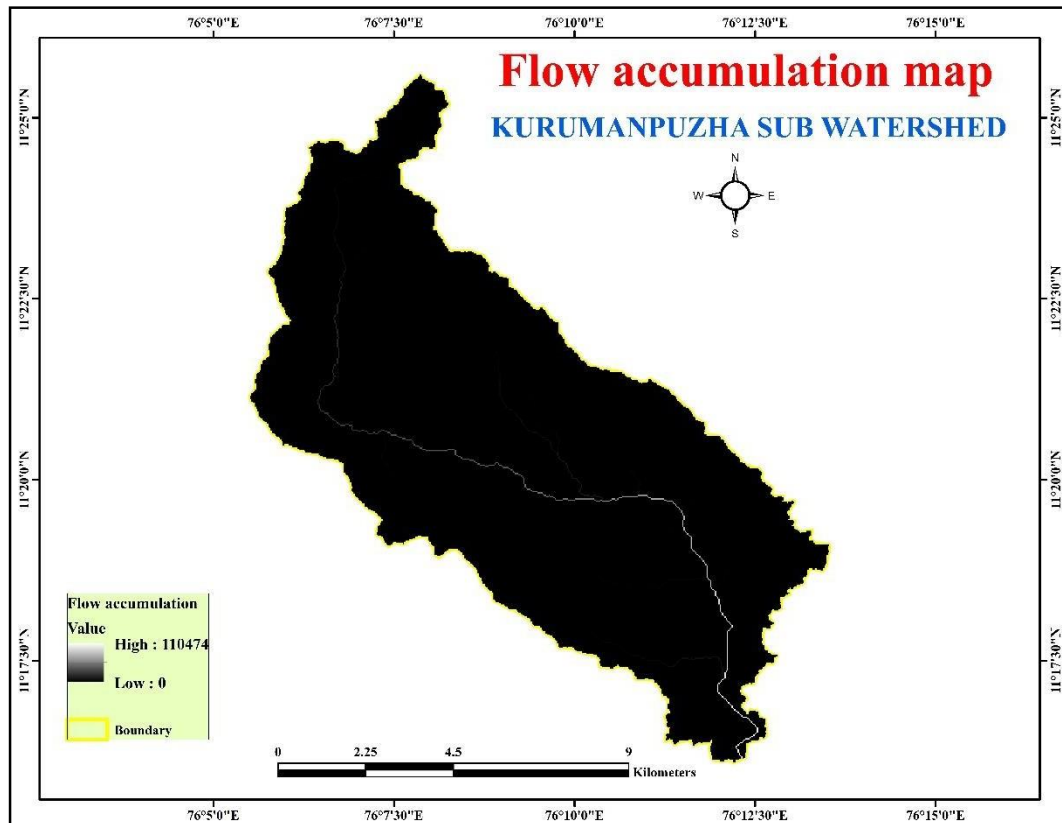


Fig. 4.3 Flow accumulation map of Kurumanpuzha sub watershed

4.1.4 Slope map

The slope map was created using the DEM of the study area. The entire watershed was divided into five distinct slope classes, ranging from 0% to more than 50%. According to the slope analysis data, around 50.67 per cent of the area has a slope of 10-25 per cent, while only 5.09 per cent of the land has less than 3 per cent. Plate 3 shows the higher elevated part in the watershed.

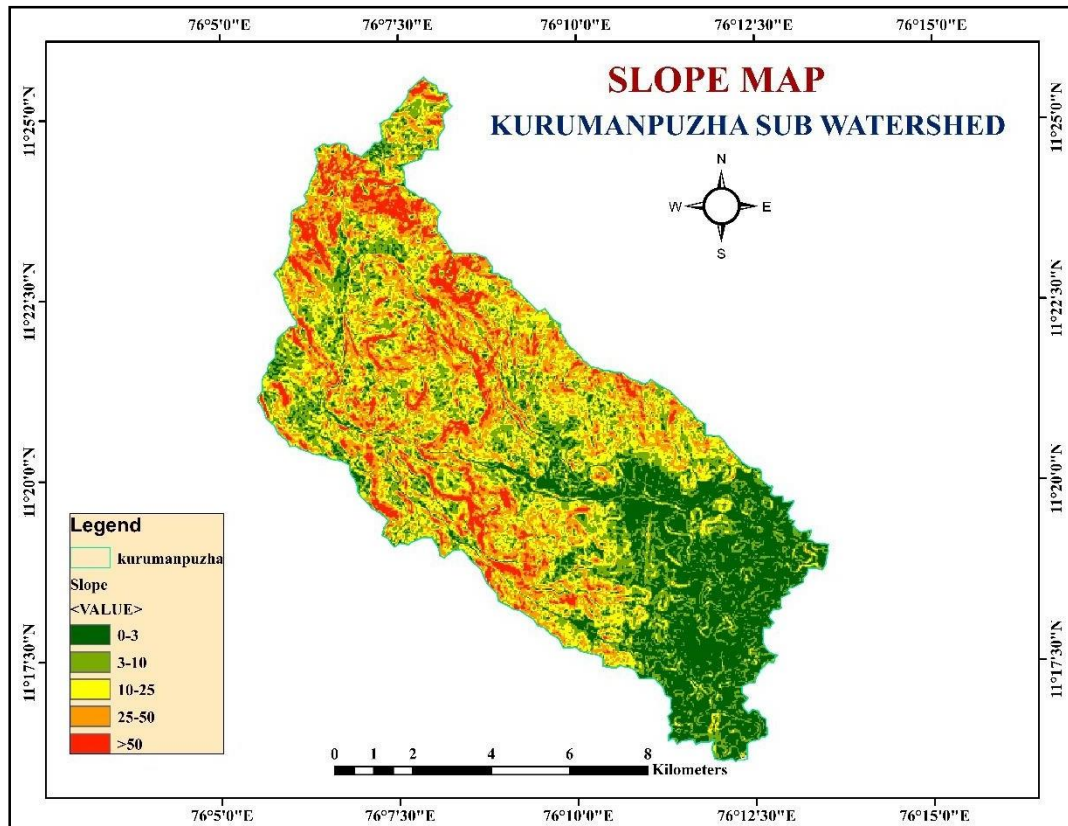


Fig. 4.4 Slope map of the watershed

Table 4.1 Slope classes identified in the watershed

Slope classes	Slope values in %	Area in ha	% of total area
Very gently sloping	0-3	527.08	5.09
Gently sloping	3-10	2298.635	22.20
Strongly sloping	10-25	5245.74	50.67
Steeply sloping	25-50	2279.858	22.02
Very steeply sloping	>50	4.97	0.04

4.1.5.Aspect

Aspect maps give the observer a sense of the direction in which various slopes derived from a DEM lie. The aspect map value -1 denotes a slope of zero, i.e., flat terrain. The value of slope direction ranges from 0 to 22.5, indicating that the slope is to the north. Similarly, other values ranging from 22.5 to 67.5 indicate a slope to the north-east, while values ranging from 67.5 to 112.5 indicate a slope to the east. Similarly, slope directions of 112.5 to 157.5, 157.5 to 202.5, 202.5 to 247.5, 247.5 to 292.5, 292.5 to 337.5, and 337.5 to 360 indicate direction towards the South East, South, South West, West, North West, and North. The majority of the flow in the Kurumanpuzha sub-watershed was south.

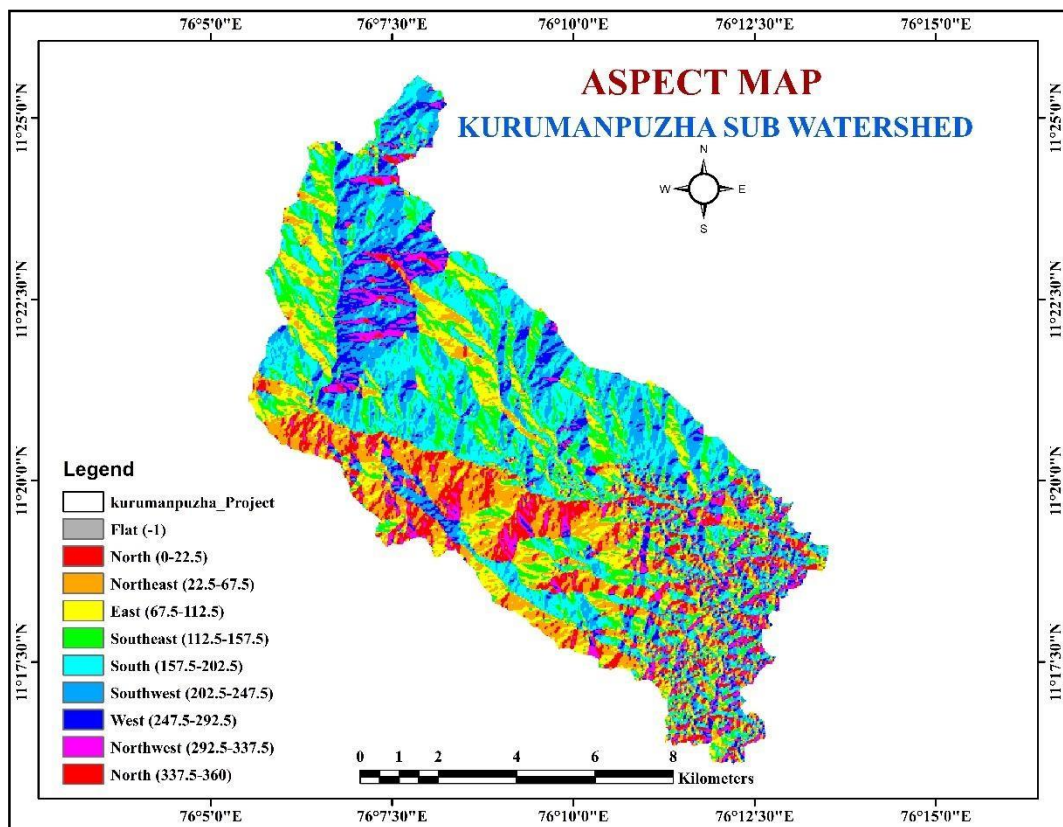


Fig.4.5 Aspect map of Kurumanpuzha sub watershed

4.1.5 Land use/Land cover

Using unsupervised classification in ERDAS imagine 2015 software land use land cover map of the study area was generated. The procedure for the preparation of a land use map was explained in section 3.5.6.

The water bodies, Forest/dense vegetation, rubber, coconut/areca nut, cropland, scrubland, and bare land are the type of land uses identified in the study area. The obtained raster map was digitally vectorized and then rasterized for spatial GIS analysis. Forest/dense vegetated area (56.46 %) was estimated as the major land use with the Rubber plantation (20.06 %). Rubber, coconut and areca nut were identified as the major crops in the study area. Some ground truth values identified the selected areas for classifying using the unsupervised method. Fig 4.6 shows the land use land classification map of the The study area. Plate 2 shows the Field photographs of different land uses of the study area.

Table 4.2. The area under different Land use/Landcover

Land use/Landcover	Area in ha	Area in %
Forest/Dense vegetation	5849.19	56.46
Rubber	2078.64	20.06
Coconut/Arecanut	993.15	9.5
Scrub land	923.22	8.91
Crop land	279.45	2.69
Bare land	138.96	1.34
Water bodies	67.23	0.64
Built up/Urban areas	28.35	0.27

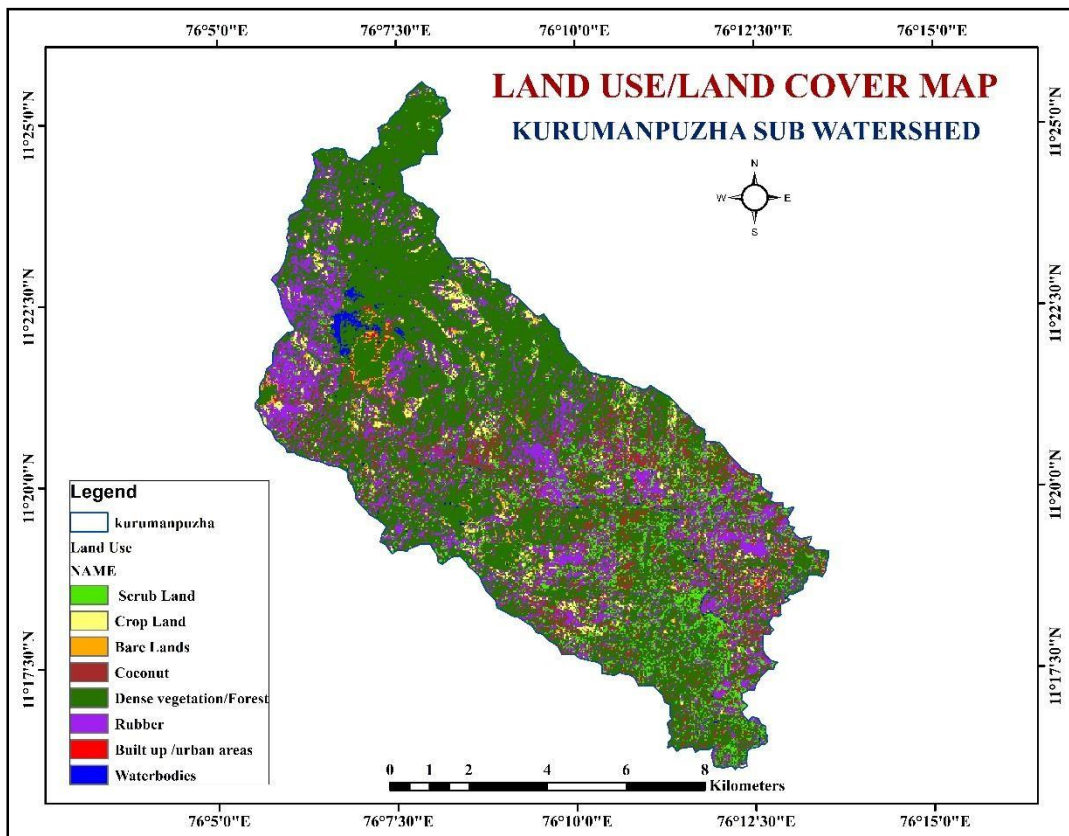


Fig 4.6 Land use land cover map of the study area



Plate .3 Higher elevated part in Kurumanpuzha subwatershed



Plate. 2 Field photographs of different land uses of the study area

4.2 GEOMORPHOLOGICAL CHARACTERISTICS OF KURUMANPUZHA SUBWATERSHED

Morphological characteristics give the basis for analyzing the drainage basin slope, rock hardness differences, structural control, and watershed geology. The geomorphologic study of the drainage area aims to collect precise data on measurable features of the stream network. By using the drainage map of the study area, morphometric analysis and basin boundary values of various morphometric parameters were measured using the methodology described in section 3.5

4.2.1 Linear aspects of the drainage network

This section examines the stream order, stream number, basin length, average basin width, mean stream length, stream length ratio, and bifurcation ratio. The study area has a 5th order stream and a dendritic drainage pattern according to the output. The maximum watershed length and the width were

19.19 and 9.20 km, respectively. The number of first, second, third, fourth and fifth order streams were 294, 137, 74, 59 and 20, respectively. According to Horton, as stream order increases, stream number decreases. In this study, the results of stream number support Horton's law. The total length of 1st, 2nd, 3rd, 4th and 5th order streams are 120.744, 62.687, 29.48, 17.22 and 10.26 km, respectively. The stream lengths of different orders and their relative mean stream lengths were calculated by digitising the stream networks in ArcGIS software.

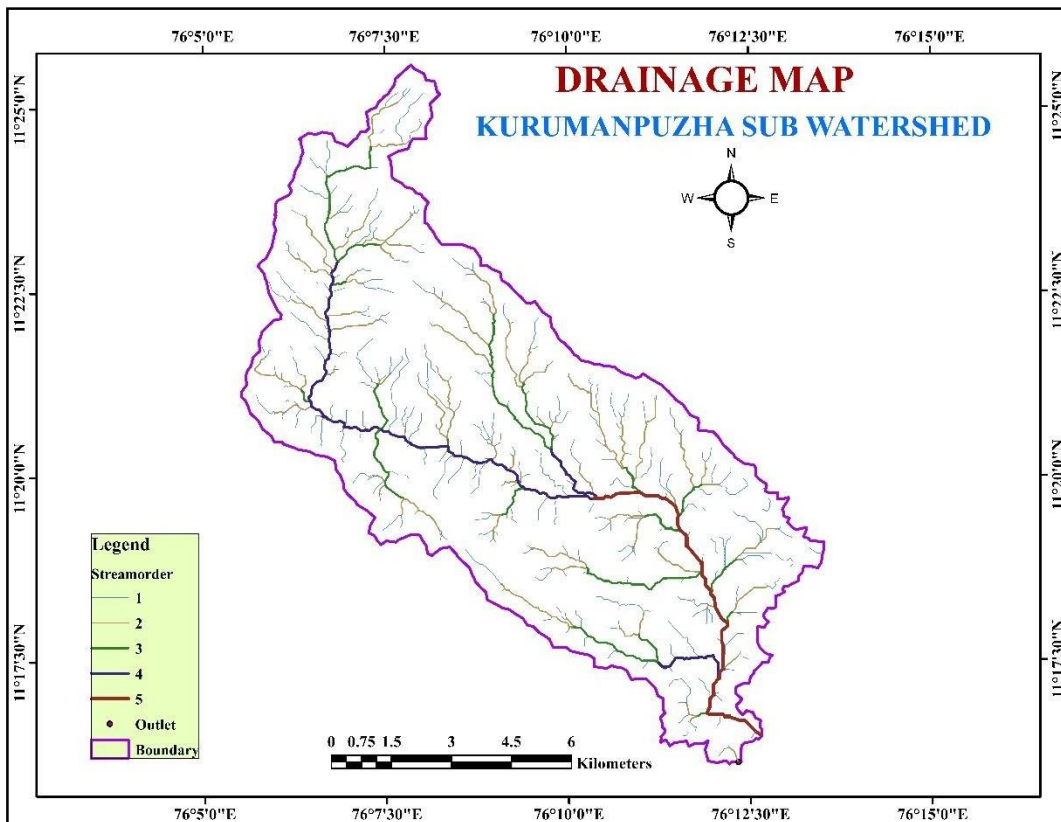


Fig.4.7 Drainage network map of the watershed

Table 4.3. Stream order and mean stream length of Kurumanpuzha sub watershed

Parameters	Stream order					Total
	I	II	III	IV	V	
No of streams	294	137	74	59	20	584
Total stream length, km	120.74	62.68	29.48	17.22	10.26	240.44
Mean stream length, km	0.842	1.808	3.348	4.200	12.391	22.589

4.2.1.1 Stream length ratio(R_L)

The stream length ratio(R_L) values for second to first, third to second, fourth to third and fifth to fourth-order streams were obtained to be 2.147, 1.851, 1.254 and 2.95, respectively (Table 4.4).

Changes in slope and topography can be compared to changes in stream length ratio. The length ratio in the study area fell from third to fourth order, indicating that the study area is in the late-stage of its geomorphic development. On the other hand, the fourth to fifth-order stream length ratio increases compared to the fourth to third order, showing that the watershed has reached its mature geographic stage. Plate 4 and 5 show the 3rd and 4th order streams in the study area.

Table 4.4. Stream length ratio of Kurumanpuzha sub watershed

Stream order	Mean stream length,km	Stream length ratio (R_L)
I	0.842	-
II	1.808	2.147
III	3.348	1.851
IV	4.200	1.254
V	12.391	2.95

4.2.1.2. Stream number and stream order relationship

For the Kurumanpuzha sub watershed, the number of streams in each order was counted and recorded, as shown in Table 4.3. The logarithm of the number of streams versus the order of the streams is plotted in Fig 4.8. The graph shows a straight line following Horton's law, which states that the number of stream segments in a drainage system has a linear relationship with minimal variance. As a result, in geometric progression, as stream order increases, the number of streams decreases.

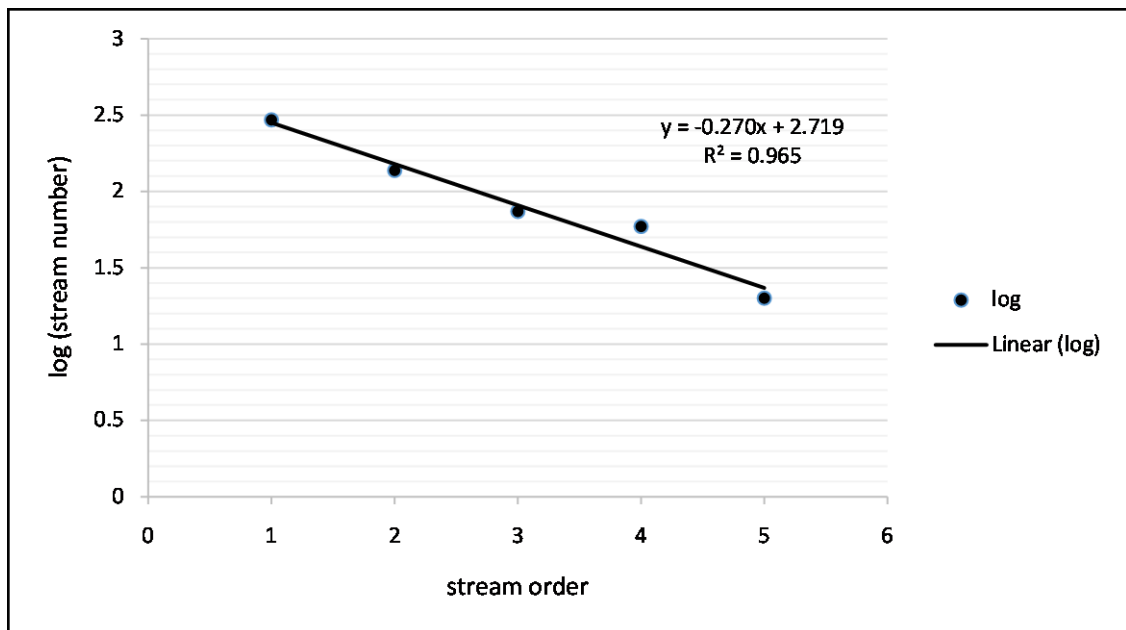


Fig.4.8 Regression plot of logarithm of stream number vs stream order

4.2.1.3. Relationship between stream order and total stream length

A graph showing the relationship between total stream length and stream order (U) was plotted. To study the geometric property of the correlation, the logarithm of total stream length was plotted as the ordinate and the stream order (U) as the abscissa on the arithmetic scale. Figure 4.9 shows a logarithmic trend line with the regression value ($R^2 = 0.994$).

In the first order, the total length of the stream segments was long. As the stream order increases, stream segments become shorter. Figure 4.9 shows a nearly straight line fit with the logarithm of cumulative stream length as the ordinate and the stream

order as the abscissa. The straight-line fit indicates that the total stream length to order ratio remains constant as the basin order increases.

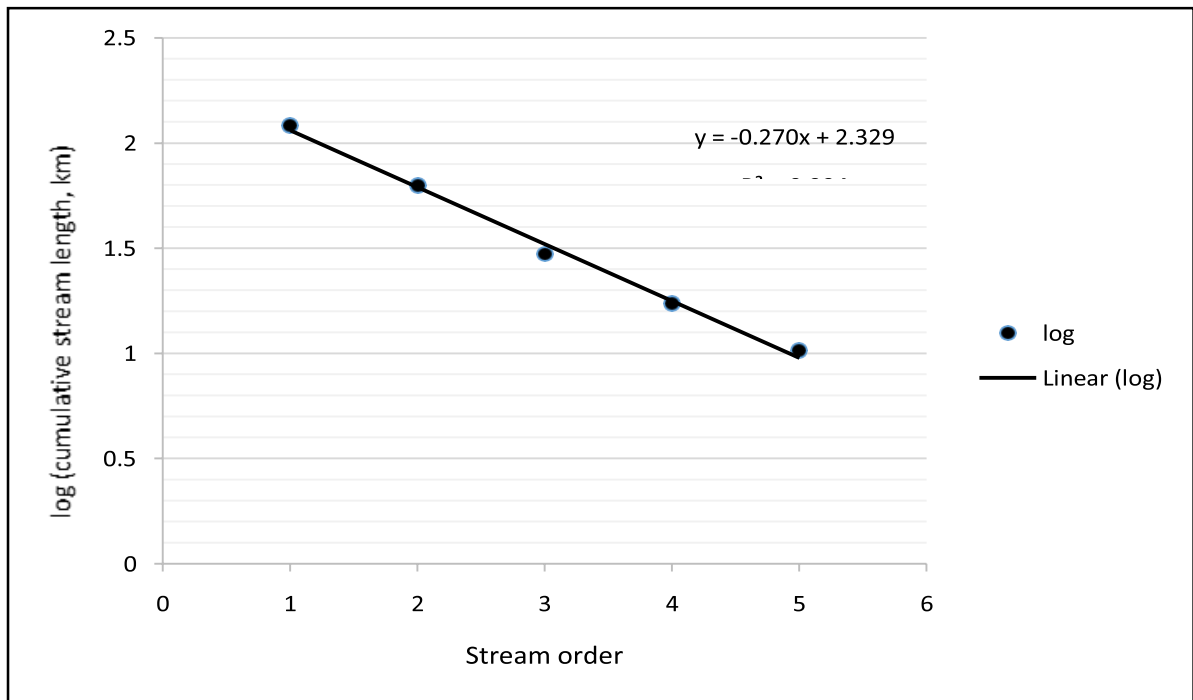


Fig .4.9 Regression plot of the logarithm of total stream length and stream order



Plate. 4 3rd order stream of Kurumanpuzha subwatershed

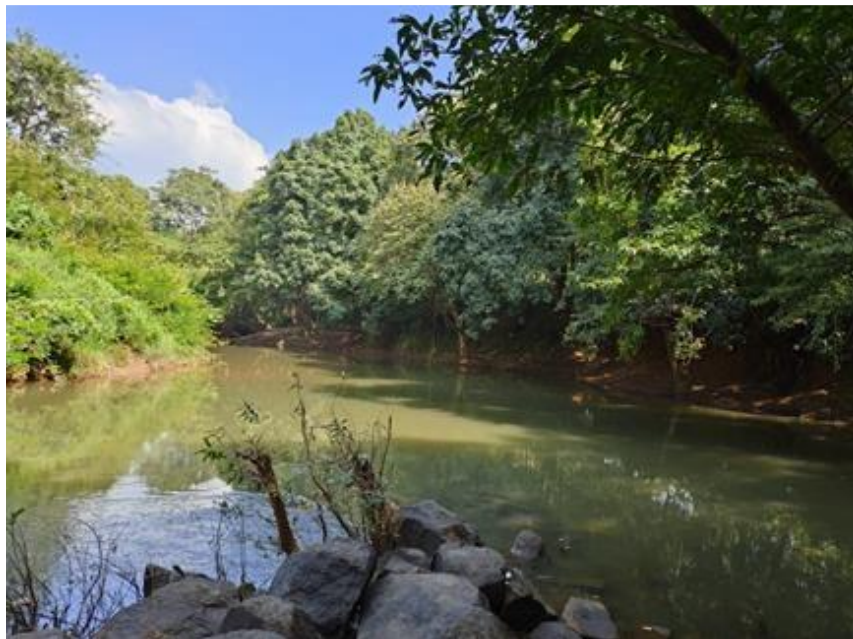


Plate .5 4th order stream of Kurumanpuzha sub watershed

4.2.1.4. Bifurcation ratio (R_b)

The bifurcation ratio (R_b) is another significant aspect of the drainage network that represents the watershed's geological and tectonic properties. The R_b values from 1st to 2nd, 2nd to 3rd, 3rd to 4th, and 4th to 5th order streams were 2.14, 1.85, 1.25 and 2.95, respectively, and the mean bifurcation ratio was 2.05 (Table 4.5). A smaller bifurcation ratio reflects that the watershed has experienced less structural disturbance, and there is no change in the drainage pattern because of the structural disturbance (Nag and Lahiri 2011).

Table 4.5 Bifurcation ratio of Kurumanpuzha Sub Watershed

Stream order	No of stream	Bifurcation ration(R_b)
I	294	2.14
II	137	1.85
III	74	1.25
IV	59	2.95
V	20	-
Mean	-	2.05

Table 4.6. Linear aspects of Kurumanpuzha sub watershed

Sl.No	Parameters	Symbol	Value
1	watershed perimeter	P	60.63 km
2	Length of main stream	L	29.13 km
3	watershed length	L	19.08 km
4	Stream length of each order	L ₁	120 km
		L ₂	62.68 km
		L ₃	29.48 km
		L ₄	17.22 km
		L ₅	10.26 km
5	Total length of all orders	L _w	240.44 km
6	Mean stream length of each order	\bar{L}_1	0.84 km
		\bar{L}_2	1.80 km
		\bar{L}_3	3.34 km
		\bar{L}_4	4.20 km
		\bar{L}_5	12.39 km
7	Number of streams of each order	N ₁	294
		N ₂	137
		N ₃	74
		N ₄	59
		N ₅	20
8	Total number of streams of all order	N _w	584
9	Bifurcation ratio	R _b	Av:2.05
10	Length of overland flow	L _g	0.209 km

4.2.2 Areal aspects of drainage network

Systematic measurements of areal elements such as watershed, form factor, drainage density, drainage texture, stream frequency, circulatory ratio, elongation ratio, compactness co-efficient, texture ratio, and length of overland flows are the part of areal aspects of a drainage network. The whole area covered by all lower-order streams is included in the area covered by the higher-order stream. Form factor, circularity ratio, elongation ratio and compactness coefficient are 0.284, 0.353, 0.598 and 0.585, respectively. The values indicate that the watershed is in a n elongated shape as the form factor value is less than 0.7854 (Horton, 1932). An elongated watershed with a lesser form factor has a flatter peak flow for a longer period; hence the flood flow will continue to flow for longer. As a result, flood flows in a watershed like this can be easily managed (Mahadevaswamy *et al.*, 2011). The lower value of the compactness coefficient (0.585) suggests that the entire watershed is less sensitive to erosion risk (Ali and Ali 2014). The lithological properties of the area, infiltration capacity, and relief characteristics all influence the texture ratio. The texture ratio (4.849) in this study shows moderate subsurface material permeability and infiltration and a moderate runoff rate.

The drainage density, drainage texture, stream frequency, and texture ratio values were estimated to be 2.392 km km⁻², 9.632 km⁻¹, 5.637 km⁻² and 4.849 respectively. The drainage density value shows the extent of channel spacing closeness and provides a quantitative measure of the average stream channel length of the entire watershed. The relatively high value of drainage texture, in this case, indicates that the watershed has very fine drainage texture, moderate infiltration rates, higher surface flow velocity, and the dominance of impermeable soft rock with moderate resistance against erosion. The watershed shows a moderate stream frequency value, indicating that the watershed has resistant or permeable subsurface material with moderate infiltration rate and good vegetation cover (Choudhari *et al.*, 2018).

The length of the overland flow is equal to half of the drainage density and is the distance that water travels over land before it is concentrated into defined stream channels (Horton, 1945). The average channel slope is inversely proportional to the

length of overland flow. In the present study, overland flow length has a lower value of 0.209 km, indicating the watershed has predominant channel flow and more stream erosion because of high drainage density Horton (1945).

Table 4.7 Areal aspects of Kurumanpuzha subwatershed

Sl.No	Parameters	Symbols	Value
1	Watershed area(A),ha	A	10359.053
2	Watershed width(B), km	B	9.200
3	Form factor (R_f)	R_f	0.281
4	Drainage density (D_d), km km ⁻²	D_d	2.392
5	Drainage texture (D_t), km ⁻¹	D_t	9.632
6	Stream frequency (F), km ⁻²	F	5.637
7	Circularity ratio (R_c)	R_c	0.353
8	Elongation ratio (R_e)	R_e	0.598
9	Compactness coefficient (C_c)	C_c	0.585
10	Texture ratio (R_t)	R_t	4.849
11	Length of overland flow (L_g), km	L_g	0.209

4.2.3 Relief aspects of drainage network

The relief aspects of land are significant elements for both usage and assessing drought-prone areas. Maximum watershed relief (H), Relative relief (R) in %, The relief ratio (Rr), ruggedness number (Rn), and time of concentration (Tc) values determined were 2307 m, 3.82, 0.12, 5.51 and 8.89 min, respectively, showing a high relief value for the watershed.

A lower relief ratio value indicates the existence of rocks exposed in the form of higher ridges and mounds with a higher degree of slope (Praveen *et al.*, 2012). The ruggedness number was calculated by using relief aspects and was found to be 5.51. The higher value of the rugged number is due to the presence of higher elevated areas

in the watershed. The ruggedness number decreases as the region becomes prone to soil erosion and has an inherent structural complexity in connection to the relief aspects and drainage density (Guha, 2015).

The watershed runoff generation is directly influenced by the time of concentration. The value obtained for concentration time is 8.89 minutes, representing the time it takes for water to travel from the farthest reaches of the watershed to its outlet. (Sreedevi *et al.*, 2012) .Table 4.8. Relief aspects of Kuruvanpuzha Sub Watershed.

Sl.No	Relief parameters	Value
1	Maximum watershed relief (H), m	2307
2	Relative relief (R_R)	3.82
3	Relief ratio (R_r)	0.12
4	Ruggedness number (R_n)	5.51
5	Time of concentration (T_c), min	8.89

4.2.2 Hypsometric integral

The hypsometric curves have been plotted between the cumulative percentage of the surface areas with respect to the elevation of the study area by using DEM in arc GIS. The hypsometric integral (HI) was estimated using the elevation relief ratio method. The HI value of the Watershed were about 0.48, indicating that elevation was in equilibrium stages. Fig 4.10 shows the Hypsometric curve of the Kurumanpuzha sub-watershed.

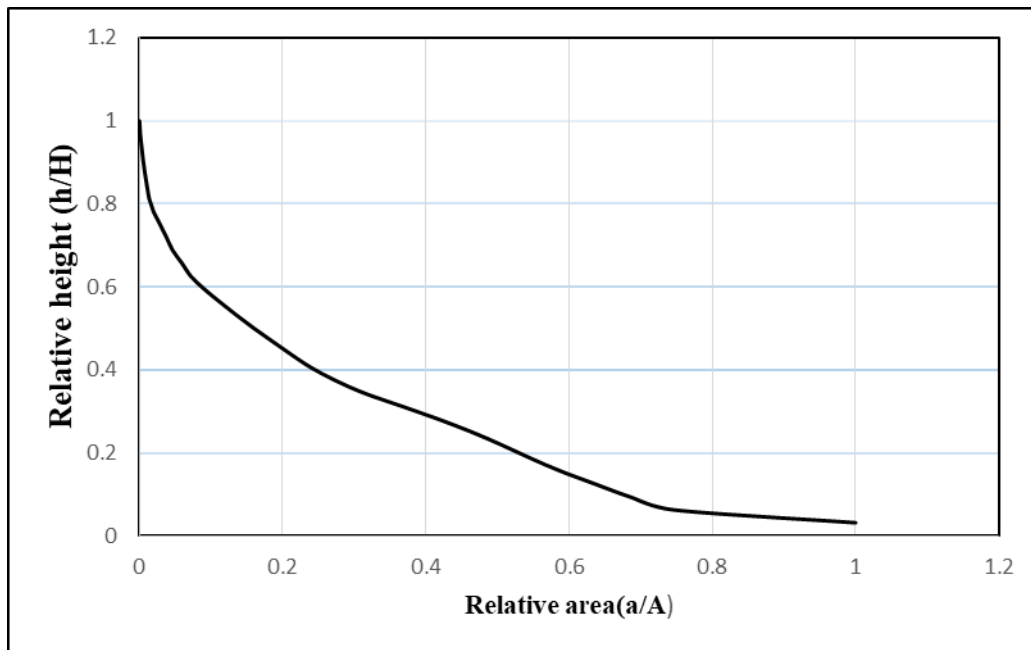


Fig.4.10. Hypsometric curve of Kurumanpuzha sub watershed

4.2 MODELING OF SOIL EROSION

4.3.1 Generation of maps for the RUSLE model

4.3.1.1 Rainfall erosivity factor (R-factor)

Soil erosion is highly dependent on rainfall distribution and, therefore erosivity (Jain *et al.*,2001). Due to a lack of rainfall intensity data in the watershed area, the erosivity index factor was calculated using the monthly rainfall amount. R-factor was calculated using the Modified Fournier Index (MFI) value because a strong correlation was identified between MFI and R factor in a study conducted by Kouli *et al.* (2008) in North-western Crete, Greece. The R factor value for the year 2000 to 2020 was calculated using a modified Arnolds equation. The average R factor value calculated was found to be 9310.538 MJ mm ha⁻¹ h⁻¹ yr⁻¹. A graph showing the annual rainfall erosivity factor for 2000 to 2020 is shown in Fig 3.2. The findings are consistent with Kartic *et al.* (2014), who found an erosivity factor ranging from 150 to 450 MJ cm ha⁻¹ h⁻¹ yr⁻¹ for their study area. Owing to the unavailability of data relating to daily rainfall intensity and the study area being small (103.6 sq km), it was influenced by only one near rain gauge station, Nilambur. Hence same R factor values were taken for

the whole watershed. Since it is a single value, no map was generated for the R factor.

Fig 4.11 denotes the variation of the R factor values with rainfall in the study area.

Table 4.9. Rainfall erosivity factor R (MJ mm ha⁻¹ h⁻¹ yr⁻¹)

Years	Annual R factor (MJ mm ha⁻¹ h⁻¹ yr⁻¹)	Years	Annual R factor (MJ mm ha⁻¹ h⁻¹ yr⁻¹)
2000	4957.21	2011	17002.41
2001	5196.15	2012	6525.46
2002	3648.58	2013	744.79
2003	4967.39	2014	12264.19
2004	5135.41	2015	7875.92
2005	12656.04	2016	6562.91
2006	18850.14	2017	5198.45
2007	23485.83	2018	18754.49
2008	4309.32	2019	14890.02
2009	12141.28	2020	5856.17
2010	4499.09		

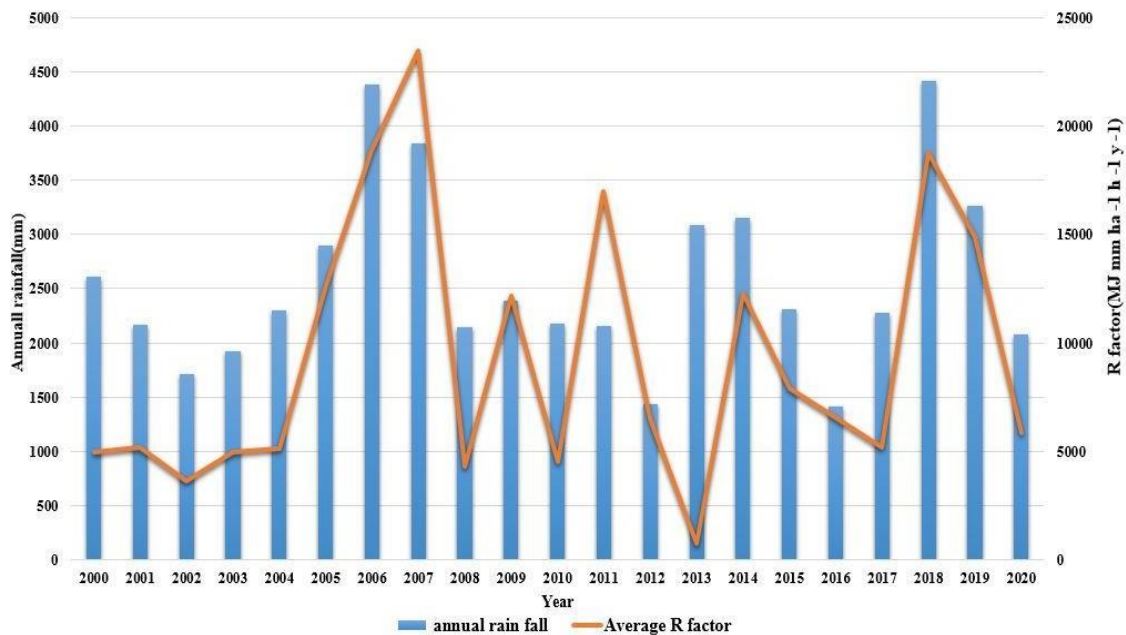


Fig.4.11 Average annual rainfall erosivity factor (R) graph for 2000-2020 Years

4.3.1.2 Soil Erodibility Factor (K-factor)

The erosion vulnerability of the soil is greatly represented by the soil erodibility factor (K factor). The soil map provided by the Department of Soil Survey and Soil Conservation, Kerala, was used in this study to extract all of the soil characteristics. In the Kurumanpuzha sub watershed, seven textural categories were identified: sandy clay loam, clay loam, sandy loam, sandy clay, gravelly sandy clay loam, and gravelly clay. According to Wischmeier and Smith (1978), K values fluctuate depending on the soil's sticky and less sticky properties, less sticky soils being more erodible than sticky soil. There were five types of soil series observed in the study area which are Mannamkulam-kuttil-Angadipuram, Vettekode-koramala-vazhikad, Arimbra-karuvarakundu-churathinmel, Nadukani-kalvarikunnu-pullangod, Walakkad-kurumbramala.

The K factor value of soils in the study area was found to be in the range of 0.25 to 0.53 t ha h ha⁻¹ MJ⁻¹ mm⁻¹. The obtained K values from this study were in agreement with the statement given by Wischmeier and Smith (1978).

The soil association Vettekode-koramala-vazhikad had the lowest amount of clay than sand and silt and had a higher K value of 0.53 t ha h ha⁻¹ MJ⁻¹ mm⁻¹, whereas the soil association Mannamkulam-kuttil-Angadipuram with more clay content had a

lower K value of $0.28 \text{ t ha h ha}^{-1} \text{ MJ}^{-1} \text{ mm}^{-1}$. It is not a suitable practice to assign K factor values only based on texture because coarse sand does not play much more in determining the K factor than it does in textural calculations. Fig 4.12 and Fig 4.13 show the soil map and K factor map, respectively.

Table 4.10 K factor values for the Kurumanpuzha sub watershed

Soil association	Soil texture			Organic Carbon (%)	Organic matter (%)	Structural code b	Permiability c	K factor
	Sand (%)	Silt (%)	Clay (%)					
Mannamkulam	22	20	58	2	2	3	5	0.19
Kutil	52	6	42	2	2	2	5	0.16
Angadipuram	58	15	27	2	1.2	2	5	0.28
Vettekode	52	6	42	2	2	4	5	0.25
Koramala	58	15	27	2	2	4	5	0.35
Vazhikad	32	34	34	2	2.76	4	5	0.37
Arimbra	43	39	18	2	2.07	4	5	0.53
karuvarakundu	22	20	58	2	2	4	5	0.23
churathinmel	32	34	34	2	2.43	4	5	0.38
Nadukani	22	20	58	2	0.83	4	5	0.24
Kalvarikunnu	52	6	42	2	2.21	4	5	0.25
Pullangod	52	6	42	2	2	4	5	0.25
Walakkad	32	34	34	2	4.22	3	5	0.29
kurumbramala	32	34	34	2	4.22	3	5	0.29

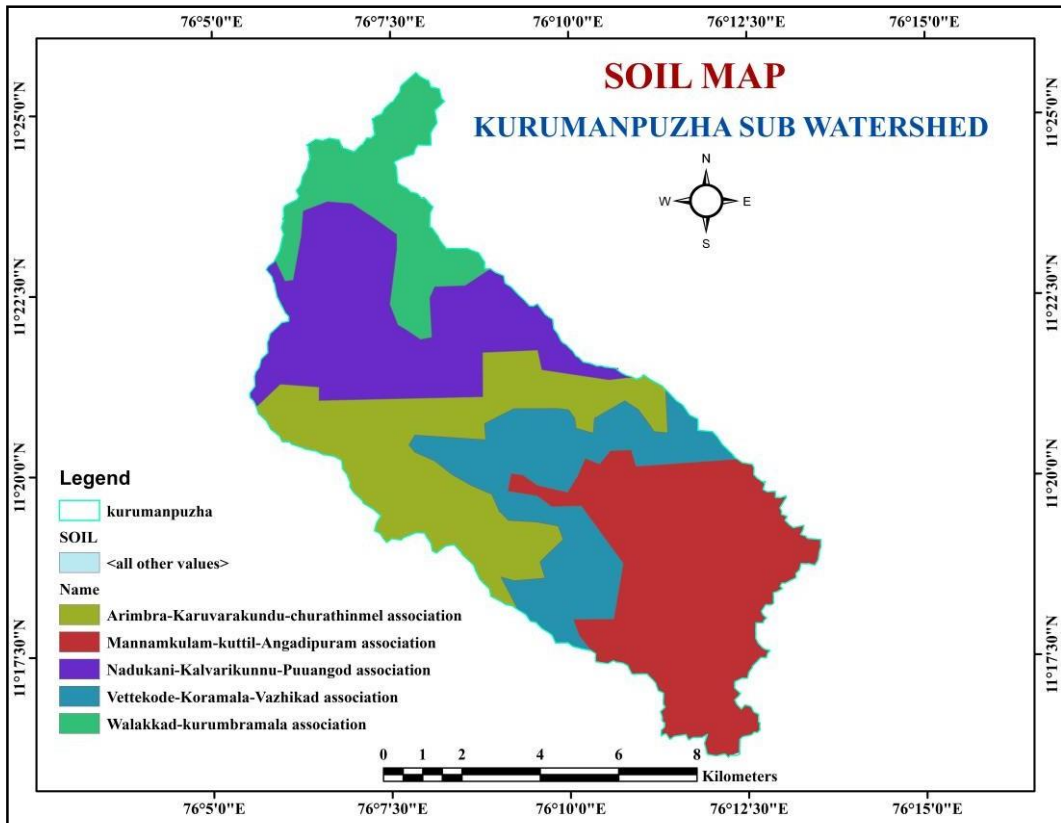


Fig. 4.12 Soil map of Kurumanpuzha sub watershed

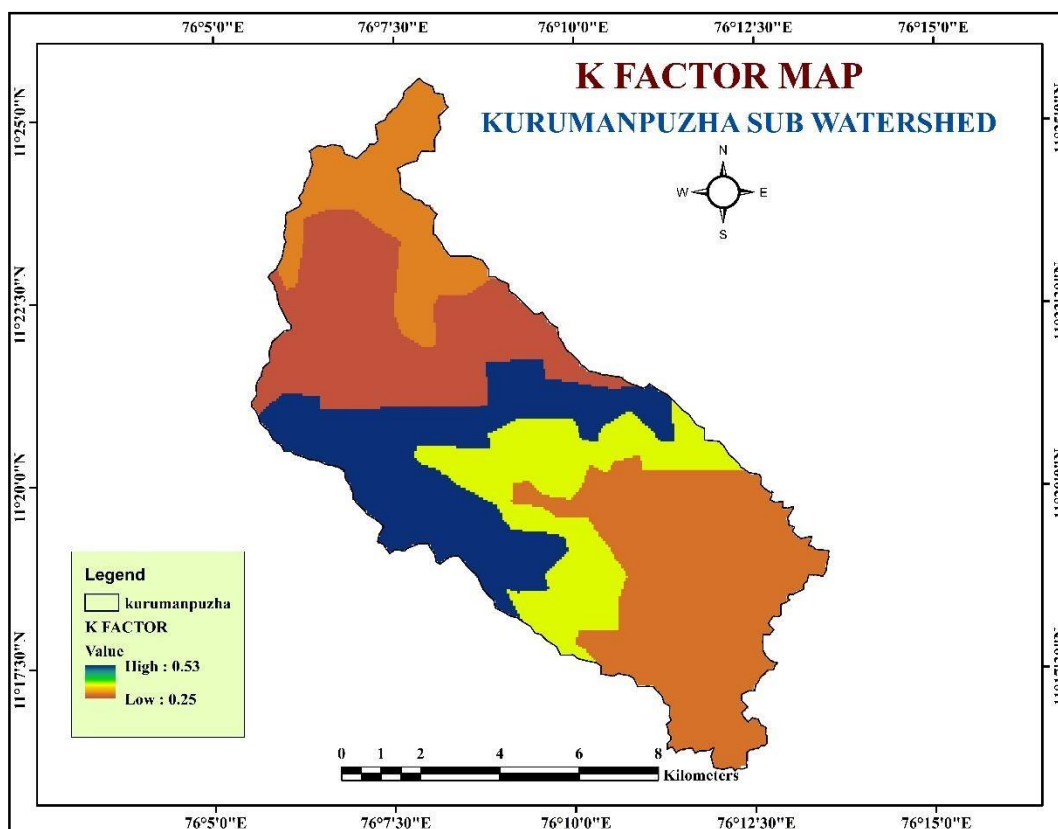


Fig.4.13 Spatial distribution of soil erodibility factor(K factor)

In the current study, erodibility index was found to be low in soil with higher clay content, as Belasri and Lakhouili (2016). Soils with higher K factor values are more prone to erosion, while those with lower values are less susceptible to erosion. The organic matter and soil texture were found to significantly influence the K factor value.

4.3.1.3 Slope length and slope steepness factor (LS-factor)

The study area DEM was used to generate flow accumulation and slope maps, which were used to estimate and generate the LS factor and LS maps, respectively. The LS factor obtained for the area was 0 to 24.59 with a mean of 0.158 and a standard deviation of 0.523. The accuracy of the LS factor can be determined by the resolution of the DEM data. High LS factor values were carried by higher elevation pixel. The spatial distribution of the LS factor in the study area is shown in Fig 4.14.

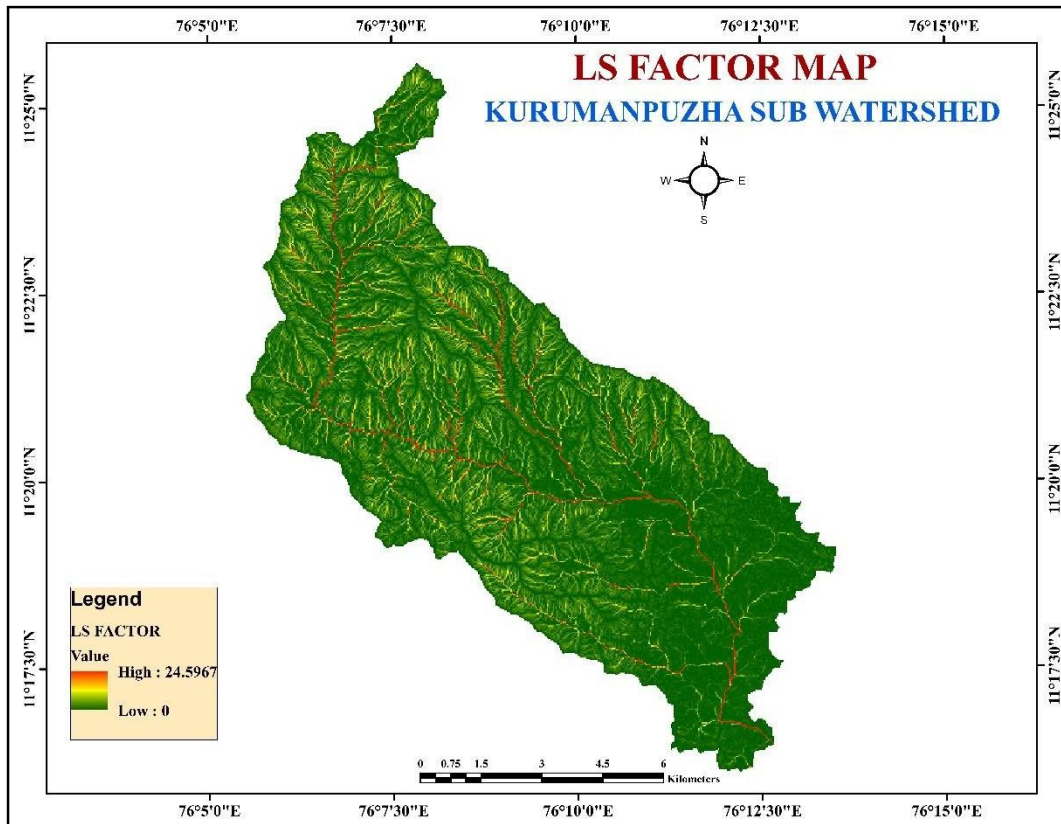


Fig. 4.14. Spatial distribution of topographic (LS factor)

A similar methodology was published by Prasannakumar *et al.* (2011b) in calculating the LS factor for the Munnar forest division, where the factor ranged from 0 to 32, with a mean of 5.32 and a standard deviation of 4.63. The LS factor was calculated using the same formula in both studies. The estimated LS values were comparable with ranges of 0.07 to 58.6 by Thomas *et al.* (2017a) in the Muthirappuzha sub-basin, 0.07 to 58.8 by Thomas *et al.* (2017b) in the Pamba river basin, 19.4 by Pradeep *et al.* (2014) in Meenachil sub-watershed, and 2.028 for the year 2005 by Prasannakumar *et al.* (2011a) in Attappady region. This research conducted in different locations of Kerala with similar topographical features helps to validate the accuracy of the resulting LS factor map.

4.3.1.4 Crop cover management factor (C-factor)

The crop cover management factor or C factor highly depends on the range of Vegetation/canopy cover present in the area. The C factor values were calculated using NDVI maps derived from Landsat imageries (Fig 4.15), which consider the field's urbanisation and major vegetation changes.

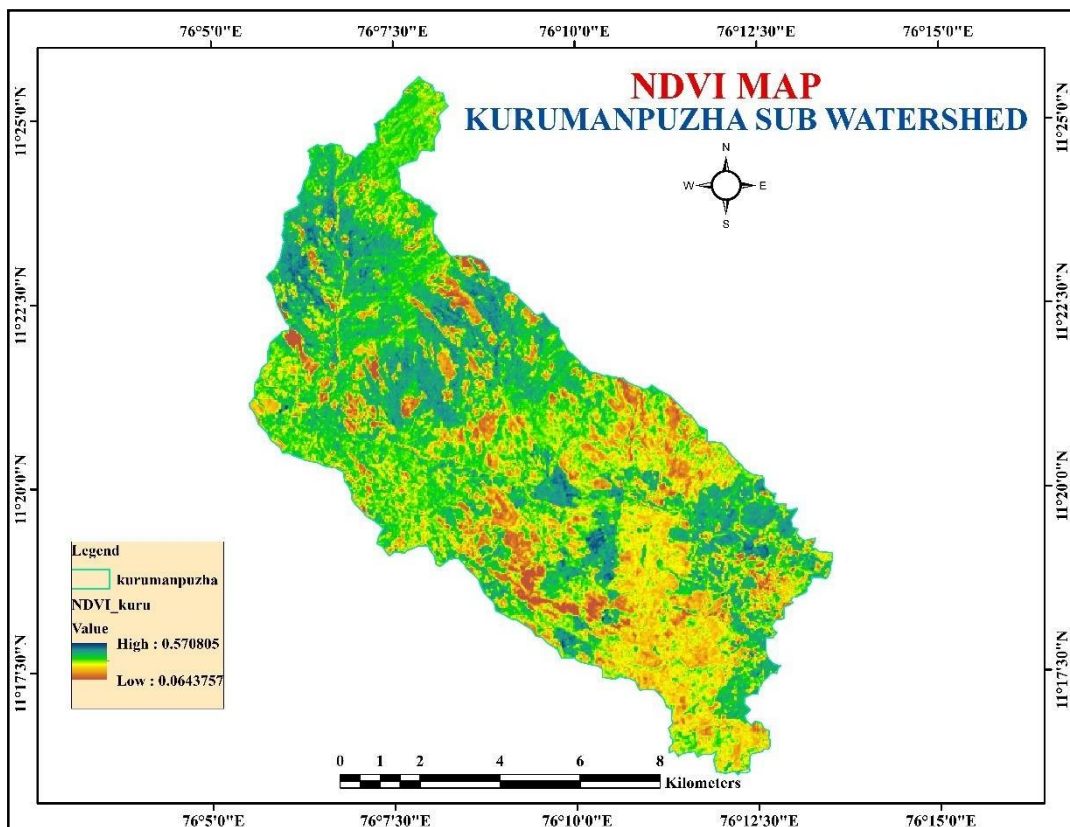


Fig. 4.15 NDVI map of Kurumanpuzha subwatershed

In this study C factor calculated by exponential scaling methods was in the range of 0.0699 to 0.87.

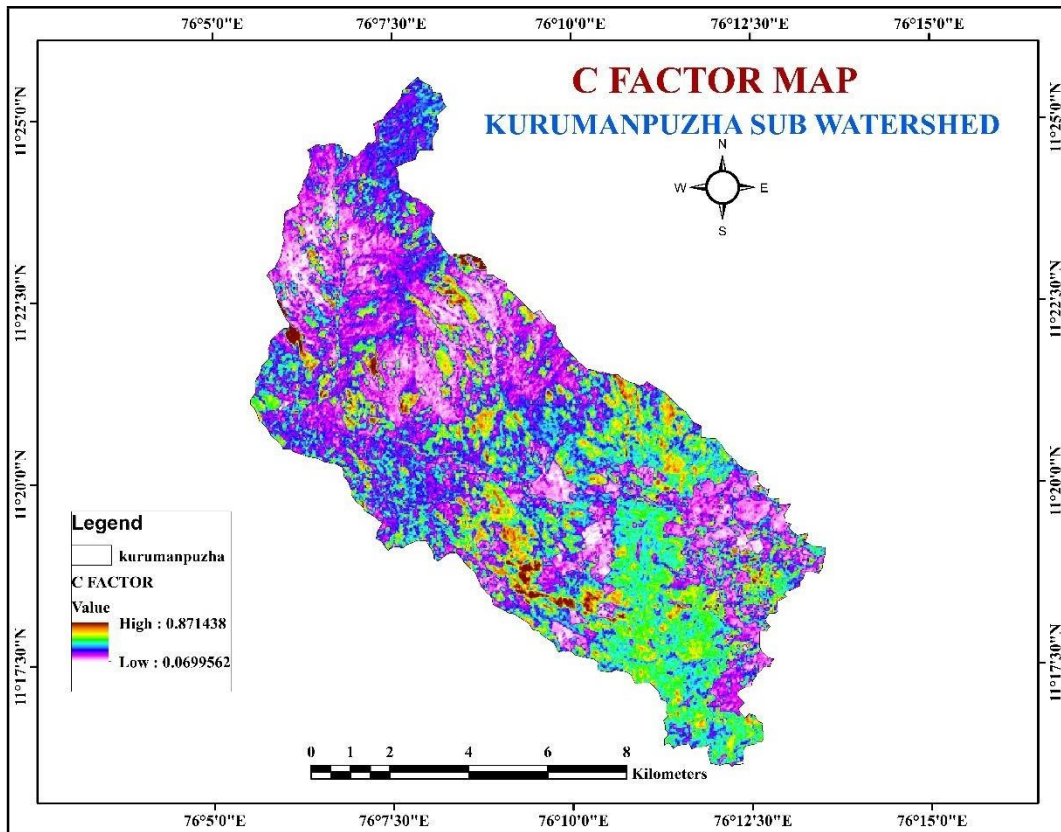


Fig.4.16 Spatial distribution of C factor of Kurumanpuzha sub watershed

The obtained C factor map was integrated with the LULC map to calculate the C factor for various land uses. The C factor value of different land uses given in Table 4.14 and Fig 4.17. From the map,, it was clear that water bodies and built-up and bare land areas have a greater C factor as it carries fewer NDVI values. Lands with vegetation have a lower C factor than built-up and bare areas because the NDVI values are comparatively high for the areas carrying high canopy cover. The results obtained were similar to those reported by Bayramov *et al.* (2013) and Thomas *et al.* (2017a).

Table 4.11 The variation of range of C factor with respect to the land use

Land uses	C factor range
Forest/Dense vegetation	0.186-0.252
Rubber	0.252-0.318
Coconut	0.318-0.384
Bare land	0.384-0.450
Scrub land	0.450-0.522
Crop land	0.522-0.616
Built/Urban area	0.616-0.871

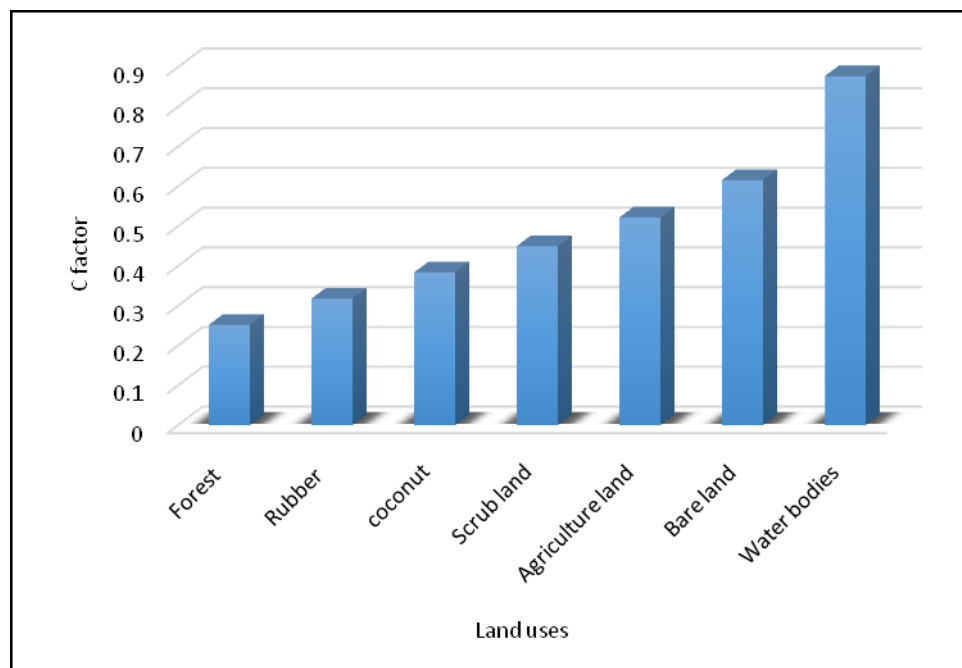


Fig.4.17 Spatial variation of C factor with respect to Land use

4.3.1.5 Conservation practice factor (P factor)

Most of the earlier studies related to RUSLE model gave the P-value for the entire watershed as '1' (Shiono *et al.*, 2002; Alexakis *et al.*, 2013). The current study considers slope and land use characteristics while calculating the P factor, as Wischmeier and Smith (1978) indicated.

By combining both slope and Land use/ land cover map by using the union tool in ArcGIS, the P factor map was generated. For agricultural areas, the P factor was assigned based on the slope of the land according to the guidelines by Wischmeier and Smith (1978) and for other land uses, the p factor was considered one. The P factor map obtained for the watershed is shown in Fig 4.18.

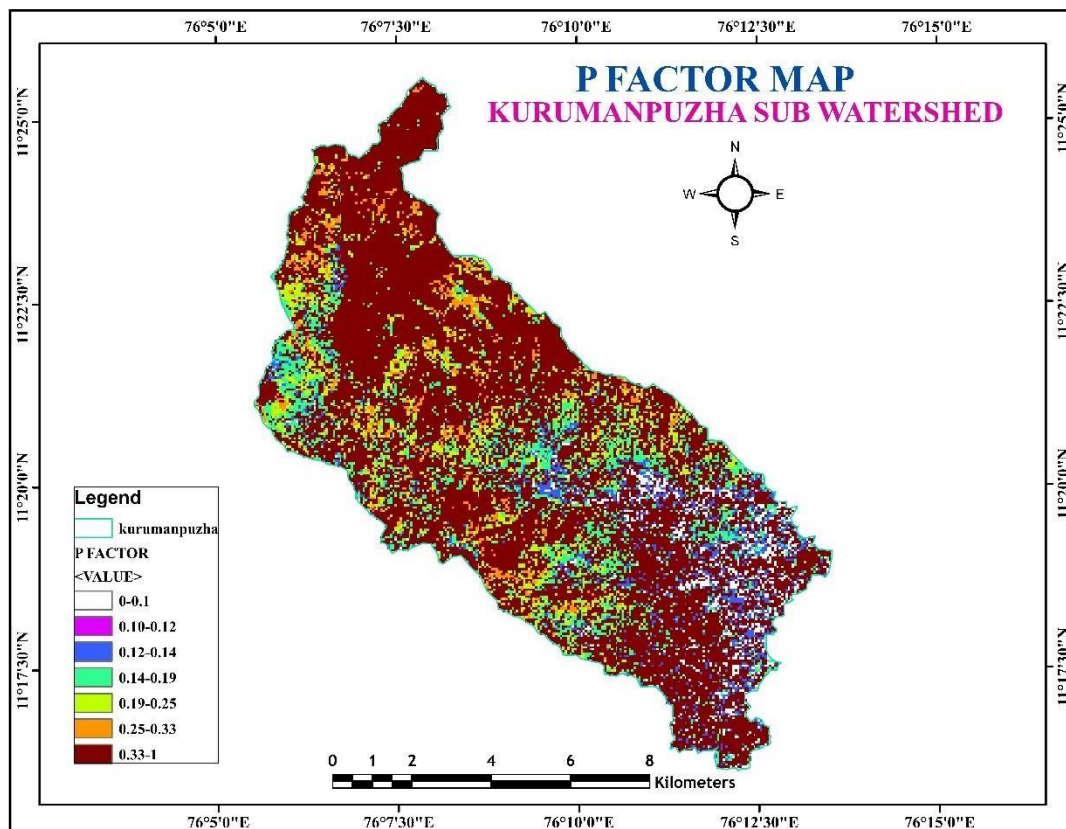


Fig.4.18 Spatial distribution of P factor for the watershed

4.3.2. Soil erosion risk assessment

To run the RUSLE model, R-factor value, K, LS, C, and P factor maps were layered using a raster calculator in a GIS environment.

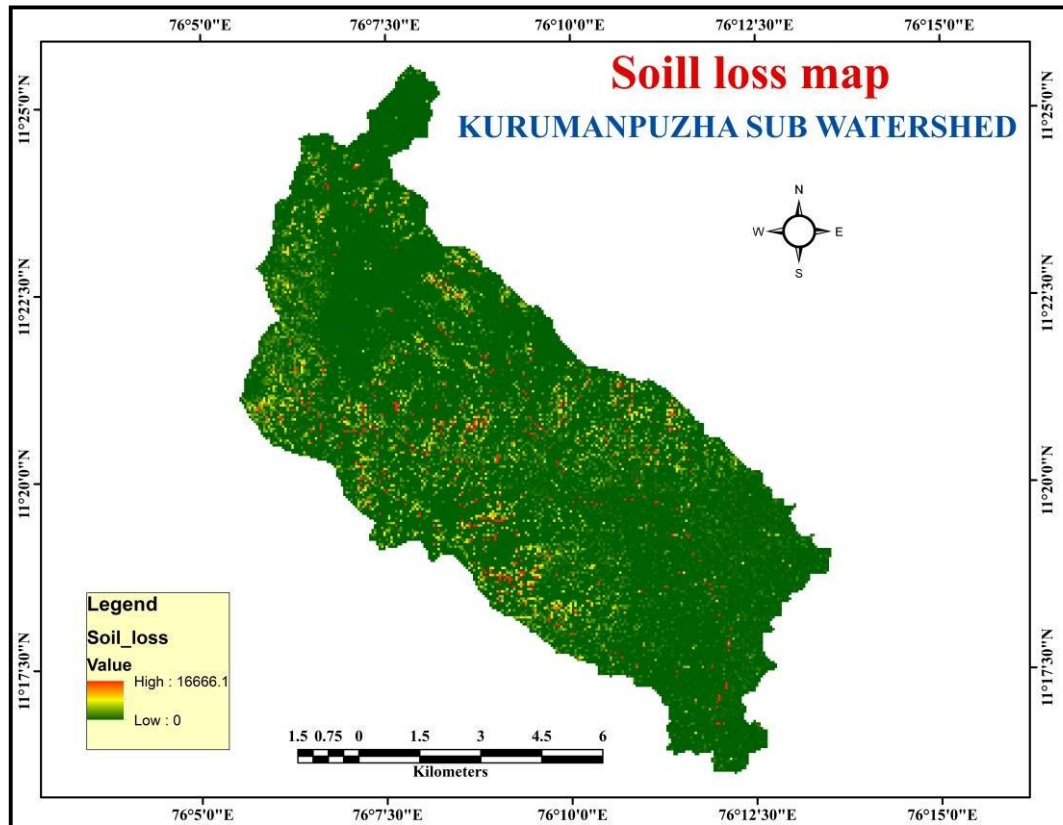


Fig.4.19 Soil loss map of Kurumanpuzha sub watershed

The average annual soil loss (A) for the watershed was calculated to be $8.00 \text{ t ha}^{-1} \text{ yr}^{-1}$ and the total quantity of soil eroded from the watershed $82,872.4 \text{ t yr}^{-1}$. The results of the soil erosion studies were consistent with those of other research conducted in different parts of Kerala with tropical climates and steep terrain. The higher values of pixels indicate the high erosion values and vice versa. It may be due to the land use and steeper slope in that area.

The study area was separated into 5 different soil erosion risk zones which are very slight ($<5 \text{ t ha}^{-1} \text{ yr}^{-1}$), slight ($5\text{-}15 \text{ t ha}^{-1} \text{ yr}^{-1}$), moderate ($15\text{-}30 \text{ t ha}^{-1} \text{ yr}^{-1}$), Severe ($30\text{-}50 \text{ t ha}^{-1} \text{ yr}^{-1}$), Very severe ($>50 \text{ t ha}^{-1} \text{ yr}^{-1}$). The result showed that about 78.79% of the watershed was in very slight erosion, 16.29% was in the slight class,

4.55% was in moderate, 0.28% was in severe and 0.07% of the land was under very severe erosion risk class. The reclassified map of the study area is shown in Fig 4.20.

Table 4.12 Soil erosion risk classification and area coverage

Soil erosion class	Soil loss (in t ha ⁻¹ yr ⁻¹)	Area (in ha)	Area (%)
Very slight	<5	8162.40	78.8
Slight	10-15	1687.67	16.3
Moderate	15-30	471.632	4.5
Severe	30-50	29.60	0.3
Very severe	>50	7.73	0.07

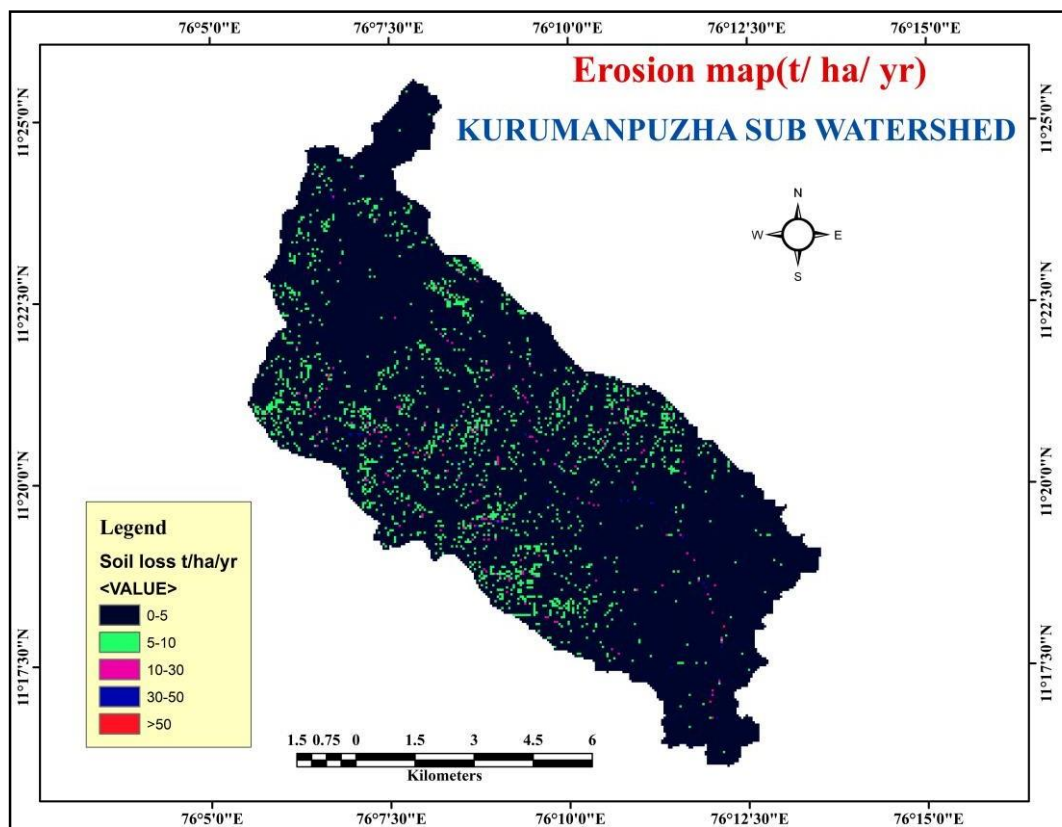


Fig. 4.20.Spatial distribution of soil erosion in Kurumanpuzha subwatershed

In comparison to the other studies performed in the Western Ghats similar results were obtained in the Kurumanpuzha subwatershed (Prasannakumar *et al.*, 2011a; Prasannakumar *et al.*, 2011b; Prasannakumar *et al.*, 2012; Pradeep *et al.*, 2014 and Thomas *et al.*, 2017a). The relatively lesser variation in soil loss observed in these studies is mainly due to the difference in rainfall distribution as well as land use characteristics.

The geomorphological characteristics of the watershed like stream frequency, drainage density, drainage texture, circulatory ratio, elongation ratio, compactness coefficient and length of overland flow indicate that the watershed is under very slight erosion risk. The results of erosion modelling using RUSLE also indicates that the major portion of the watershed is under very slight erosion risk.

4.2. SUGGESTION OF SUITABLE SOIL CONSERVATION AND MANAGEMENT PROTOCOL FOR THE WATERSHED

To preserve the production potential of soil, sustain productivity, and prevent soil erosion in a given area, soil conservation and management methods are to be adopted. These methods result in soil and water conservation, which contributes to groundwater recharge by increasing the rate of infiltration and increasing the opportunity time. Contour bunds, graded bunds, trenches, nalla bunds, check dams/gully plugs, and other agronomical and biological practices are examples of these measures.

The soil loss from different land uses, and different slope classes of the watershed were identified based on the procedure explained in section 3.10. and the results are given in Tables 4.13 and 4.14.

Table 4.13 Average annual soil loss (A in t ha⁻¹yr⁻¹) in different land uses

Land use/Landcover	Area (ha)	Area %	A
Bare land	138.96	1.34	8.55
Forest/Dense vegetation	5849.19	56.46	3.10
Rubber plantations	2078.64	20.06	3.94
Built/urban areas	28.35	0.27	3.60
Coconut	993.15	9.5	3.35
Scrub land	923.22	8.91	5.27
Crop land	279.45	2.69	2.72

Table 4.13 helps to conclude concerning the relation between the different land use/land cover and average annual soil loss using the average annual soil loss map. From the result, it is clearly shown that the soil erosion was high, i.e., 8.55 t ha⁻¹ yr⁻¹ with a standard deviation of 18.2 t ha⁻¹ yr⁻¹ in bare lands, which can be attributed to the fact that bare lands have no are less vegetation cover and conservation practices are less. Followed by the Scrubland where the soil loss was in the tune of 5.27 t ha⁻¹ yr⁻¹ with a standard deviation of 12.35 t ha⁻¹ yr⁻¹. The lowest values of A were found in forest, rubber, coconut/areacanut, and crop lands, which may be due to the farmers' canopy cover and conservation practices.

Table 4.14 Average annual soil loss (A) corresponds to different slope lands

Slope range in %	Area in ha	A in t ha ⁻¹ yr ⁻¹
0-3	527.08	4.215
3-10	2298.635	6.830
10-25	5245.74	7.826
25-50	2279.858	5.248
>50	4.97	1.566

Table 4.14 shows the results after combining the slope map and average annual soil loss map in ArcGIS environment. From the above table values,, it is very clear that average soil loss varies differently with respect to different slopes. The area with very gentle slope lands accounted for 527.08 ha, gently sloping accounts for 2298.635 ha, strongly sloping for 5245.74 ha, steeply slopes for 2279.858 ha and very strongly slopes for 4.97 ha out of the total area of the watershed respectively. The RUSLE model found that average soil loss from each slope land area is 4.215, 6.830, 7.826, 5.248, and 1.566 t ha⁻¹ yr⁻¹ respectively. As the slope increases, the erosion is more, but the area covered is less so in this watershed, lands with a a slope of 10-25% range are more prone to erosion.

Considering the current study results from varying slope ranges, the following soil conservation measures are suggested for the study area:

1. For slopes ranging between 0-3%, having a slight slope with very slight and slight erosion, soil conservation measures such as agronomical measures including contour farming, intercropping, strip cropping, tillage practice, and mulching are suggested.
2. For slopes ranging between 3-10%, with a gentle slope with moderate erosion, mechanical measures such as contour bunds are suggested as soil conservation measures.
3. Since the watershed has an annual rainfall of 2419 mm, Graded bunds are suggested
4. Slope ranging between 10-25% amounts to a major portion of the study area. Inward sloping bench terracing is suggested for this study area facing moderate soil erosion and graded bunds for selected patches of lesser soil erosion.
5. Slopes ranging from 25-50% occupy a considerable area of the study watershed. This area is composed of either forest or rubber and farmers have already adopted terracing as conservation measures in that area .
6. Slopes >50% is composed of forest area. Due to negligible soil erosion, no soil conservation measure is suggested.
7. Since the length of overland flow is less and Channel flow is predominant in the watershed. Even though RUSLE modelling doesn't estimate channel erosion or gully erosion, drainage line treatments are to be given in the watershed.
8. For the first order streams, check dams, loose stone brush wood, and log brush wood

dams are suggested.

9. For higher order streams permanent check dams along the drainage lines are suggested.

10. Steep slopes can also be stabilised by constructing logwood crib structures filled with stone/brushwood.

Field measurements on a long term basis are required to validate the results of erosion models. Since the study was conducted during the covid pandemic and lock down field validation of model results could not be performed well.

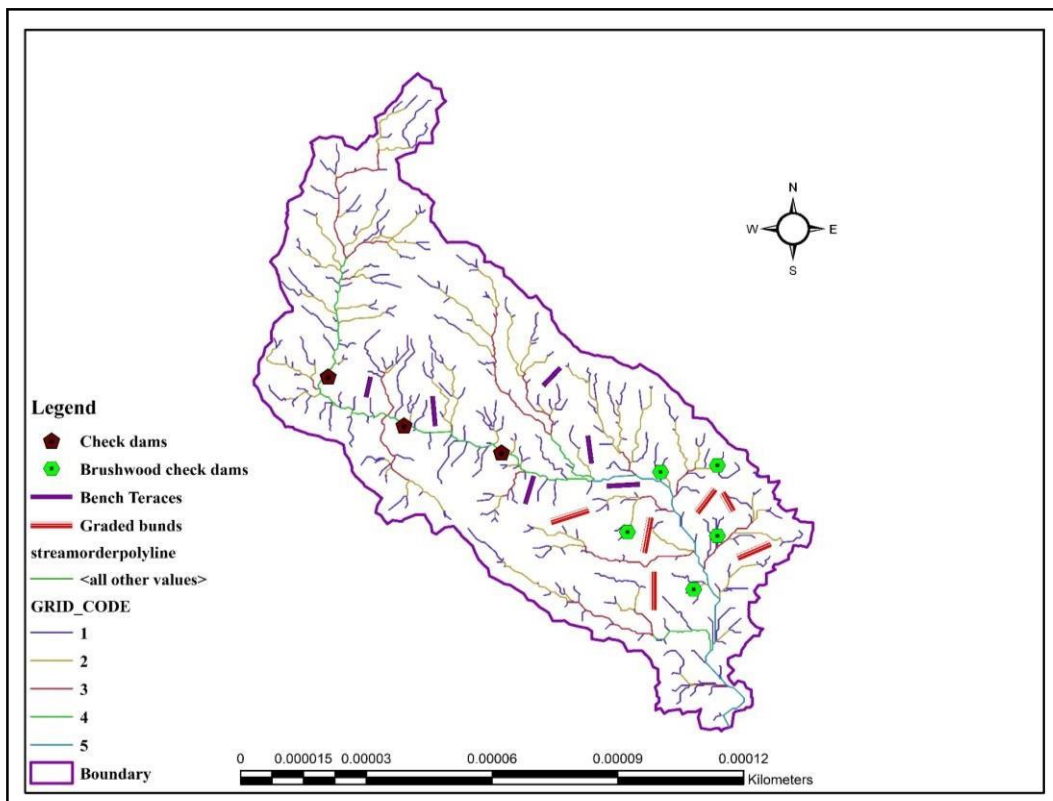


Fig.4.21 Soil conservation measures suggested for the study area

SUMMARY AND CONCLUSIONS

CHAPTER -V

SUMMARY AND CONCLUSION

Soil is the topmost weathered and disintegrated layer of the earth's crust that is made of minerals and organic substances with the potential of sustaining plant life. Soil depth varies from place to place from zero to several meters. However, the top 30 cm of soil depth is extremely beneficial to both humans and animal life. The top layer of soil is frequently subjected to the effects of atmospheric activities. Wind and water are the two primary active forces responsible for dislodging the top soil layer and transporting it from one location to another. Erosion is a recognisable intrinsic, natural process, but it is magnified in many places by human activity. Poor land use practices are always a major cause of soil erosion. Erosion-producing land activities include deforestation, overgrazing, unmanaged construction activities, etc. The GIS technology with remote sensing data, which can provide more reliable predictions, was used in this study because conventional methods to estimating soil erosion rate are very expensive and time consuming.

The present study was undertaken in the Kurumanpuzha sub watershed of the Chaliyar river basin, Kerala to estimate the soil loss with the existing land use and management practices in a sub watershed of Chaliyar river basin and to identify erosion prone areas for implementation of best management practices and policy decisions. Kurumanpuzha sub watershed is located between 11^o17'30" North, 76^o7'0" East and 11^o23'0" North, 76^o12'30" East Chaliyar river basin in middle part of Chaliyar river basin in Malappuram district of Kerala, covering an area of 103.6 km².

In this investigation, watershed was delineated using ArcGIS 10.2 and an effort was made to emphasize the use of RS and GIS for the prediction of soil loss from the sub watershed and to identify the erosion prone areas in order to suggest some suitable soil erosion conservation and management protocol for the watershed. The remote sensing data of research area was derived from Landsat 8 satellite imagery, which was downloaded from the official Bhuvan and USGS earthexplorer websites. The soil map of the research area obtained from the Department of Soil Survey and Soil Conservation served as an input data for estimating soil loss, from which soil erodibility map was prepared.

From the geomorphological analysis it can be concluded that The Kurumanpuzha sub watershed is of 5th order type, with a dendritic drainage pattern indicating textural homogeneity and a lack of structural control. The watershed's maximum length and width were 19.084 km and 9.2km, respectively. Different morphometric parameters determined can be grouped as Linear, areal, relief aspects. The linear aspect viz., stream number (N_u), stream order (U), average basin width (B), basin length (L_b), mean stream length (L_u), stream length (L), stream length ratio (R_L) bifurcation ratio (R_b). Areal aspects viz., drainage area (A), drainage density (D_d), form factor (R_f), stream frequency (F), drainage texture (D_t), circulatory ratio (R_c), compactness coefficient (C_c), elongation ratio (R_e), texture ratio (R_t). Length of overland flow (L_g). Relief aspects viz., maximum watershed relief (H), relief ratio (R_r), relative relief (R_R), time of concentration (T_c) and ruggedness number (R_n).

When the logarithm of the number of streams is plotted against the stream order, a straight line was obtained, confirming Horton's law, which states that the number of stream segments in the drainage network has a linear relationship with the stream order. A low Bifurcation ratio (2.05) indicated less structural disturbance in the watershed and that the drainage pattern has not changed as a result of structural disturbance.

The drainage density was approximately 2.392 km km^{-3} , indicating that the region has very fine drainage texture. The stream frequency was found to be around 5.637 km^{-2} , indicating that the study basin had a high stream frequency.

The maximum watershed relief (H), relative relief (R_R), and relief ratio (R_r) were discovered to be 2307 m, 3.82 and 0.12 respectively. A lower relief ratio value indicates the presence of exposed rocks in the form of higher ridges and mounds with a steeper slope. The hypsometric integral shows the watershed was in equilibrium stage.

Most of the watershed area comes under a strongly sloping class (50.67% of total study area) followed by gently sloping land (22.20% of total study area). Both strongly sloping and steeply sloping areas are distributed over the entire sub watershed. Only a few parts of the sub watershed have a gentle slope (5.09% of total land area).

Out of total watershed area, Forest/Dense vegetation, Rubber, Coconut/Areca nut, Scrub land, Crop land, Bare land, Water bodies, Built up/Urban areas occupy about 56.46%, 20.06%, 9.5%, 8.91%, 2.69%, 1.34%, 0.64% and 0.27% of the

total area respectively.

Five soil associations were identified in the study area. They are Mannamkulam-kuttil-Angadipuram, Nadukani–kalvarikunnu-pullangod, Arimbra- karuvarakundu-churathinmel, Vettekode-koramala-vazhikad, Walakkad- kurumbramala. These soil associations occupy 29.10%, 22.11%, 21.82%, 16.44%, and 22.11% of the total. Sandy clay loam forms the major soil group in the watershed and followed by clay loam.

The geomorphological characters of the watershed like stream frequency, drainage density, drainage texture, circulatory ratio, elongation ratio, compactness coefficient and length of overland flow indicates that watershed is under very slight erosion risk.

For the RUSLE model to run, map layers corresponding to the R, K, LS, C, and P factors were created and analysed for spatial variation within the watershed. The rainfall data was collected from IMD Pune for the year 2000 to 2020 and the soil related data were collected from the Department of soil survey and soil conservation. The slope and vegetation related parameters were derived from the remote sensing data viz. digital elevation models and Landsat 8 satellite imageries. The average value of R factor estimated using the monthly rainfall data of the years 2000 to 2020 was $9310.538 \text{ MJ cm ha}^{-1} \text{ h}^{-1} \text{ y}^{-1}$. The estimated K factor ranged from 0.25 to $0.53 \text{ t ha h ha}^{-1} \text{ MJ}^{-1} \text{ mm}^{-1}$. The majority of the watershed has an LS factor ranging from 0 to 0.38, indicating slight erosion.

The C factor was calculated using the NDVI values derived from the satellite imageries. The obtained C values ranged from 0.0699 to 0.87 depending on the NDVI values. The P factor was calculated by assigning values found from the literature according to land use as well as percentage slope.

The average annual soil loss was calculated by multiplying the developed raster files for each RUSLE factors. The average annual soil loss was estimated to be $8.00 \text{ t ha}^{-1} \text{ yr}^{-1}$ and the total quantity of soil eroded from the watershed was $82,872.4 \text{ t yr}^{-1}$. Based on the RUSLE model, there were five erosion classes identified in the study area they are 0-5, 5-10, 10-30, 30-50 and $> 50 \text{ t ha}^{-1} \text{ yr}^{-1}$. Out of which 78.8% of the area experienced very slight erosion, 16.3% were under slight erosion, and 4.5% were under moderate erosion severity class. The percentage under severe erosion range was 0.3% and under very severe erosion range was 0.07%.

Based on the erosion classes and slope of the watershed soil conservation measures were suggested by using the guidelines of NBSSLUP & CSWCRTI (2014).

1. For slopes ranging between 0-3%, having slight slope with very slight and slight erosion, soil conservation measures such as agronomical measures which includes contour farming, intercropping, strip cropping, tillage practice, mulching are suggested.
2. For slopes ranging between 3-10%, with a gentle slope with moderate erosion, mechanical measures such as contour bunds are suggested as soil conservation measures. Since the watershed has annual rainfall of 2419 mm Graded bunds are suggested
3. Slope ranging between 10-25% amounts to major portion of the study area. Inward sloping bench terracing is suggested for this study area facing moderate soil erosion along with graded bunds for selected patches of lesser soil erosion.
4. Slopes ranging from 25-50% occupies considerable area of the study watershed. This area is composed of either forest or rubber and farmers have already adopted terracing as conservation measures in that area.
5. Slopes >50% is composed of forest area. Due to negligible soil erosion, no soil conservation measure is suggested.
6. Since length of overland flow is less and Channel flow is predominant in the watershed. Even though RUSLE modelling doesn't estimate channel erosion or gully erosion, drainage line treatments are to be given in the watershed.
7. For the first order streams, check dams, loose stone brush wood, and log brush wood dams. For higher order streams permanent check dams along the drainage lines are suggested. Steep slopes can also be stabilised by construction of logwood crib structures filled with stone/brushwood.

Scope of future work

The following are the suggestions for future work

1. Comparison of erosion using slope maps derived from different DEMs can be done.
2. Gridded rainfall data and gridded soil data can be used to detailed spatial representation of erosion.
3. Validation of model by field measurements on a long term basis can be done to evaluate

the model performance.

REFERENCES

REFERENCES

- Abdel Rahman, M.A., Natarajan, A., Srinivasamurthy, C.A. and Hegde, R. 2016. Estimating soil fertility status in physically degraded land using GIS and remote sensing techniques in Chamarajanagar district, Karnataka, India. *The Egyptian J. Remote Sensing and Space Sci.* 19(1), : 95-108.
- Abdo, H. and Salloum, J. 2017. Mapping the soil loss in Marqya basin: Syria using RUSLE model in GIS and RS techniques. *Envi. Earth Sci.* 76(3). p.114.
- Al-Ali, A. M. A. 2016. *Temperature effects on fine-grained soil erodibility* (Doctoral dissertation, Kansas State University).
- Ali, U. and Ali, S.A., 2014. Analysis of drainage morphometry and watershed prioritization of Romushi-Sasar catchment, Kashmir Valley, India using remote sensing and GIS technology. *Int. J. of Adv. Res.* 2(12), pp.5-23.
- Alexakis, D.D., Hadjimitsis, D.G. and Agapiou, A. 2013. Integrated use of remote sensing, GIS and precipitation data for the assessment of soil erosion rate in the catchment area of “Yialias” in Cyprus. *Atmos. Res.* 13:108-124.
- Alexandridis, T. K., Sotiropoulou, A. M., Bilas, G., Karapetsas, N. and Silleos, N. G. 2015. The effects of seasonality in estimating the C-factor of soil erosion studies. *Land Degradation & Development.* 26(6) :596-603.
- Alewell, C., Borrelli, P., Meusburger, K. and Panagos, P., 2019. Using the USLE: Chances, challenges and limitations of soil erosion modelling. *Int. soil and water Conserv. Res.*, 7(3), pp.203-225.
- Ali, U. and Ali, S. A. 2014. Analysis of drainage morphometry and watershed prioritization of Romushi-Sasar catchment, Kashmir Valley, India using remote sensing and GIS technology. *Int. J. Adva. Res.* 2(12):5-23.
- Alkharabsheh, M. M., Alexandridis, T. K., Bilas, G., Misopolinos, N. and Silleos, N. 2013. Impact of land cover change on soil erosion hazard in northern Jordan using remote sensing andGIS. *Procedia Envi. Sci.* 19:912-921.
- Amdihun, A., Gebremariam, E., Rebelo, L.M. and Zeleke, G., 2014. Suitability and scenario

- modeling to support soil and water conservation interventions in the Blue Nile Basin, Ethiopia. *Environ. Syst. Res.*, 3(1), pp.1-13.
- Amore, E., Modica, C., Nearing, M.A. and Santoro, V.C. 2004. Scale effect in USLE and WEPP application for soil erosion computation from three Sicilian basins. *J. Hydrology*, 293:100-114.
- Arekhi, S., Niazi, Y. and Kalteh, A.M. 2012. Soil erosion and sediment yield modeling using RS and GIS techniques: a case study, Iran. *Arabian J. Geosciences*, 5(2):285-296.
- Arekhi, S., Shabani, A. and Rostamizad, G. 2012. Application of the modified universal soil loss equation (MUSLE) in prediction of sediment yield (Case study: Kengir Watershed, Iran). *Arabian J. Geosciences*. 5(6):1259-1267.
- Arnaez, J., Lasanta, T., Ruiz-Flaño, P. and Ortigosa, L. 2007. Factors affecting runoff and erosion under simulated rainfall in Mediterranean vineyards. *Soil and Tillage Res.* 93(2):324-334.
- Arnoldus, H. M. J. 1977. Methodology used to determine the maximum potential average annual soil loss due to sheet and rill erosion in Morocco.
- Arnoldus, H.M.J. 1980. An approximation of the rainfall factor in the Universal Soil Loss Equation. *An approximation of the rainfall factor in the Universal Soil Loss Equation.*, :127-132.
- Bahadur, K. K. 2009. Mapping soil erosion susceptibility using remote sensing and GIS: a case of the Upper Nam Wa Watershed, Nan Province, Thailand. *Envi. Geol.* 57(3):695-705.
- Balasubramanian, A. 2017. Soil erosion—causes and effects. *Centre for Advanced Studies in Earth Science, University of Mysore, Mysore.*
- Barger, N.N., Herrick, J.E., Van Zee, J. and Belnap, J. 2006. Impacts of biological soil crust disturbance and composition on C and N loss from water erosion. *Biogeochemistry.*, 77(2):247-263.
- Barman, B.K., Rao, K.S., Sonowal, K., Prasad, N.S.R. and Sahoo, U.K., 2020. Soil erosion assessment using revised universal soil loss equation model and geo-spatial technology:

- A case study of upper Tuirial river basin, Mizoram, India. *AIMS Geosciences*, 6(4), pp.525-545.
- Basic, F., Kistic, I., Mesic, M., Nestroy, O. and Butorac, A. 2004. Tillage and crop management effects on soil erosion in central Croatia. *Soil and Tillage Res.* 78(2):197-206.
- Bayramov, E., Buchroithner, M. F. and McGurty, E. 2013. Differences of MMF and USLE models for soil loss prediction along BTC and SCP pipelines. *J. Pipeline Syst. Engineer.Practice.* 4(1) :81-96.
- Belasri, A. and Lakhouili, A. 2016. Estimation of soil erosion risk using the universal soil loss equation (USLE) and geo-information technology in Oued El Makhazine Watershed, Morocco. *J. Geograph. Info. Syst.* 8(1):98.
- Belayneh, M., Yirgu, T. and Tsegaye, D. 2019. Potential soil erosion estimation and area prioritization for better conservation planning in Gumara watershed using RUSLE and GIS techniques'. *Envi. Systems Res.* 8(1):1-17.
- Bhattacharai, R. and Dutta, D. 2007. Estimation of soil erosion and sediment yield using GIS at catchment scale. *Water Resources Management.*, 21(10):1635-1647.
- Biswas, S. S. and Pani, P. 2015. Estimation of soil erosion using RUSLE and GIS techniques: a case study of Barakar River basin, Jharkhand, India. *Modeling Earth Systems and Environment.*, 1(4):1-13.
- Biswas, S., 2012. Estimation of soil erosion using remote sensing and GIS and prioritization of catchments. *Int. J. Emerging Technol. Advanced Engineer.* 2(7):124-128.
- Borrelli, P., Alewell, C., Alvarez, P., Anache, J. A. A., Baartman, J., Ballabio, C., Bezak, N., Biddoccu, M., Cerdà, A., Chalise, D. and Chen, S. 2021. Soil erosion modelling: A global review and statistical analysis. *Sci. Total environment.* :146494.
- Borrelli, P., Panagos, P., Ballabio, C., Lugato, E., Weynants, M. and Montanarella, L. 2016. Towards a pan-European assessment of land susceptibility to wind erosion. *Land Degradation & Development.* 27(4):1093-1105.
- Borrelli, P., Robinson, D.A., Panagos, P., Lugato, E., Yang, J.E., Alewell, C., Wuepper, D., Montanarella, L. and Ballabio, C. 2020. Land use and climate change impacts on global

- soil erosion by water (2015-2070). *Proceedings of the National Academy of Sciences*. 117(36):21994-22001.
- Borrelli, P., Robinson, D.A., Fleischer, L.R., Lugato, E., Ballabio, C., Alewell, C., Meusburger, K., Modugno, S., Schütt, B., Ferro, V. and Bagarello, V., 2017. An assessment of the global impact of 21st century land use change on soil erosion. *Nature communications*, 8(1), pp.1-13.
- Brodie, I. and Rosewell, C. 2007. Theoretical relationships between rainfall intensity and kinetic energy variants associated with stormwater particle wash off. *J. Hydrology*. 340(1):40-47.
- Busari, M. A., Kukal, S. S., Kaur, A., Bhatt, R. and Dulazi, A. A. 2015. Conservation tillage impacts on soil, crop and the environment. *Int. Soil and water conservation res.* 3(2):119-129.
- Chandrashekar, H., Lokesh, K.V., Sameena, M. and Ranganna, G. 2015. GIS-based morphometric analysis of two reservoir catchments of Arkavati River, Ramanagaram District, Karnataka. *Aquatic Proceedings.*, 4:1345-1353.
- Choudhari, P.P., Nigam, G.K., Singh, S.K. and Thakur, S. 2018. Morphometric based prioritization of watershed for groundwater potential of Mula river basin, Maharashtra, India. *Geol. Ecol. Landscapes*. 2(4) :256-267.
- Cooper, K. 2011. Evaluation of the relationship between the RUSLE R-Factor and mean annual precipitation. *Colorado State University, Fort Collins*.
- Demirci, A. and Karaburun, A. 2012. Estimation of soil erosion using RUSLE in a GIS framework: a case study in the Buyukcekmece Lake watershed, northwest Turkey. *Envi. Earth Sci.* 66(3):903-913.
- Djoukbal, O., Mazour, M., Hasbaia, M. and Benselama, O. 2018. Estimating of water erosion in semiarid regions using RUSLE equation under GIS environment. *Envi. Earth sci.* 77(9):1-13.
- Durán Zuazo, V. H., Rodríguez Pleguezuelo, C. R., Francia Martínez, J. R. and Martín Peinado, F. J. 2013. Land-use changes in a small watershed in the Mediterranean landscape (SE Spain): environmental implications of a shift towards subtropical crops.

J. Land UseSci. 8(1):47-58.

- Dutta, D., Das, S., Kundu, A. and Taj, A. 2015. Soil erosion risk assessment in Sanjal watershed, Jharkhand (India) using geo-informatics, RUSLE model and TRMM data. *Modeling Earth systems and environment*, 1(4), :1-9.
- Dvorák, J. and Novák, L. 1994. *Soil conservation and silviculture*. Elsevier.
- Elias, E.A., Cichota, R., Torriani, H.H. and De Jong Van Lier, Q. 2004. Analytical soil–temperature model: Correction for temporal variation of daily amplitude. *Soil Sci. Society of America J.* 68(3):784-788.
- El-Swaify, S. A. and Dangler, E.W. 1976. Erodibilities of selected tropical soils in relation to structural and hydrologic parameters.
- Eltaif, N. I. Gharaibeh, M. A. Al-Zaitawi, F. and Alhamad, M. N. 2010. Approximation of rainfall erosivity factors in North Jordan. *Pedosphere*, 20(6):711-717.
- Farhan, Y. and Nawaiseh, S. 2015. Spatial assessment of soil erosion risk using RUSLE and GIS techniques. *Envi. Earth Sci.* 74(6):4649-4669.
- Farhan, Y., Zregat, D. and Farhan, I. 2013. Spatial estimation of soil erosion risk using RUSLE approach, RS, and GIS techniques: a case study of Kufranja watershed, Northern Jordan. *J. Water Resource and Protection.*, 5(12):1247.
- Ferro, V., Giordano, G. and Iovino, M., 1991. Isoerosivity and erosion risk map for Sicily. *Hydrol. Sci. J.*, 36(6), pp.549-564.
- Flanagan, D. C., Ascough II, J. C., Nieber, J. L. Misra, D. and Douglas-Mankin, K. R. 2013. Advances in soil erosion research: Processes, measurement, and modelling. *Transactions of the ASABE.* 56(2):455-463.
- Ganasri, B.P. and Ramesh, H. 2016. Assessment of soil erosion by RUSLE model using remote sensing and GIS-A case study of Nethravathi Basin. *Geoscience Frontiers.*, 7(6):953-961.
- Gessesse, B., Bewket, W. and Bräuning, A. 2015. Model-based characterization and monitoring of runoff and soil erosion in response to land use/land cover changes in the Modjo watershed, Ethiopia. *Land degradation & development.*, 26(7):711-724.

- Graaff, J. D. 1993. *Soil conservation and sustainable land use: an economic approach*.
- Guerra, C.A., Rosa, I., Valentini, E., Wolf, F., Filipponi, F., Karger, D.N., Nguyen Xuan, A., Mathieu, J., Lavelle, P. and Eisenhauer, N., 2020. Global vulnerability of soil ecosystems to erosion. *Landscape Ecol.*, 35(4), pp.823-842.
- Guha, S. 2015. Mathematical analysis of Solani Watershed, North India. *Int. J. Geomatics and Geosci.* 6(2) :1512-1529.
- Handbook of Agriculture. 2009. Sixth (Revised) Edition, Directorate of Information and Publications of Agriculture, Indian Council of Agricultural Research, New Delhi-12.
- Hao, C. H. E. N., Oguchi, T. and Pan, W.U. 2017. Assessment for soil loss by using a scheme of alterative sub-models based on the RUSLE in a Karst Basin of Southwest China. *J. Integrative Agric.* 16(2):377-388.
- Haregeweyn, N., Fikadu, G., Tsunekawa, A., Tsubo, M. and Meshesha, D.T. 2012. The dynamics of urban expansion and its impacts on land use/land cover change and small-scale farmers living near the urban fringe: A case study of Bahir Dar, Ethiopia. *Landscape and urban planning.* 106(2):149-157.
- Haregeweyn, N., Tsunekawa, A., Nyssen, J., Poesen, J., Tsubo, M., Tsegaye Meshesha, D., Schütt, B., Adgo, E. and Tegegne, F. 2015. Soil erosion and conservation in Ethiopia: a review. *Progress in Physical Geography.* 39(6):750-774.
- Horton, R. E. 1932. Drainage-basin characteristics. *Eos, transactions american geophysical union*, 13(1):350-361.
- Horton, R. E. 1945. Erosional development of streams and their drainage basins; hydrophysical approach to quantitative morphology. *Geological society of America bulletin*, 56(3):275-370.
- Huang, C.H., Wells, L.K. and Norton, L.D. 1999. Sediment transport capacity and erosion processes: Model concepts and reality. *Earth Surface Processes and Landforms: The J. The British Geomorphological Research Group.* 24(6):503-516.

- Hurni, H. 1985. Soil conservation manual for Ethiopia. First draft. Ministry of Agriculture. *Natural Resources Conservation and Development Department, Community Forests and Soil Conservation Development Department. Addis Ababa.*
- Hurni, H. 1986. *Guidelines for development agents on soil conservation in Ethiopia.* Community Forests and Soil Conservation.
- Hurni, H., Herweg, K., Portner, B. and Liniger, H. 2008. Soil erosion and conservation in global agriculture. In *Land use and soil resources.* Springer, Dordrecht. : 41-71
- Igwe, P. U., Onuigbo, A. A., Chinedu, O. C., Ezeaku, I. I. and Muoneke, M. M. 2017. Soil erosion: a review of models and applications. *Int. J. Adva. Engineer. Res. Sci.* 4(12):237341.
- Jackson, W. L., Gebhardt, K. and Van Haveren, B. P. 1986. Use of the modified universal soil loss equation for average annual sediment yield estimates on small rangeland drainage basins. *IAHS-AISH publication.* (159):413-423.
- Jain, S. K., Kumar, S. and Varghese, J. 2001. Estimation of soil erosion for a Himalayan watershed using GIS technique. *Water Resources Management*, 15(1):41-54.
- Kabite, G. and Gessesse, B. 2018. Hydro-geomorphological characterization of Dhidhessa River basin, Ethiopia. . *Int. Soil and Water Conservation Res.* 6(2):175-183.
- Kalambukattu, J. and Kumar, S. 2017. Modelling soil erosion risk in a mountainous watershed of Mid-Himalaya by integrating RUSLE model with GIS. *Eurasian J. Soil Sci.* 6(2) :92-105.
- Kandel, D. D., Western, A.W., Grayson, R. B. and Turrall, H. N. 2004. Process parameterization and temporal scaling in surface runoff and erosion modelling. *Hydrological Processes.* 18(8):1423-1446.
- Kartic, K. M., Annadurai, R. and Ravichandran, P. T. 2014. Assessment of soil erosion susceptibility in Kothagiri Taluk using revised universal soil loss equation (RUSLE) and geo-spatial technology. *Int. J. Sci. Res. Public.* 4 :10-13.
- Karthick, P., Lakshumanan, C. and Ramki, P., 2017. Estimation of soil erosion vulnerability in Perambalur Taluk, Tamilnadu using revised universal soil loss equation model (RUSLE) and geo information technology. *Int. Res. J. Earth Sci.*, 5(8), pp.8-14.

- Kathiravelu, G., Lucke, T. and Nichols, P., 2016. Rain drop measurement techniques: a review. *Water*, 8(1), p.29.
- Kayet, N., Pathak, K., Chakrabarty, A. and Sahoo, S. 2018. Evaluation of soil loss estimation using the RUSLE model and SCS-CN method in hillslope mining areas. *Int. Soil and Water Conservation Res.* 6(1):31-42.
- Kebede, Y. S., Endalamaw, N. T., Sinshaw, B. G. and Atinkut, H. B. 2021. Modeling soil erosion using RUSLE and GIS at watershed level in the upper beles, Ethiopia. *Envi. Challenges*, 2:100009.
- Keesstra, S. D., Bouma, J., Wallinga, J., Tittonell, P., Smith, P., Cerdà, A., Montanarella, L., Quinton, J. N., Pachepsky, Y., Van Der Putten, W. H. and Bardgett, R. D. 2016. The significance of soils and soil science towards realization of the United Nations Sustainable Development Goals. *Soil*. 2(2):111-128.
- Keesstra, S. D., Davis, J., Masselink, R. H., Casali, J., Peeters, E.T. and Dijkema, R. 2019. Coupling hysteresis analysis with sediment and hydrological connectivity in three agricultural catchments in Navarre, Spain. *J. of Soils and Sediments*. 19(3):1598-1612.
- Keno, K. and Suryabagavan, K.V. 2014. Multi-temporal remote sensing of landscape dynamics and pattern change in Dire district, Southern Ethiopia. *J. Geom.* 8(2):189-194.
- Kim, H.S. and Julien, P.Y. 2006. Soil erosion modeling using RUSLE and GIS on the IMHA Watershed. *Water Engineer. Res.* 7(1).29-41.
- Kouli, M., Soupios, P. and Vallianatos, F. 2009. Soil erosion prediction using the revised universal soil loss equation (RUSLE) in a GIS framework, Chania, Northwestern Crete, Greece. *Envi. Geol.* 57(3):483-497.
- Krishna, V.S., Lakshmi, S.J. and Ramana, M.V., 2018. Estimation of soil and water conservation measures in micro-watershed. *J. Pharmacognosy and Phytochemistry*, 7(5), pp.2600-2604.
- Krois, J. and Schulte, A., 2014. GIS-based multi-criteria evaluation to identify potential sites for soil and water conservation techniques in the Ronquillo watershed, northern Peru. *Applied Geogr.*, 51, pp.131-142.

- Laflen, J. M. and Roose, E. J. 1998. Methodologies for assessment of soil degradation due to water erosion. *Methods for assessment of soil degradation*, pp. 31-55.
- Lampurlanés, J. and Cantero-Martínez, C. 2003. Soil bulk density and penetration resistance under different tillage and crop management systems and their relationship with barley root growth. *Agron. J.* 95(3). 526-536.
- Le Bissonnais, Y., Renaux, B. and Delouche, H. 1995. Interactions between soil properties and moisture content in crust formation, runoff and inter rill erosion from tilled loess soils. *Catena.* 25(1-4):33-46.
- L.G.K. Naidu, A.K. Sikka, S. Srinivas, V. Selvi, P. Krishnan, D.V. Singh, Dipak Sarkar, S.K. Singh, M. Madhu and P.K. Mishra (2014). Soil Erosion of Kerala. *NBSS Publ.* 163, NBSS&LUP, Nagpur, p 36.
- Libin, B. S., Sukanya, S. N., Thrivikramji, K. P. and Chrips, N. R. 2019. Geomatics Model of Soil Erosion in Chittar Sub-Watersed, Vamanapuram River Basin, Kerala, India. *InternationalResearch Journal of Engineering and Technology*, 6(3) :1658-1664.
- Liu, B. Y., Nearing, M. A. and Risse, L. M. 1994. Slope gradient effects on soil loss for steep slopes. *Transactions of the ASAE*, 37(6):1835-1840.
- Liu, B. Y., Nearing, M. A., Shi, P. J. and Jia, Z. W. 2000. Slope length effects on soil loss for steep slopes.
- Lu, D., Li, G., Valladares, G. S. and Batistella, M. 2004. Mapping soil erosion risk in Rondonia, Brazilian Amazonia: using RUSLE, remote sensing and GIS. *Land degradation & development.* 15(5). 499-512.
- Mahadevaswamy, G., Nagaraju, D., Siddalingamurthy, S., Nagesh, P. C. and Rao, K. 2011. Morphometric analysis of Nanjangud taluk, Mysore District, Karnataka, India, using GIS Techniques. *Int. J. Geomatics and Geosci.* 1(4) :721-734.
- Maitra, S. and Pramanick, B. Causes and Effect of Soil Erosion and its Preventive Measures.
- Mandal, D. and Sharda, V.N., 2013. Appraisal of soil erosion risk in the Eastern Himalayan region of India for soil conservation planning. *Land Degradation & Dev*, 24(5), pp.430-437.

- Markose, V. J. and Jayappa, K. S. 2016. Soil loss estimation and prioritization of sub-watersheds of Kali River basin, Karnataka, India, using RUSLE and GIS. *Envi. Monitor. Assess.* 188(4):225.
- Mati, B. M., Morgan, R. P., Gichuki, F. N., Quinton, J. N., Brewer, T. R. and Liniger, H. P. 2000. Assessment of erosion hazard with the USLE and GIS: A case study of the Upper Ewaso Ng'iro North basin of Kenya. *Int. J. A: Earth Observation and Geoinfo.* 2(2):78-86.
- McCool, D. K. and Renard, K. G. 1990. Water erosion and water quality. In *Advances in soil science*. Springer, New York, NY.pp :175-185
- McCool, D. K., Brown, L. C., Foster, G. R., Mutchler, C. K. and Meyer, L. D. 1987. Revised slope steepness factor for the Universal Soil Loss Equation. *Transactions of the ASAE*, 30(5):1387-1396.
- McCool, D. K., Foster, G. R., Mutchler, C. K. and Meyer, L. D. 1989. Revised slope length factor for the Universal Soil Loss Equation. *Transactions of the ASAE.* 32(5):1571-1576.
- Merritt, W. S., Letcher, R. A. and Jakeman, A. J. 2003. A review of erosion and sediment transport models. *Environ. modelling & software.* 18(8-9):761-799.
- Mhazo, N., Chivenge, P. and Chaplot, V. 2016. Tillage impact on soil erosion by water: discrepancies due to climate and soil characteristics. *Agric. Ecosystems & Environ.* 230:231-241.
- Misra, R. K. and Rose, C.W. 1996. Application and sensitivity analysis of process-based erosion model GUEST. *European J. Soil Sci.* 47(4):593-604.
- Mitasova, H., Hofierka, J., Zlocha, M. and Iverson, L. R. 1996. Modelling topographic potential for erosion and deposition using GIS. *Int. J. Geo. Info. Syst.* 10(5):629-641.
- Mitasova, H., Mitas, L., Brown, W.M., Gerdes, D.P., Kosinovsky, I. and Baker, T. 1995. Modelling spatially and temporally distributed phenomena: new methods and tools for GRASS GIS. *Int. J. Geo. Info. Systems.* 9(4): 433-446.
- Mohamadi, M. A. and Kavian, A. 2015. Effects of rainfall patterns on runoff and soil erosion in field plots. *Int. Soil and Water Conservation Res.* 3(4):273-281.
- Mohammed, S., Alsafadi, K., Talukdar, S., Kiwan, S., Hennawi, S., Alshihabi, O., Sharaf, M.

- andHarsanyie, E. 2020. Estimation of soil erosion risk in southern part of Syria by using RUSLE integrating geo informatics approach. *Remote Sensing Appl. Society and Environ.*20:100375.
- Morgan, R. P. C., Quinton, J.N., Smith, R. E., Govers, G., Poesen, J. W. A., Auerswald, K., Chisci, G., Torri, D. and Styczen, M. E. 1998. The European Soil Erosion Model (EUROSEM): a dynamic approach for predicting sediment transport from fields and small catchments. *Earth Surface Processes and Landforms. The J. The British Geomorphological Research Group.* 23(6):527-544.
- Morgan, R.P.C. 2009. *Soil erosion and conservation.* John Wiley & Sons.
- Moore, I.D. and Burch, G.J., 1986. Physical basis of the length-slope factor in the universal soil loss equation. *Soil Science Society of America Journal*, 50(5), pp.1294-1298.
- Moore, I.D. and Wilson, J.P., 1992. Length-slope factors for the Revised Universal Soil Loss Equation: Simplified method of estimation. *J. soil and water Conserv.*, 47(5), pp.423-428.
- Muluneh, T. and Mamo, W. 2014. Morphometric analysis of Didessa River catchment in Blue Nile Basin, Western Ethiopia. *Sci. Technol. Arts Res. J.* 3(3): 191-197.
- Nag, S.K. and Lahiri, A., 2011. Morphometric analysis of Dwarakeswar watershed, Bankura district, West Bengal, India, using spatial information technology. *Int. J. Water Resources and Environ. Eng.*, 3(10), pp.212-219.
- Naylor, L. A., Viles, H. A. and Carter, N. E. A. 2002. Biogeomorphology revisited: looking towards the future. *Geom.* 47(1):3-14.
- Ndolo Goy, P. 2015. GIS-based soil erosion modeling and sediment yield of the N'djili River basin, *Democratic Republic of Congo* (Doctoral dissertation, Colorado State University).
- Nearing, M. A., Foster, G. R., Lane, L. J. and Finkner, S. C. 1989. A process-based soil erosion model for USDA-Water Erosion Prediction Project technology. *Transactions of the ASAE.* 32(5):1587-1593.

- Olorunfemi, I. E., Komolafe, A. A., Fasinmirin, J. T., Olufayo, A. A. and Akande, S. O. 2020. A GIS-based assessment of the potential soil erosion and flood hazard zones in Ekiti State, Southwestern Nigeria using integrated RUSLE and HAND models. *Catena*. 194:104725.
- Onwuka, B. and Mang, B. 2018. Effects of soil temperature on some soil properties and plant growth. *Adv. Plants Agric. Res*, 8(1):34.
- Ostovari, Y., Ghorbani-Dashtaki, S., Bahrami, H. A., Naderi, M. and Dematte, J. A. M. 2017. Soilloss estimation using RUSLE model, GIS and remote sensing techniques: A case study from the Dembecha Watershed, Northwestern Ethiopia. *Geoderma regional*. 11:28-36.
- Panagos, P., Borrelli, P., Meusburger, K., Van der Zanden, E.H., Poesen, J. and Alewell, C. 2015. Modelling the effect of support practices (P-factor) on the reduction of soil erosion by water at European scale. *Envi. Sci. policy*. 51:23-34.
- Pandey, A., Chowdary, V. M. and Mal, B.C. 2007. Identification of critical erosion prone areas in the small agricultural watershed using USLE, GIS and remote sensing. *Water reso. Manage*. 21(4):729-746.
- Pandey, A., Himanshu, S. K., Mishra, S. K. and Singh, V. P. 2016. Physically based soil erosion and sediment yield models revisited. *Catena*. 147:595-620.
- Parsons, A. J. and Stone, P. M. 2006. Effects of intra-storm variations in rainfall intensity on inter rill runoff and erosion. *Catena*. 67(1):68-78.
- Parveen, R., Kumar, U. and Singh, V. K. 2012. Geomorphometric characterization of Upper South Koel Basin, Jharkhand: a remote sensing & GIS approach. *J. Water Resource and Protec*. 4(12):1042.
- Patode, R.S., Pande, C.B., Nagdeve, M.B., Moharir, K.N. and Wankhade, R.M., 2017. Planning of conservation measures for watershed management and development by using geospatial technology—A case study of Patur watershed in Akola District of Maharashtra. *Curr World Envi*, 12(3), p.708.
- Pedersen, H. S. and Hasholt, B. 1995. Influence of wind speed on rainsplash erosion. *Catena*. 24(1):39-54.

- Prasannakumar, V., Shiny, R., Geetha, N. and Vijith, H. 2011. Spatial prediction of soil erosion risk by remote sensing, GIS and RUSLE approach: a case study of Siruvani river watershed in Attapady valley, Kerala, India. *Envi. Earth Sci.* 64(4):965-972.
- Prasannakumar, V., Vijith, H., Abinod, S. and Geetha, N. J. G. F., 2012. Estimation of soil erosion risk within a small mountainous sub-watershed in Kerala, India, using Revised Universal Soil Loss Equation (RUSLE) and geo-information technology. *Geosci. Front.* 3(2):209- 215.
- Prasannakumar, V., Vijith, H., Geetha, N. and Shiny, R., 2011. Regional scale erosion assessment of a sub-tropical highland segment in the Western Ghats of Kerala, South India. *Water Res. Management*, 25(14):3715-3727.
- Puigdefábregas, J. 2005. The role of vegetation patterns in structuring runoff and sediment fluxes in drylands. *Earth Surface Processes and Landforms: The J. The British Geomorphological Research Group.* 30(2):133-147.
- Rahaman, S.A., Aruchamy, S., Jegankumar, R. and Ajeez, S.A., 2015. Estimation of annual average soil loss, based on RUSLE model in Kallar watershed, Bhavani basin, Tamil Nadu, India. *ISPRS Annals Photogrammetry, Remote Sensing and Spatial Infr. Scie.*, 2(2), p.207.
- Renard, K. G. and Freimund, J. R. 1994. Using monthly precipitation data to estimate the R-factor in the revised USLE. *J. Hydrology*, 157(1-4) :287-306.
- Renard, K. G., Foster, G. R., Weesies, G. A., McCool, D. K. and Yoder, D. C. 1996. Predicting soil erosion by water: A guide to conservation planning with the Revised Universal Soil Loss Equation (RUSLE). *Agric. Handbook.* 703:25-28.
- Renschler, C. S. and Harbor, J. 2002. Soil erosion assessment tools from point to regional scales—the role of geomorphologists in land management research and implementation. *Geom.* 47(2-4):189-209.
- Renschler, C. S., Mannaerts, C. and Dieckkrüger, B. 1999. Evaluating spatial and temporal variability in soil erosion risk—rainfall erosivity and soil loss ratios in Andalusia, Spain. *Catena.* 34(3-4) :209-225.

- Rey, F. 2003. Influence of vegetation distribution on sediment yield in forested marly gullies. *Catena*. 50(2-4) :549-562.
- Richter, G. 1980. On the soil erosion problem in the temperate humid area of Central Europe. *Geo. J.* 4(3) :279-287.
- Richter, G. 1980. On the soil erosion problem in the temperate humid area of Central Europe. *Geo. J.* 4(3) :279-287.
- Rickson, R. J. 2005. Soil Erosion and Conservation. BY RPC MORGAN x+ 304 :, 17× 24.4× 2 cm, ISBN 1 40511 781 8 paperback, GB£ 29.95, Oxford, UK: Blackwell Publishing, 2004. *Environ. Conserv.*32(4) :374-375.
- Romkens, M. J., Helming, K. and Prasad, S. N. 2002. Soil erosion under different rainfall intensities, surface roughness, and soil water regimes. *Catena*. 46(2-3):103-123.
- Roose, E. J. 1977. Use of the universal soil loss equation to predict erosion in West Africa. In *Soilerosion: prediction and control* Soil Conservation Society of America Ankeny, IA. 21. pp. 60-74.
- Roose, E. J. 1986. Runoff and erosion before and after clearing depending on the type of crop in western Africa. *Land clearing and development in the tropics*”(R. Lal, ed.) :317-330.
- Rudra, R. P., Dickinson, W. T., Clark, D. J. and Wall, G. J. 1986. GAMES—A screening model of soil erosion and fluvial sedimentation on agricultural watershed. *Canadian Water Resources Journal*. 11(4):58-71.
- Sabzevari, T. and Talebi, A. 2019. Effect of hillslope topography on soil erosion and sediment yield using USLE model. *Acta Geophysica*, 67(6) :1587-1597.
- Sadeghi, S. H. R., Gholami, L., Khaledi Darvishan, A. and Saeidi, P. 2014. A review of the application of the MUSLE model worldwide. *Hydrological Sci. J.* 59(2):365-375.
- Sadeghi, S. H., Mizuyama, T. and Vangah, B. G.,2007. Conformity of MUSLE estimates and erosion plot data for storm-wise sediment yield estimation. *TAO: Terrestrial, Atmospheric and Oceanic Sciences*. 18(1):117.

- Sadgir, P.A., Patil, G.K. and Takalkar, V.G., 2006, November. Sustainable watershed development by refilled continuous contour trenching technology. In *National Seminar on Rainwater Harvesting and Water Manag.* (pp. 331-338).
- Sahu, A., Baghel, T., Sinha, M.K., Ahmad, I. and Verma, M.K., 2017. Soil erosion modeling using rusle and GIS on Dudhawa Catchment. *Intern. J. Applied Environ. Scie.*, 12(6), pp.1147-1158.
- Saroha, J., 2017. Soil Erosion: Causes, Extent, and Management in India. *Int. J. Creative Res. Thoughts.* 5(4) :1321-1330.
- Schmidt, J., Werner, M. V. and Schindewolf, M. 2017. Wind effects on soil erosion by water—Asensitivity analysis using model simulations on catchment scale. *Catena.* 148 :168-175.
- Schmidt, J., Werner, M.V. and Schindewolf, M. 2017. Wind effects on soil erosion by water—Asensitivity analysis using model simulations on catchment scale. *Catena.* 148 :168-175.
- Schumm, S. A. 1956. Evolution of drainage systems and slopes in badlands at Perth Amboy, NewJersey. *Geological society of America bulletin.* 67(5):597-646.
- Senanayake, Sumudu, Biswajeet Pradhan, Alfredo Huete, and Jane Brennan. 2020. Assessing SoilErosion Hazards Using Land-Use Change and Landslide Frequency Ratio Method: A Case Study of Sabaragamuwa Province, Sri Lanka. *Remote Sensing* 12 (9):1483.
- Sharma, A. 2010. Integrating terrain and vegetation indices for identifying potential soil erosion risk area. *Geo-Spat. Info. Sc.* 13(3) :201-209.
- Sharon, D. and Arazi, A., 1997. The distribution of wind-driven rainfall in a small valley: an empirical basis for numerical model verification. *J. Hydrology*, 201(1-4) :21-48.
- Shi, P., Yan, P., Yuan, Y. and Nearing, M. A. 2004. Wind erosion research in China: past, present and future. *Progress in physical geography.*, 28(3) :366-386.
- Shiono, T., Kamimura, K. I., Okushima, S. and Fukumoto, M. 2002. Soil loss estimation on a local

- scale for soil conservation planning. *Japan Agric. Res. Quart: JARQ*. 36(3):157-161.
- Singh, G. and Panda, R. K. 2017. Grid-cell based assessment of soil erosion potential for identification of critical erosion prone areas using USLE, GIS and remote sensing: A case study in the Kapgari watershed, India. *Int. Soil and Water Conserv. Res.* 5(3) :202-211.
- Singh, V. P. 1994 Elementary Hydrology, Prentice Hall.
- Smith, D. D. and Whitt, D. M. 1948. Estimating soil losses from field areas of claypan soil. *Soil Sci. Society of America J.* 12(C):485-490.
- Soni, S. 2017. Assessment of morphometric characteristics of Chakrar watershed in Madhya Pradesh India using geospatial technique. *App. Water Sci.* 7(5) :2089-2102.
- Sreedevi, P. D., Owais, S. H. H. K., Khan, H. H. and Ahmed, S. 2009. Morphometric analysis of a watershed of South India using SRTM data and GIS. *J. The geological society of India.* 73(4):543-552.
- Sreedevi, P. D., Sreekanth, P. D., Khan, H. H. and Ahmed, S. 2013. Drainage morphometry and its influence on hydrology in an semi arid region: using SRTM data and GIS. *Envi. Earth Sci.* 70(2) :839-848.
- Srinivas, C. V., Maji, A. K., Reddy, G. and Chary, G. R. 2002. Assessment of soil erosion using remote sensing and GIS in Nagpur district, Maharashtra for prioritisation and delineation of conservation units. *J. Indian Society of Remote Sensing.* 30(4) :197-212.
- Stone, R.P. and Hilborn, D. 2000. Universal Soil Loss Equation (USLE). Ontario. Ministry of Agriculture. *Food and Rural Affairs.* pp.9.
- Strahler, A. N. 1964. Quantitative geomorphology of drainage basin and channel networks. *Handbook. A: Hydrol.*
- Sukristiyanti, S., Maria, R. and Lestiana, H., 2018, February. Watershed-based morphometric analysis: a review. In *IOP conference series: earth and environ sci* (Vol. 118, No. 1, p. 012028). IOP Publishing.
- Suma, B.N. and Srinivasa, C.V., 2017. A study on morphometric parameter of a watershed for sustainable water conservation. *Int J. of Civil Eng. and Technol*, 8(9), pp.271-278.

- Sun, W., Shao, Q., Liu, J. and Zhai, J. 2014. Assessing the effects of land use and topography on soil erosion on the Loess Plateau in China. *Catena*. 121 :151-163.
- Tadesse, L., Suryabagavan, K. V., Sridhar, G. and Legesse, G., 2017. Land use and land cover changes and Soil erosion in Yezat Watershed, North Western Ethiopia. *Int. Soil and Water Conserv. Res.* 5(2) :85-94.
- Thakural, L.N., Kumar, S.A. and Ansari, M.I., 2018. Trend analysis of rainfall for the Chaliyar Basin, South India. *Int. J. for Res. in Appl Sci. and Eng. Technol.*, 6(7), pp.91-100.
- Teng, H., Liang, Z., Chen, S., Liu, Y., Rossel, R. A. V., Chappell, A., Yu, W. and Shi, Z. 2018. Current and future assessments of soil erosion by water on the Tibetan Plateau based on RUSLE and CMIP5 climate models. *Sci. Total Envi.* 635 :673-686.
- Terranova, O., Antronico, L., Coscarelli, R. and Iaquina, P. 2009. Soil erosion risk scenarios in the Mediterranean environment using RUSLE and GIS: an application model for Calabria(southern Italy). *Geomorph.* 112(4) :228-245.
- Thomas, J., Joseph, S. and Thirvikramji, K.P., 2018. Assessment of soil erosion in a monsoon-dominated mountain river basin in India using RUSLE-SDR and AHP. *Hydrol. Sci. J.*, 63(4), pp.542-560.
- Thomas, J., Joseph, S. and Thirvikramji, K. P. 2018. Assessment of soil erosion in a tropical mountain river basin of the southern Western Ghats, India using RUSLE and GIS. *Geosci.Front.* 9(3):893-906.
- Thomas, J., Joseph, S. and Thirvikramji, K. P. 2018. Estimation of soil erosion in a rain shadow river basin in the southern Western Ghats, India using RUSLE and transport limited sediment delivery function. *Int. Soil and Water Conserv. Res.* 6(2) :111-122.
- Toy, T.J., Foster, G.R. and Renard, K.G., 1999. RUSLE for mining, construction and reclamation lands. *J. Soil and Water Conserv.*, 54(2), pp.462-467.
- Turner, B. L., Fuhrer, J., Wuellner, M., Menendez, H. M., Dunn, B. H. and Gates, R. 2018. Scientific case studies in land-use driven soil erosion in the central United States: Why soil potential and risk concepts should be included in the principles of soil health. *Int. Soiland Water Conserv. Res.* 6(1) :63-78.

- Van Dijk, A. I. J. M., Bruijnzeel, L. A. and Rosewell, C. J. 2002. Rainfall intensity–kinetic energy relationships: a critical literature appraisal. *J. Hydrol.* 261(1-4) :1-23.
- Van Haveren, B.P., Jackson, W.L. and Lusby, G.C., 1987. Sediment deposition behind Sheep Creek barrier dam, southern Utah. *J. Hydrol. (New Zealand)*, pp.185-196.
- Vannoppen, W., De Baets, S., Keeble, J., Dong, Y. and Poesen, J. 2017. How do root and soil characteristics affect the erosion-reducing potential of plant species? *Ecological Engineer.* 109:186-195.
- Vemu, S. and Pinnamaneni, U. B., 2011. Estimation of spatial patterns of soil erosion using remote sensing and GIS: a case study of Indravati catchment. *Natural Hazards.* 59(3) :1299-1315.
- Wainwright, J., Parsons, A. J., Schlesinger, W. H. and Abrahams, A. D. 2002. Hydrology–vegetation interactions in areas of discontinuous flow on a semi-arid bajada, southern New Mexico. *J. Arid Envi.* 51(3):319-338.
- Williams, J. R. and Berndt, H. D. 1977. Sediment yield prediction based on watershed hydrology. *Transactions of the ASAE.* 20(6) :1100-1104.
- Wischmeier, W. H, Smith, D. D. 1978. Predicting rainfall erosion losses: a guide to conservation planning. U.S. Department of Agriculture, Agriculture Handbook, No. 537
- Wischmeier, W. H., Johnson, C. B. and Cross, B. V. 1971. Soil erodibility nomograph for farmland and construction sites.
- Smith, D. D. and Uhland, R. E. 1958. Evaluation of factors in the soil loss equation. *Agric. Engineer.* 39(8) :458-462.
- Wu, X., Fan, J., Sun, L., Zhang, H., Xu, Y., Yao, Y., Yan, X., Zhou, J., Jia, Y. and Chi, W. 2021. Wind erosion and its ecological effects on soil in the northern piedmont of the Yinshan Mountains. *Ecological Indicators.* 128:107825.
- Xie, Y., Liu, B. and Nearing, M. A. 2002. Practical thresholds for separating erosive and non-erosive storms. *Transactions of the ASAE.* 45(6):1843.
- Yang, C. S., Li, Q. F., Wen, H. Y. and Cai, T. 2012. Simulation of soil and water loss in the Upper Huaihe River Basin using the Xinanjiang Model. *Procedia Engineer.* 28 :501-505.

- Zare, M., Panagopoulos, T. and Loures, L. 2017. Simulating the impacts of future land use change on soil erosion in the Kasilian watershed, Iran. *Land Use Policy*. 67:558-572.
- Zerihun, M., Mohammedyasin, M. S., Sewnet, D., Adem, A. A. and Lakew, M. 2018. Assessment of soil erosion using RUSLE, GIS and remote sensing in NW Ethiopia. *Geoderma regional*. 12:83-90.
- Zhang, Y., Degroote, J., Wolter, C. and Sugumaran, R. 2009. Integration of modified universal soil loss equation (MUSLE) into a GIS framework to assess soil erosion risk. *Land Degradation & Development*. 20(1):84-91.
- Zheng, F.L., 2006. Effect of vegetation changes on soil erosion on the Loess Plateau. *Pedospher*. 16(4):420-427.
- Zhou, P., Luukkanen, O., Tokola, T. and Nieminen, J. 2008. Effect of vegetation cover on soil erosion in a mountainous watershed. *Catena*. 75(3) :319-325.
- Ziegler, A. D. and Giambelluca, T. W. 1998. Influence of revegetation efforts on hydrologic response and erosion, Kaho'olawe Island, Hawai'i. *Land Degradation & Development*. 9(3):189-206.
- Zorn, M. and Komac, B. 2011. The importance of measuring erosion processes on the example of Slovenia. *Hrvatski geografski glasnik*, 73(2):19-34.
- Zuazo, V. D., Martinez-Raya, A. and Ruiz, J. A. 2002. Control de la erosión en los taludes de banales, en terrenos con fuertes pendientes. *Edafología*, 9(1):1-10.
- Zuazo, V. D., Pleguezuelo, C. R., Martínez, J. F., Rodríguez, B. C., Raya, A. M. and Galindo, P.P. 2008. Harvest intensity of aromatic shrubs vs. soil erosion: An equilibrium for sustainable agriculture (SE Spain). *Catena*. 73(1):107-116.
- Zuazo, V. H. D. and Pleguezuelo, C. R. R. 2009. Soil-erosion and runoff prevention by plant covers: a review. *Sustainable agric*. 12:785-811.

APPENDICES

APPENDICES

APPENDIX I

Sample calculation of R factor for the year 2000

MONTH	P _i	P	P _i ²	P _i ² /P	R factor
Jan	35	2060.1	1225	0.594631	0.658857
Feb	10	2060.1	100	0.048541	0.768433
Mar	0	2060.1	0	0	0
Apr	137	2060.1	18769	9.110723	39.51379
May	28	2060.1	784	0.380564	0.337335
Jun	537.2	2060.1	288583.8	140.0824	2382.292
Jul	293.4	2060.1	86083.56	41.78611	388.1212
Aug	494.9	2060.1	244926	118.8903	1862.685
Sep	254.6	2060.1	64821.16	31.46506	253.6076
Oct	115	2060.1	13225	6.419591	23.37117
Nov	41	2060.1	1681	0.81598	1.059104
Dec	74	2060.1	5476	2.658123	6.227048
					4957.214

To calculate monthly R value

Consider month July with annual rainfall of 2060.1 mm

According to equation

$$R = \sum_{i=1}^{12} 1.735 \times 10^{(1.5 \log_{10} \frac{P_i^2}{P} - 0.08188)}$$

$$= 1.735 \times 10^{(1.5 \log 41.78611 - 0.08188)}$$

$$= 388.1212 \text{ MJ mm ha}^{-1} \text{ h}^{-1} \text{ y}^{-1}$$

APPENDIX II

Calculation of erodibility factor K

Soil association	Soil texture %			Organic carbon%	Organic matter %	Structural code b	Permiability c	K factor
	Sand	silt	clay					
Mannamkulam	22	20	58	2	2	3	5	0.19
Kutil	52	6	42	2	2	2	5	0.16
Angadipuram	58	15	27	2	1.2	2	5	0.28
Vettekcode	52	6	42	2	2	4	5	0.25
Koramala	58	15	27	2	2	4	5	0.35
Vazhikad	32	34	34	2	2.76	4	5	0.37
Arimbra	43	39	18	2	2.07	4	5	0.53
karuvarakundu	22	20	58	2	2	4	5	0.23
churathinmel	32	34	34	2	2.43	4	5	0.38
Nadukani	22	20	58	2	0.83	4	5	0.24
Kalvarikunnu	52	6	42	2	2.21	4	5	0.25
Pullangod	52	6	42	2	2	4	5	0.25
Walakkad	32	34	34	2	4.22	3	5	0.29
kurumbramala	32	34	34	2	4.22	3	5	0.29

Sample calculation of K factor

For Vazhikkad series,

$$K = \{2.1 \times M^{1.14} \times 10^{-4} \times (12-a) + 3.25 \times (b-2) + 2.5 \times (c-3)\} / 100$$

In which, M = (% of silt + % of very fine sand) x (100 - % of clay), 'a' is the % of organic matter content in the soil, 'b' indicates value corresponding to structural classes and c indicates the value corresponding to the permeability class.

$$\{ M = (20+7) * (100-58) = 2904.00, a = 2.76, b = 4, c = 5 \}$$

$$\text{Therefore } K = \{2.1 * 1134.00^{1.14} * (12-2.76) + 3.25 * (4-2) + 2.5 * 2\} / 100$$

$$= 0.37 \text{ t ha h}^{-1} \text{ MJ}^{-1} \text{ mm}^{-1}$$

**SOIL LOSS ESTIMATION AND SPATIAL MAPPING USING
RUSLE AND GIS- A CASE STUDY IN KURUMANPUZHA SUB
WATERSHED OF CHALIYAR RIVER BASIN**

By

AISHWARYA M S

(2019-18-002)

ABSTRACT OF THESIS

Submitted in partial fulfillment of the

Requirement for the award of degree of

Master of Technology

In

Agricultural Engineering

(Soil and Water Conservation Engineering)

Faculty of Agricultural Engineering and Technology

Kerala Agricultural University



Department of Irrigation and Drainage Engineering

Kelappaji College of Agricultural Engineering and Technology

Tavanur-679 573, Malappuram.

2022

ABSTRACT

Land degradation is a problem of grave concern and one major factor leading to it is soil erosion. The main aim of the study is to calculate the soil loss in the sub watershed. This study also analysed the quantitative analysis of morphometric parameters of Kurumanpuzha sub watershed using remote sensing data and geographic information system. Morphometric parameters were evaluated from three perspectives: Linear, Areal and relief characteristics. A fifth-order river drains Kurumanpuzha watershed and the drainage network is mainly dendritic type. The mean bifurcation ratio (R_b) was 2.05. The watershed has elongated shape suggesting low peak flows for longer duration and hence easier flood management. The drainage texture analysis revealed fine drainage which implies the dominance of impermeable soft rock with low resistance against erosion. High relief and steep slopes dominates, by which rough landforms (hills, breaks, and low mountains) make up major portion of the watershed. The hypsometric curve with hypsometric integral of 0.48 suggests that Kurumanpuzha watershed is in equilibrium or mature stage of geomorphic evolution. At sub-watershed scale, the derived morphometric parameters were grouped into three clusters (low, moderate, and high) and considerable spatial variability was observed. The results of this study provide information on drainage morphometry that can help better understand the watershed characteristics and serve as a basis for improved planning, management, and decision making to ensure sustainable use of watershed resources.

Soil erosion is caused by the action of various factors which are intrinsic to the soil or related to the environment surrounding the soil. These factors include rainfall, soil erodibility, topographic characteristics, crop cover and conservation practices. The Revised universal soil loss equation (RUSLE) is a well-renowned empirical formula which is used to compute the average annual soil loss of a particular area. Remote sensing (RS) and geographical information system (GIS) technologies make modelling and execution of RUSLE easy, reliable and cost effective. So, these were employed to compute the spatial distribution of soil erosion risk area in Kurumanpuzha sub watershed in Kerala state, India. All the factors were generated using metrological data, CartoSat DEM, Landsat 8 imagery using GIS software and integrated in a GIS environment to estimate the soil loss rate. It was found that forest/Dense vegetation

(56.46%) was the dominant land use followed by rubber plantation (20.06%) and o scrub land (8.91%). The average annual soil loss of the watershed was estimated to be 8.00 t ha⁻¹ yr⁻¹ and the total quantity of soil eroded was 82,872.4 t yr⁻¹. The average annual soil loss was highest in bare land (8.55 t ha⁻¹ yr⁻¹) followed by scrub land (5.27 t ha⁻¹ yr⁻¹). The soil erosion map thus generated can serve as a basis for adopting suitable measures in the watershed for sustainable management of the resources in it.